# SYNTHESIS OF ISOQUINOLINE DERIVATIVES AS POTENTIAL DRUG MOLECULES ACTIVE AGAINST PROSTATE CANCER

by

Halenur Karakaya

B.S., Chemistry, Boğaziçi University, 2013

Submitted to the Institute for Graduate Studies in
Science and Engineering in partial fulfillment of
the requirements for the degree of
Master of Science

Graduate Program in Chemistry
Boğaziçi University

2015

To my mother and sister,
and to the memory of my father...

# ACKNOWLEDGEMENTS

The main insight I have gained throughout this master study is the key importance of being a member of a harmonious team. Therefore, first and foremost, I would like to express my deepest sincere to my advisor Assoc. Prof. A. Ersin Acar for giving me the opportunity to be a part of his research group. I am grateful to him for his guidance, moral support, patience and academic mentorship over the years.

I would like to express my missing and gratitude to Prof. Bedi Ziver, who suddenly passed away. He always believed in me and supported me. To become acquainted with such a kind and generous person was truly precious.

I would like to thank the thesis committee members Prof. Duygu Avcı Semiz and Assoc. Prof. İ. Halil Kavaklı for sparing their valuable time for reviewing my thesis. I also would like to express my gratitude to Prof. Metin Türkay and Assoc. Prof. İ. Halil Kavaklı for providing us with this cancer research project. I also want to thank to Halise Büşra Angın, Selma Bulut for performing computational and biological tests and Begüm Alaybeyoğlu for providing me a large number of NMR data. The contribution of my lab friends is very valuable to me. I would like to express my gratitude to Turan and Ahmet for sharing their experiences and for their help. Particularly, I wish to extend my great thanks to each member of Acar Lab family: Ayşenur, Duygu, Kâmil, Sedef, Seda, Aylin, Işıl and Didem for the times we spent together in lab. They provided such a friendly and endearious lab environment that I just felt peaceful while working in lab for hours. I also would like to thank to Sare and Refia for their help during the experiments. I especially would like to thank to my dearest friend Vildan for standing with me whenever I need, for her support, encouragement and affection. My sincere gratitude belongs to Mücahid for sharing my happiness, sorrow and even my childhood over these years, and for his understanding and patience.

Last but not least, I would like to express my inmost gratitude to my dear mother Gülsüm and my sister Gülnur, who make me feel the luckiest person in the world with their everlasting loves, eternal sacrifices and endless supports.

And I specially dedicate this thesis to the memory of my beloved father Recep, who never deprived me of his love.

This research has been funded by Bogazici University Research Funds (BAP, Project No: 5085) and The Scientific and Technological Research Council of Turkey (TÜBİTAK, Project No: 109T431).

# ABSTRACT


## SYNTHESIS OF ISOQUINOLINE DERIVATIVES AS POTENTIAL DRUG MOLECULES ACTIVE AGAINST PROSTATE CANCER

Cancer is the most common neoplasm of the prostate in developed countries. About 80% of prostatic tumors are based on elevated levels of androgens because androgen stimulates the cellular proliferation of human prostate cancer. Therefore, deprivation of androgen level constitutes a good strategy in order to treat castration-resistant prostate cancer. Enzymes in androgen biosynthesis are favorable targets, such as CYP17A1. Although the androgens are secreted from three different sites, namely the testes, adrenal glands, and PCa cells, androgen production depends on catalysis by one enzyme, CYP17, which is also known as P450-C17. Being a pivotal enzyme in the biosynthetic route to steroidal hormones, CYP17A1 has a key role in the conversion of progesterone and pregnenolone to androstenedione and dehydroepiandrostenedione (DHEA) respectively, which constitute as the direct precursors of 5α-dihydrotestosterone (DHT) and testosterone (T). Since the crystal structure of CYP17 has been absent for a long term, natural substrates (pregnenolone and progesterone) have been used as scaffolds of potential drug candidates. Although Abiraterone was launched as a potent steroidal CYP17 inhibitor, due to the potential side effects of steroidal CYP17A1 inhibitors resulting from inhibition of other steroid receptors, there is a certain need to develop nonsteroidal inhibitors. In this project, several derivatives of a nonsteroidal lead compound were designed: Mainly the synthesis of isoquinoline derivatives was endeavored. Besides, a library of final products was built by synthesizing several aromatic carboxamides including benzofuran-2-carboxylic acid, benzo[b]thiophene-2-carboxylic acid and 4-(1H-tetrazol-5-yl)benzoic acid derivatives.

# ÖZET

## PROSTAT KANSERİNE KARŞI AKTİF, POTANSİYEL İLAÇ MOLEKÜLLERİ OLARAK İZOKİNOLİN TÜREVLERİNİN SENTEZİ

Gelişmiş ülkelerde kanser, prostatın en yaygın görülen tümör türüdür. Prostat kanserinin yayılmasının nedeni androjenlerin prostat kanserli hücrelerde çokça üretilen androjen reseptörüne bağlanmaları olması nedeniyle prostat kanserinin yayılmasının % 80'i androjenlere bağlıdır. Dolayısıyla, androjen seviyesinin azaltılması, kastrasyon-dirençli prostat kanserinin tedavisi için iyi bir stratejidir. Androjen biyosentezindeki enzimler, örneğin CYP17A1, tercih edilebilir hedeflerdir. Androjenlerin erbezleri, adrenal bezleri ve prostat kanser hücreleri olarak üç farklı bölgeden salınmalarına rağmen, androjen üretimi anahtar enzim olan P450-C17 olarak da bilinen CYP17A1'in katalizine dayanmaktadır. Steroidal hormonların biyosentezinde merkezi bir öneme sahip olan bir enzim olarak CYP17A1, pregnenolon ve progesteronun, sırasıyla, DHT ve T öncül maddeleri olan androstendion ve DHEA'ya dönüştürlmesinde anahtar bir rol oynamaktadır. CYP17A1'in kristal yapısı uzun süre boyunca mecvut olmadığı için, doğal sübstratlar (pregnenolone ve progesterone), potansiyel ilaç adaylarının yapı iskeleti olarak kullanılmıştır. Abirateron asetat, CYP17A1 potent steroid yapıda bir ilaç olarak çıkarılmasına rağmen, steroid yapıdaki CYP17A1 inhibitörlerinin diğer steroid reseptörlerini inhibe etmesinden kaynaklanan potansiyel yan etkilerinden dolayı steroidal olmayan inhibitörlerin geliştirilmesine kesin bir ihtiyaç vardır. Bu çalışmada steroidal olmayan bir öncü bileşiğin çeşitli türevleri tasarlandı: Temel olarak izokinolin türevlerinin sentezi amaçlandı. Bunun yanı sıra, benzofuran-2-karboksilik asit, benzo[b]tiyofen-2-karboksilik asit ve 4-(1H-tetrazol-5-yl)benzoik asit içeren çeşitli karboksamit türevleri sentezlenerek bir son ürün kütüphanesi oluşturuldu.

# TABLE OF CONTENTS

# LIST OF FIGURES

# LIST OF TABLES

# LIST OF ACRONYMS/ABBREVIATIONS

| | |
|---|---|
| $Ac_2O$ | Acetic Anhydride |
| ADMET | Adsorption, Distribution, Metabolism, Elimination and Toxicity |
| ADT | Androgen Deprivation Therapy |
| AR | Androgen Receptor |
| BC | Before Christ |
| BE | Binding Energy |
| BPH | Benign Prostatic Hyperplasia |
| BtOH | Hydroxybenzotriazole |
| $CDCl_3$ | Deuterated chloroform |
| $CH_2Cl_2$ | Dichloromethane |
| CRH | Corticotropin-Releasing Hormone |
| CRPC | Castration Resistant Prostate Cancer |
| CYP | Cytochrome P-450 |
| CYP17A1 | 17 alpha-hydroxylase cytochrome P-450 (P-$450_{17\alpha}$) |
| DHT | 5α-dihydrotestosterone |
| DE | Docking Energy |
| DCM | Dichloromethane |
| DHEA | Dehydroepiandrostenedione |
| DHT | 5α-dihydrotestosterone |
| DMF | N,N-Dimethylformamide |
| DNA | Deoxyribonucleic Acid |
| DRE | Digital Rectal Exam |
| EtOAC | Ethyl Acetate |
| EDC | 1-Ethyl-3-(3-dimethylaminopropyl)carbodiimide |
| *et al.* | Et Alii (and Others) |
| FDA | Food and Drug Administration |
| FSH | Follicle stimulating Hormones |
| GnRH | Gonadotropin Releasing Hormone |

| | |
|---|---|
| Gn | Gonadotropin |
| HEK 293T | Human Embryonic Kidney Cell Line |
| $IC_{50}$ | Inhibitory Concentration |
| IARC | International Agency for Research on Cancer |
| LDA | Lithium Diisopropylamide |
| LH | Luteinizing Hormone |
| NMR | Nuclear Magnetic Resonance |
| P450-C17 | 17 alpha-hydroxylase cytochrome (CYP17) |
| PCa | Prostate Cancer |
| PDB ID | Protein Data Bank Identification |
| PSA | Prostate-Specific Antigen |
| QSAR | Quantitative Structure Activity Relationship |
| RT | Room Temperature |
| SBDD | Structure Based Drug Design |
| T | Testosterone |
| THF | Tetrahydrofuran |
| TLC | Thin Layer Chromatography |
| US | Ultrasound Imaging |
| USA | United States of America |

# 1. INTRODUCTION

## 1.1. The Ongoing Problem: Cancer

### 1.1.1. What Is Cancer?

Cancer is a group of more than a hundred diseases characterized by the growth and spread of abnormal cells in an uncontrolled manner. Compared to normal cells, cancer cells have the distinction of possessing damaged DNA and not dying as they are supposed to. Instead, the cancerous cell continues to make new cells which have the same damaged DNA as the first cell does. Invading other tissues may end up with death unless the spread is controlled [1].

The cancerous cells can get into the body's bloodstream or lymph vessels and travel to other parts of body, which is called metastatis. Different types of cancer can act very differently in terms of growth rates or their response to various treatments. For this reason, regardless of the location of metastatis, the nomenclature of cancer is based on the part of the body where the cancer is originated. As an example, a cancer which has stemmed from prostate gland and has spread to the liver is called metastatic prostate cancer, not liver cancer.

Some inherited genetic mutations, hormones or immune charachteristics can cause cancer. However, DNA is predominantly damaged during a normal cell is reproducing or if the person is exposed to external factors such as tobacco, infectious organisms, and an unhealthy diet. These factors may act together or sequentially to induce cancer [1].

### 1.1.2. Early History of Cancer

One of the earliest evidence of cancer has been recorded in an ancient Egypt manuscript, which is thought to be written in 3000 BC. The textbook defines the undeveloped portraiture of breast cancer and states that there is no treatment for this

disease. As well as literature, fossilized bone tumors belonging to human mummies exemplifies that the history of cancer dates back to the dawn of ancient times.

The origin of the word cancer is attributed to the Greek physician Hippocrates (460-370 BC), who is recognized as “Father of Medicine.” Due to the resemblance of spreading cancer to a crab with its extended claws, Hippocrates used the terms carcinos, the corresponding Greek word for crab. One of the most well-known Roman physician, Celsus (28-50 BC), later translated the carcinos into cancer, the Latin term used for the word “crab”, to describe malignant tumors [2].

### 1.1.3. Cancer in the Contemporary Era

The modern understanding of cancer biology has pioneered to noteworthy progress in cancer prevention, early detection, and treatment. By the middle of 20$^{th}$ century, some of the complicated problems of chemistry and biology have been started to be clarified as a result of invention of advanced instruments. Beyond any doubt, the most important development was the discovery of the exact chemical structure of DNA by James Watson and Francis Crick. They received a Nobel Prize in 1962 for their impressive study.

Scienctists have already conceived that both external factors and family history could lead to the cancer, but the understanding of DNA has brought scientists about determining the effect of chemicals and radiation as well as the inherited defective genes on cancer development.

Remarkably, the contemporaneous scientists have gained a more advanced perspective about cancer in the last two decades. Especially the intellectual and practical developments such as more targeted therapies, immunotheraphy, nanotechnology, robotic surgery, cancer genetics, and expression profiling and proteomics are the inevitable consequences of very promising progression in cancer research.

As of 2014, more than a hundred chemical, physical and biological carcinogens have been determined by the World Health Organization’s International Agency for Research on

Cancer (IARC). Today, researchers are still discovering new carcinogens, explaining their influence on cancer, and supplying novel insights in order to prevent cancer [3].

### 1.1.4. Estimated Number of New Cancer Cases and Deaths for 2015

By the year 2015, approximately 1,658,370 new cancer cases are expected to be diagnosed. Additionally almost 589,430 Americans are expected to die of cancer, corresponding to 1,620 people per day. Cancer is the second most prevailing cause of death in the US (Figure 1.1.), exceeded only by heart disease, accounts for about 1 of every 4 deaths [4].

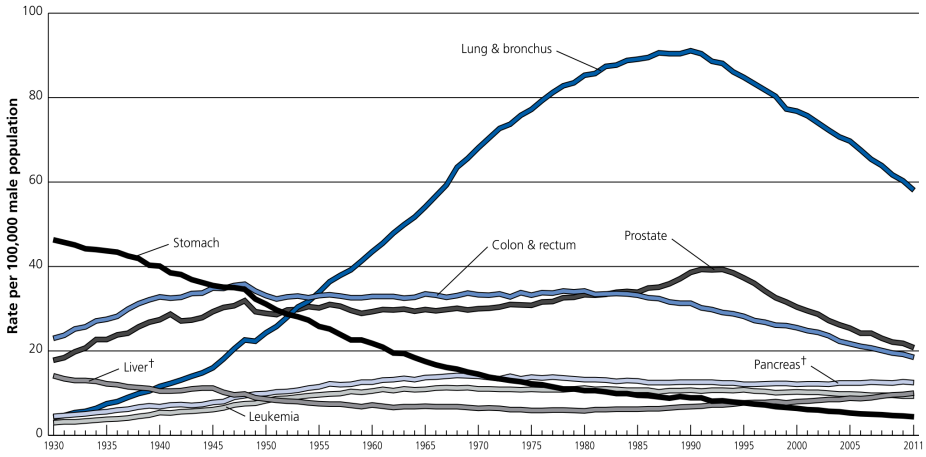


Figure 1.1. Age-adjusted Cancer Death Rates, Males by Site, US, 1930-2006 [4].

## 1.2. Prostate Cancer

Prostate cancer is the most commonly diagnosed cancer and the second most common cause of cancer death among men in US. It accounts for about 1 in 4 newly diagnosed cancers each year among US men. Approximately 217,730 new cases of prostate cancer diagnosed in the US, in 2010. In the same year, 32,050 men were expected to die by reason of prostate cancer (Figure 1.2) [1].

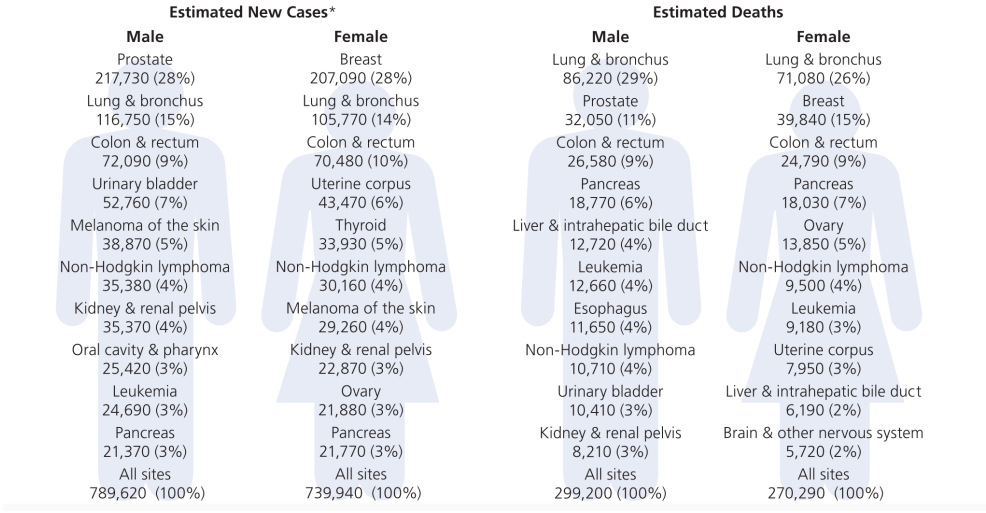


Figure 1.2. Leading Sites of New Cancer Cases and Deaths – 2010 Estimates [1].

### 1.2.1. What are the risk factors for prostate cancer?

In epidemology, a risk factor is a variable associated with an increased risk of disease or infection [5]. Although the causes of prostate cancer are not completely understood, researchers have determined some factors that might trigger the risk of getting prostate cancer.

- Prostate cancer is uncommon in men who are younger than 40, however the risk accelerates rapidly after the age 50. Approximately 6 in 10 cases of prostate cancer are found in men over the age of 65.
- Prostate cancer emerges more frequently in Afro-American men and Caribbean men of African ancestry than in men of other races. Afro-American men are also two times more likely to die of prostate cancer than white men (Figure 1.3) . Prostate cancer occurs less frequent in Asian-American and Hispanic/Latino men than in non-Hispanic whites. The reasons why the racial and ethnic differences contibute to the development of prostate cancer have not been explained yet.

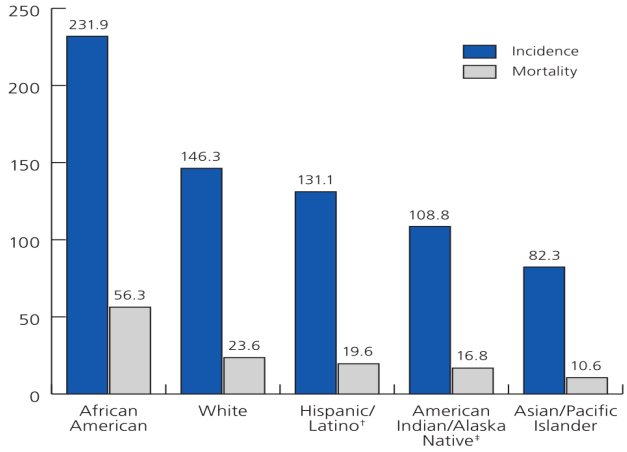


Figure 1.3. Prostate Cancer Incidence and Mortality Rates by Race and Ethnicity, US, 2002-2006 [1].

- Prostate cancer is most frequent in North America, Northwestern Europe, Australia, and on Caribbean islands. Besides, Asia, Africa, Central America, and South America are the regions among where prostate cancer is less common [1]. The difference in prevelance between industrialized and developing countries is caused to a certain extent by the extensive employment of PSA screening in economically developed regions [6].
- Some clinical findings suggest that prostate cancer may depend on genetic factor. Having a father or brother with prostate cancer doubles a man's risk of developing prostate cancer. The risk is higher for men who have a brother with the disease than for those with an affected father [7]. Recently, some common gene variations have been linked to a higher risk of prostate cancer. Men with BRCA-2 mutations are at elevated risk of having prostate cancer which is more aggressive and develops at a younger age [1].
- Although several nutritional factors have been proposed in order to alter the risk of prostate cancer in cohort studies, the exact role of diet in prostate cancer is not clear. Some studies revealed that diets with over consumption of red and processed meat or high levels of calcium (>1,500 mg/day) may be associated with an increased risk of developing prostate cancer.

- Some studies have demonstrated that obesity may alter the stage of prostate cancer as following: Overweighted men have a lower risk of developing prostate cancer with a higher risk of getting more aggressive form.
- There is some evidence that firefighters exposed to toxic combustion products may have higher risk of developing prostate cancer [1].

### 1.2.2. Prostate Gland

Prostate gland (Greek προστάτης, prostates, literally "one who stands before", "protector", "guardian") is part of male reproductive system in most mammal as a compound tubuloalveolar exorcrine gland) (Figure 1.4). The role of the prostate gland is to secrete a slightly alkaline fluid whose color is milky or white, comprises of semen, spermatozoa and seminal vesical fluid. A healthy human male prostate gland is typically about 11 grams, ranging between 7 to 16 grams. Prostate gland is located below the male's urinary bladder, in front of the penis and it surrounds the urethra [8].

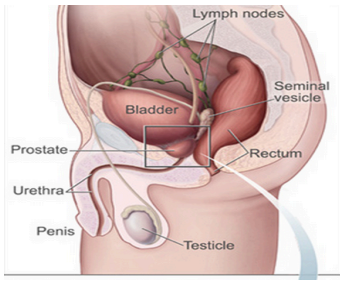


Figure 1.4. Prostate Gland [8].

### 1.2.3. Signs and Symptoms

Early stages of prostate cancer usually have no symptoms. As the disease progresses, men may experience inability to urination (Figure 1.5); weak or interrupted urine flow; difficulty in starting or stopping the urine flow; the need to urinate frequently; blood in the urine; or pain or burning with urination. Advanced prostate cancer commonly spreads to the bones, which can cause pain in the pelvic area such as hips, spine, ribs, or other areas [1].

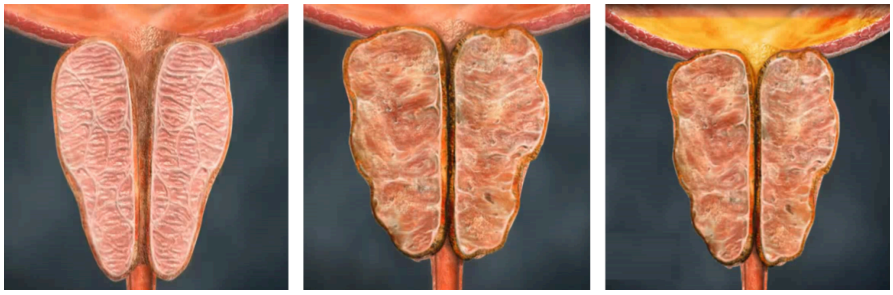

Figure 1.5. Normal Prostate Gland (left); Cancerous Prostate Gland (middle); Prostatic Obstruction (right) [9].

### 1.2.4. Diagnosis

Prostate Spesific Antigen (PSA) is a chymotypsin- like serine protease [10] that is specifically produced by the prostate gland. Hence it is employed as a biomarker for the detection of prostate cancer [11]. Although there is no definite borderline between a normal and an abnormal PSA level, >4 ng/mL has adopted as a positive test for screening programs in the US. When patients show more than 4 ng/mL of PSA concentration in plasma, prostate cancer can be a potential risk [12]. PSA screening has numerous limitations. Many men who do not have prostate cancer may screen positive PSA results and require a biopsy for diagnosis. On the other hand, some men with prostate cancer do not have elevated PSA levels. PSA secreening usually causes false alarms because high PSA levels can also be triggered by prostatitis or benign prostatic hyperplasia. Notwithstanding PSA screening is acknowledged to be successful in reducing prostate cancer mortality [13].

Digital Rectal Examination (DRE) involves the investigation of the prostate gland with respect to its size, shape and texture with a finger through the rectum. DRE is still reliable since most prostate cancer stems from there despite the fact that only the posterior part of the prostate gland is detectable by DRE. Inspections of irregular lumps and shapes, and increased stiffness reveal potential prostate cancer risk [6].

Most prostate cancer cases can be determined *via* PSA or DRE but some are finally scrutinized with the help of ultrasound or magnetic resonance imaging. Conslusively, the type, stage and grade of prostate cancer under microscopy are confirmed by prostate

biopsy. Gleason score, a grade showing the stage of prostate cancer, can be determined *via* transrectal ultrasound (TRUS) and transrectal biopsy [14].

There are basicly four stages in the progress of PC (Figure 1.6).

- Stage I: The Gleason level is low and DRE is normal; then it is accidentally found out during false surgeries, such as BPH.
- Stage II: Observable; cancerous tumor spreads over only in the prostate, detectable during DRE.
- Stage III: Carcinoma has evolved outside of the gland and started to invade seminal vesicles.
- Stage IV: More advanced stage; metastasis occurs and the tumor continually invades other parts of the body [15].

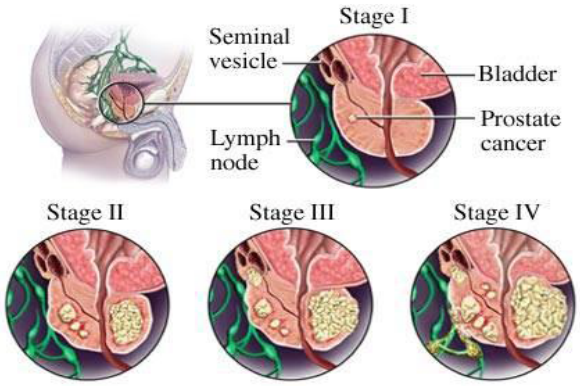


Figure 1.6. Progression of Prostate Cancer [15].

### 1.2.5. Current Treatment of Prostate Cancer

Depending on the patient's situation such as age, health and life expectancy, the treatment options for men with prostate cancer include:

- Active Surveillance
- Prostetoctomy
- Radiation therapy

- Cryosurgery (cryotherapy)
- Hormone therapy
- Chemotherapy
- Radiopharmaceuticals
- Immunotherapy

These treatments are generally used one at a time, although in some cases they may be used in combination [6].

Active Surveillance is the strategy providing carefully monitoring for signs of PC progression. It is usually preferred for patients with a life expentancy of less than ten years in order to prevent from side effects until the quality of their life is reduced; because for these patients, it is very probable that the cause of their death will not be prostate cancer. PSA and DRE are usually employed regularly along with a recurring biopsy of the prostate once a year and then at specific intervals.

Local therapy includes nonpharmaceutical approaches to PCa treatment, such as prostatectomy, radiation therapy, and cryotherapy, which are convenient for early-stage patients. Prostatectomy is the removal of the prostate gland and seminal vesicles. It is employed for the first-line therapy for first and second stage-prostate cancer patients if they are younger than 70 and otherwise healthy. Radiation therapy can be carried out in two alternative procedures depending on the location of the radiation source: external beam radiation therapy (outside the body of patient); and brachytherapy (implanted into the tumor tissue). Cryotherapy is the strategy that proposes the freezing of the prostate gland and sometimes seminal vesicles with liquid nitrogen.

Local prostate cancer in early stages can be cured with local therapy strategies; however, for advanced cases, spesifically cases with metastatis, death is an inevitable consequence if not sufficiently controlled. These patients are generally treated with hormone therapy [16].

Chemotherapy, in which cytotoxic agents are administered in order to destroy the cancerous cells, is the last option for later stage diseases because cytotoxic agents

simultaneously damage the normal cells, leading severe side effects. Still, the taxane drugs such as docataxel and cabazitaxel have been shown to improve median survival time when administered in combination with prednisone [17].

Radiopharmaceuticals targeting bone metastatis such as Strontium-89, Samarium-153 and Rhenium-186 were applied only for pain relief. However, Radium-223 has shown an amelioration of overall survival of 19 weeks [18]. Alpharadin (Radium-223 chloride) causes comparably less damage to normal tissue than other radiopharmaceuticals. Therefore nowadays it is likely to be approved by the US Food and Drug Administration (FDA) and is expected to be launched in 2013.

Immunotherapy aims to stimulate the immune system of a patient in order to destroy the cancer cells after interference with vaccines [6].

### 1.3. Androgens and Hormone Therapy

About 80% of prostatic tumors are based on elevated levels of androgens because androgen stimulates the cellular proliferation of human prostate cancer. Therefore, deprivation of androgen level is a good strategy in order to overcome advanced PCa.

There are two targets which are related to androgen stimulation:

- Blockade of the AR by AR antagonists
- Interruption of androgen biosyntheses (androgen deprivation therapy (ADT))

For the latter one, several nodes in androgen biosynthesis system are significant; yet not all of them are conventient targets.

- The hypothalamus-pituitary-adrenal axis should be kept off because ACTH controls the biosynthesis of glucocorticoids, mineralocorticoids as well as androgens, leading to severe side effects due to the hormonal imbalance [19].
- Deprivation of androgen biosynthesis *via* interference with the hypothalamus-pituitary-testes axis is feasible.

- Castration can eradicate androgen production from testes; however a small amount of androgens will be definitely produced by adrenal glands or *via de novo* path.
- Utilization of GnRH analogs results in decreasing the Gn secretion *via* either antagonizing the GnRH receptors in pituitary (antagonist) or desensitizing the gonadotrope cells (agonist). Agonists do not immediately dissociate from the GnRH receptor. Consequently, initially there is an incline in FSH and LH secretion, which is called "flare effect"; however after about ten days, a significant hypogonadal effect is obtained *via* receptor downregulation by internalization of receptors.
- Enzymes in androgen biosynthesis are also favorable targets, such as CYP17A1. CYP17A1 is in the charge of conversion of progesterogens into androgens and its inhibiton diminishes the plasma testosteron level to less than 1 ng/dL [20].
- 5α-reductase inhibitors for intervention of DHT biosynthesis are utilized for benign prostatic hyperplasia (BPH) but not for PCa because of the fact that testosterone as the DHT precursor causes proliferation of cancer cell [21].

The production of androgens is coordinated by the hypothalamic-pituitary-gonadal-adrenal axes. Hypothalamus is a vital modulator and it secretes several hormones directly targeting the pituitary gland such as gonadotropin-releasing hormone (GnRH, also known as luteinizing hormone-releasing hormone - LHRH ) and corticotropic-releasing hormone (CRH). GnRH and CRH stimulates the production of gonadotropins (Gn) in testicles and the adrenocortico-tropic hormone in adrenal glands from anterior pituitary, respectively. After binding to the corresponding receptors, cholesterol is synthesized. The biosynthesis of androgens starts with cholesterol, which is also produced during the metabolism of fatty acids. The side chain of cholesterol is cleaved by the enzyme called CYP11A1 (cholesterol side-chain cleavage enzyme, P450scc), and pregnenolone is formed. Pregnenolone is converted into progesterone after an additional dehydrogenation step which is catalyzed by 3β-hydroxysteroid dehydrogenase/Δ4-5 isomerase (3β-HSD). CYP17A1 hydroxylates the mineralocorticoid precursor substrates, pregnenolone and progesterone, at their $17^{th}$ carbons to form 17α- hydroxypregnenolone and 17α-progesterone, respectively. The consequent C17-hydroxylated substrates are used for either glucocorticoid biosynthesis or

for the 7,20 lyase reaction to produce androgens dehydroepiandrosterone (DHEA) and androstenedione (Figure 1.7) [19].

Finally, dehydroepiandrosterone (DHEA) and androstenedione produce testosterone and dihydrotestosterone (DHT), which is the last step of androgen biosynthesis. Approximately 90% of androgens are produced in the testes and less than 10% in the adrenals. Besides, androgen formation is likely to be carried out inside PCa *via de novo* androgen biosynthesis from adrenal steroids or even cholesterol, and this is a major reason for castration resistant prostate cancer. The biosynthesis inside cancer cell depends on CYP17A1, as well. Therefore, inhibition of CYP17 can entirely block androgen production, preventing further proliferation of PCa cells.

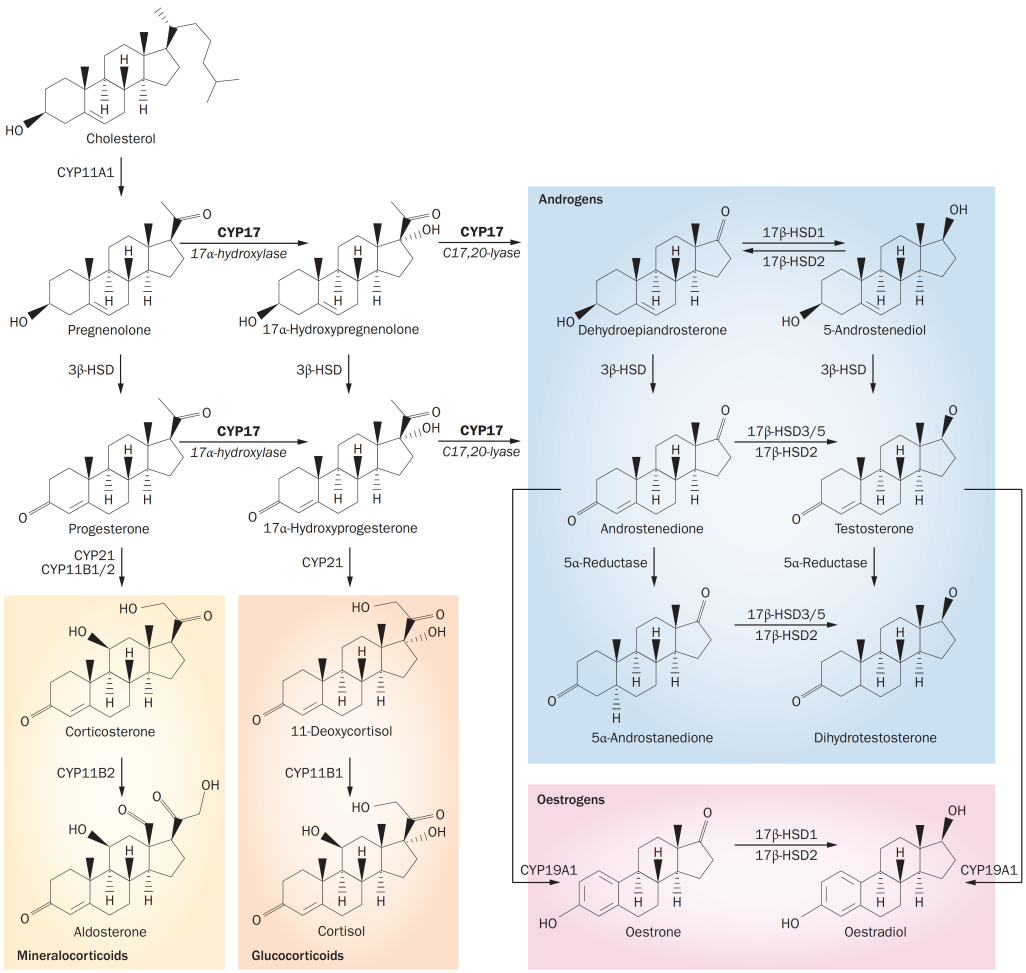


Figure 1.7. Biosynthetic pathway for androgen production [22].

Androgens subsequently bind to the androgen receptors (AR), which are overexpressed in PCa cells. AR which floats in the cytoplasm is a member of steroid and nuclear receptor superfamily. It resembles to other steroid receptors in terms of its structure and function and acts as an intercellular transcription factor. After androgens bind to AR, a series of conformational changes occur, resulting in dimer formation and phosphorylation. Above-mentioned ARs consequently translocate into the nucleus and bind to the corresponding androgen response element which is located in the promoter region of the target gene. Involvement of other transcriptional coregulators stimulates the transcriptional machinery and triggers the expression of AR regulated genes and causes mitogenic effects in PCa cells, eventuating in proliferation of cancer cells [23].

### 1.4. Specifying Target Enzyme: CYP17

The cytochrome P450 superfamily of heme monooxygenases is involved in a variety of difference physiological activities such as drug/xenobiotic metabolism or hormone biosynthesis [19]. The human cytochrome P450 monooxygenase 17α-hydroxylase / 17,20-lyase (CYP17A1) is positioned at a critical juncture in human steroidogenesis because the 17α-hydroxylase activity of CYP17A1 is necessary for the production of glucocorticoids and both hydroxylase and 17,20-lyase activities of the enzyme are required for androgenic and oestrogenic sex steroid formation [24]. Therefore, understanding the multi-functional biochemistry of CYP17A1 enzyme is significant in order to figure out the catalytic activity, substrate and reaction selectivity; and consequently to treat prostate and breast cancers, subfertility, blood pressure and other diseases [19].

CYP17A1 is a microsomal cysteinato-heme enzyme containing a heme group which is covalently linked to the protein through the sulfur atom of proximal cystein amino acid. The enzyme is coded by the gene CYP17, which is located in chromosome 10q24.3 and it consists of 508 amino acids, with a nearly 57 kDa of weight [23]. Since CYP17A1 is a microsomal P450 and binds to the endoplasmic reticulum, its crystal structure was not determined until very recently due to the difficulties in crystallization; however, studies on computer-generated models prefigured the protein or active site structures [25].

According to the modeled structure dissertated in Emre Özdemir's thesis, the active site has a mono-lobed, hydrophobic binding pocket, which means that both 17α-hydroxylase / 17,20-lyase reactions catalyzed by the enzyme occurs in one active site [25].

- The heme, which is located as the floor of the active site of the monolobed enzyme, is the reactive center that serves to activate the molecular oxygen and trigger the oxidation of substrates.
- They rise ~60º with respect to the heme and lean on I helix.
- The unique intermolecular hydrogen bond occurs between Asn202 and the hydroxy or carbonyl oxygen substitution located on $C_3$ (Figure 1.8).

Catalytic activity of the enzyme depends on residue T306, which is a proton donor. The location of the corresponding amino acid is homologous to another cytochrome P450 crystal structures. The proton of hydroxy group on threonine amino acid allows 17α-hydroxylase reaction by participating in dioxygen protonation and O-O bond cleavage, and discharge of products [24].

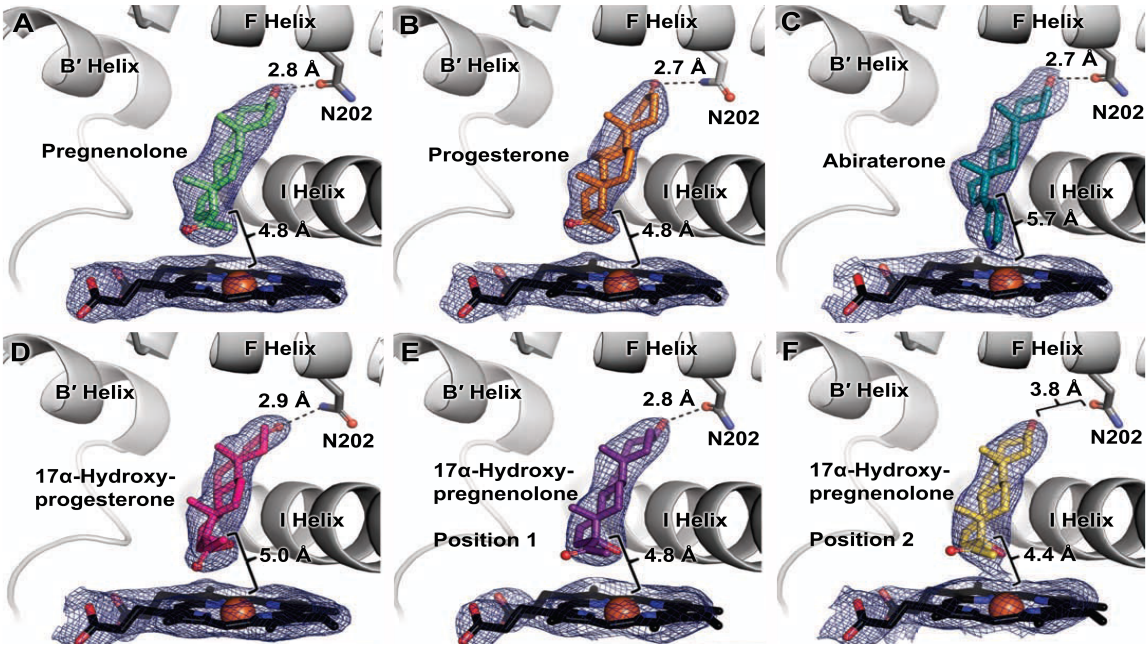


Figure 1.8. X-Ray Structures of CYP17 with its natural substrates and abiraterone [19].

## 1.5. Steroidal CYP17 Inhibitors

Since the crystal structure of CYP17 has been absent for a long term, the inhibitory studies have used the natural substrates (pregnenolone and progesterone) as scaffolds of potential drug candidates. Abiraterone acetate, for instance, is a first-in-class FDA-approved prodrug for CYP17 inhibiton. Pregnenolone scaffold with an extra Δ16,17 double bond as well as 3-pyridyl substitution as the heme coordinating group (Figure 1.9) constitutes the abiraterone structure.

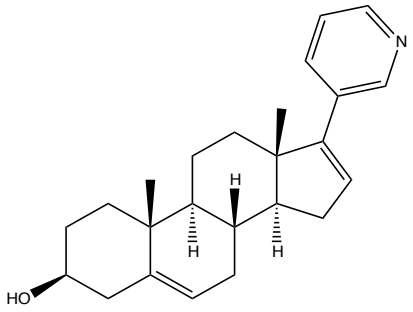


Figure 1.9. The structure of Abiraterone [23].

Abiraterone acetate is an orally-administered drug and strongly inhibits both 17α-hydroxylase / 17,20-lyase activities of CYP17 with $IC_{50}$ values of 4 nm and 2.9 nm, respectively. The additional Δ16,17 double bond reveals a 12-fold more irreversible inhibition effect. Although abiraterone has shown no affinity for CYP19 and 5α-R steroidal receptors; it is a moderate inhibitor for CYP11B1 and CYP11B2.

Also it potentially interferes with hepatic CYP1A2, CYP2D6, and CYP2C8 and moderately inhibits CYP2B6, CYP2C9, CYP2C19, CYP3A4 and CYP3A5. Besides, 3β-hydroxysteroid dehydrogenase which is involved in the conversion of DHEA and adrostenediol to androstenedione and testosterone is inhibited by abiraterone acetate, contributing to its anti tumor effect. According to the recent literature, it is demonstrated that abiraterone can interfere with AR and has an ability to inhibit AR translocation to the nucleus [23].

Abiraterone effectively binds to the CYP17A1 active site heme iron (Figure 1.10) [19] and systematically prevents androgen production; nevertheless, by doing so, the pool of precursors for mineralocorticoid generation is increased and CYP17A1-mediated formation of glucocorticoids is interrupted (Figure 1.7). Consequently, this steroid imbalances lead to hypertension, hypokalemia, and adrenocortical deficiency in PCa patient treated with abiraterone, requiring additional treatments. Moreover, accumulation in mineralocorticoid levels related to the complete inhibiton of CYP17A1 might promote the flow of androgen precursors through a "backdoor" androgen biosynthesis pathway, serving a conceivable escape gate which is likely to result in cancer progression.

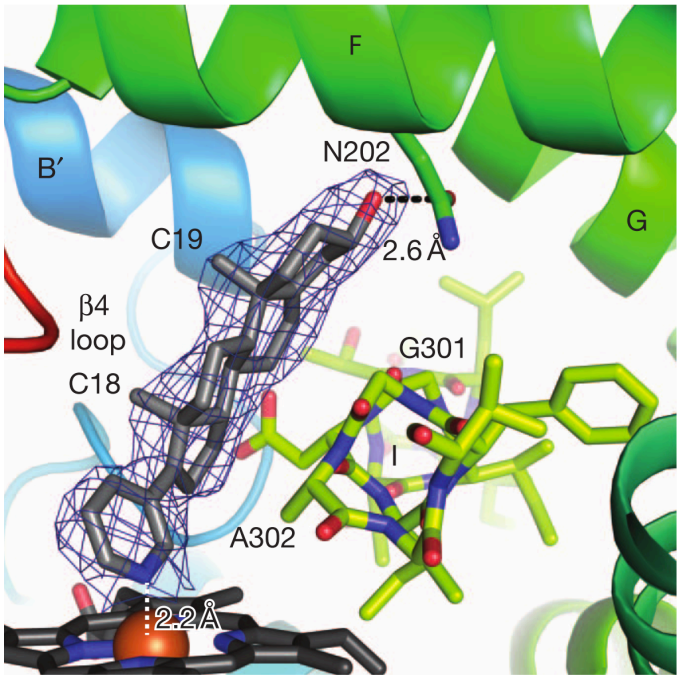


Figure 1.10. The X-ray structure of abiraterone with CYP17A1 [23].

TOK-001 (Gleterone, Figure 1.11), on the other hand, is a novel inhibitor of CYP17A1 that is currently undergoing clinical trials. There is only a minor structural difference between abiraterone and gleterone: Substituion of 1-benzimidazolyl group whose 1-N is attached to the pregnenolone scaffold instead of 3-pyridyl group of abiraterone. However, gleterone has shown 2.7-fold more potency in an assay which uses CYP17A1 expressed from *Escherichia coli*. Gleterone demonstrates a similar binding

mode for CYP17 as abiraterone, with the exception that it occupies an additional hydrophobic pocket (Figure 1.12).

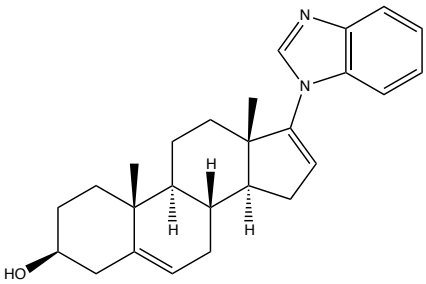


Figure 1.11. Structure of gleterone [23].

According to the phase I clinical trial data for gleterone, 11 out of 49 PCa patients demonstrated 50% or more deprivation in PSA levels. Moreover, the multi-mechanism of gleterone is still well tolerated even at elevated dose of 2600 mg/day with only a few non-serious side effects, such as fatigue, nausea, and diarrhea.

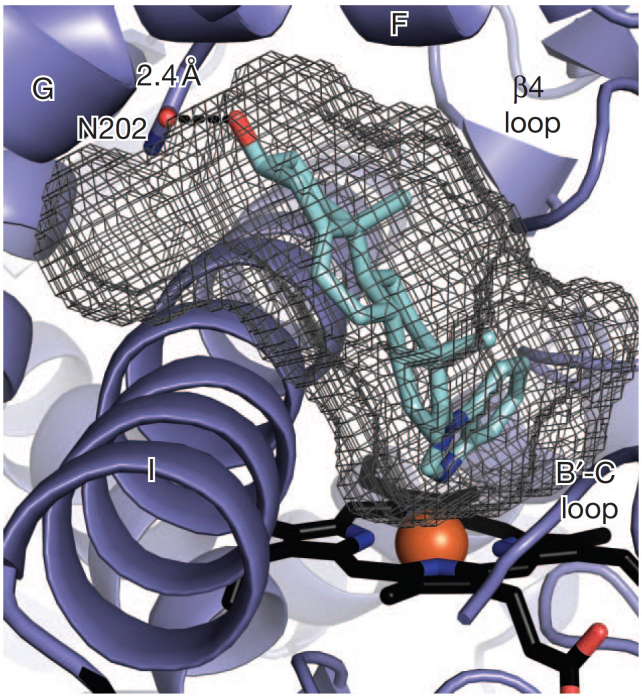


Figure 1.12. X-Ray structure of CYP17A1 with gleterone [24].

### 1.5.1. Structures of CYP17 with Abiraterone and TOK-001

Understanding CYP17A1 multifunctional biochemistry and various steric and hydrogen bonding features that will facilitate a better interpretation of the enzyme's dual hydroxylase and lyase catalytic capabilities and assist in rational drug design.

Abiraterone and TOK-001 covalently bind to the heme iron with the nitrogen of the C17 pyridine or benzimidazole, respectively. As reported by a recent spectral binding data, titrations of CYP17 with both inhibitors reveal progressive shifts in the ultraviolet-visible difference spectrum, confirming the nitrogen binding to the heme iron (type II interaction) (Figure 1.13). The similar titration protocol applied to natural substrates pregnenolone and progesterone and has demonstrated a decline in absorbance at 419 nm and an incline in 385 nm, indicating water displacement from heme iron (type I interaction)[24].

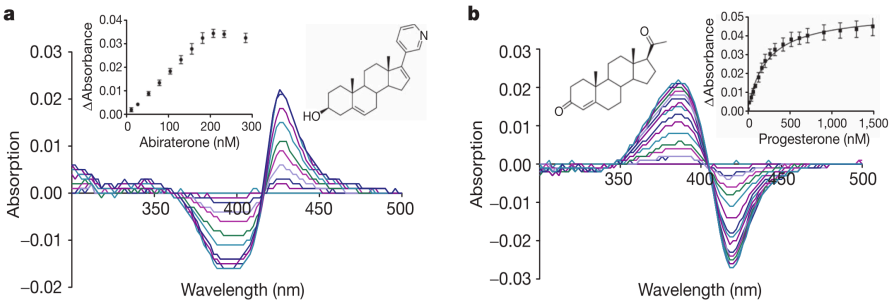


Figure 1.13. Titration of CYP17A1 with abiraterone and progesterone [24].

As stated before, both inhibitors have shown similar binding mode for CYP17A1; they almost overlap with each other.

- The steroidal scaffolds rise at an angle of 60º from the plane of heme
- The unsubstituted α-faces of steroidal cores lean on the I helix, and form a highly integrative hydrophobic planar surface, except the fact that gleterone occupies an extra hydrophobic pocket.
- The 3β-OH groups of both inhibitors make hydrogen bond with N202 in the F helix (~2.6 Å and ~2.4 Å, respectively).

This unique direct hydrogen bond between inhibitors and the protein, actually, is a part of an extensive hydrogen bonding network (Figure 1.14). In abiraterone, and similarly in TOK-001, N202, E305, several conserved water, R239 and the backbone carbonyl of G297 comprise this network. These hydrogen bond interactions are evocative of the interactions preserved in the adrogen, oestrogen, glucocorticoid, mineralocorticoid and progesterone receptors. The ligand recognition by hormone receptor and CYP17A1 selectivity over pregnenolone, progesterone and their 17α-hydroxy metabolites are likely to be stemmed from these interactions. Remarkably, TOK-001 is both CYP17A1 inhibitor and androgen receptor antagonist, and the similarity of binding modes may be the origin of the dual mechanism of action of TOK-001 [24].

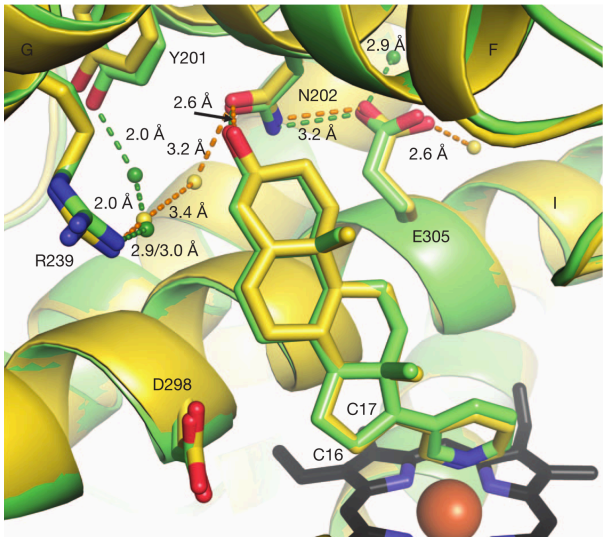


Figure 1.14. Hydrogen bonding network with abiraterone [24].

The final feature of CYP17A1 which must be highlighted is that pregnenolone (Δ5,3-ol steroid) is hydroxylated by CYP17 only at 17$^{th}$ carbon whereas progesterone (Δ4,3-keto steroid) is hydroxylated at 17$^{th}$ carbon as the major product and also at 16$^{th}$ carbon as the minor product, constituting 10-30% of total hydroxylated metabolites (Figure 1.15) [19]**.** There are some functional and structural evidences for an artificial A105L mutation demonstrates a reduction of the minor 16α-hydroxyprogesterone metabolite [24]. The A105L mutation implies an additional bulk due to the substitution of leucine instead of alanine at the position 105. Therefore this steric rationale is consistent with the location

of A105L in the active site facing the β-face where this additional bulk is likely to reduce the steroid motion within active site, providing a perspective for hydroxylase regioselectivity [19].

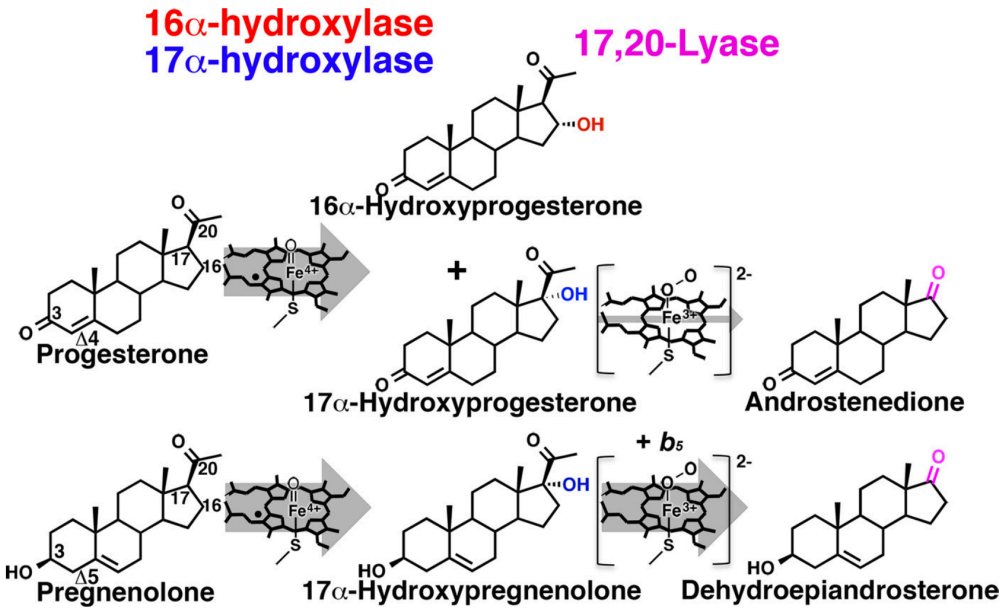


Figure 1.15. Summary of human cytochrome P450 17A1 reactions [19].

### 1.6. Non-Steroidal CYP17A1 Inhibitors

Although the steroidal CYP17A1 inhibitors abiraterone and gleterone are used in clinics or in the late clinical developments, respectively, there are some drawbacks associated with their steroidal scaffolds:

- Poor absorption
- Low bioavailability
- Low first-pass effect when orally administered
- Affinity for other steroid receptors
- Relative short half-life
- Poor acid stability

Therefore, non-steroidal CYP17A1 inhibitors are considered as being advantagous alternatives and some of them are anticipated to be more advanced than current steroidal drugs in use (Figure 1.16) [23].

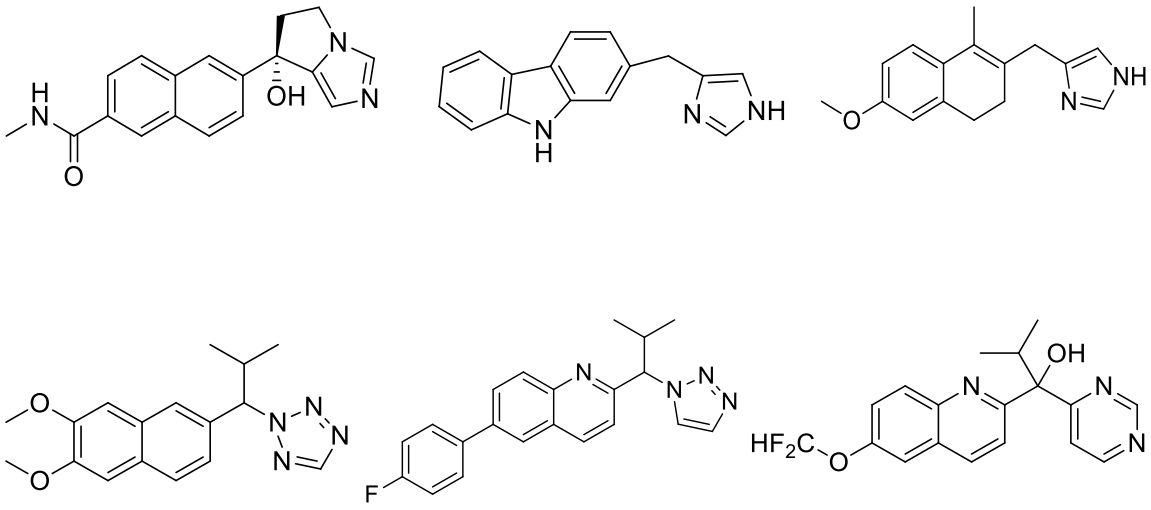

Figure 1.16. Examples on non-steroidal inhibitors [16].

A lead compound was discovered by Armutlu *et al.* using *in silico* and experimental methods (Figure 1.17) [26]. The lead compound can be used as a lead for discovery of more active nonsteroidal CYP17 inhibitors, which constitutes as the basis of this dissertation project which will be explained in details in Section 1.8.

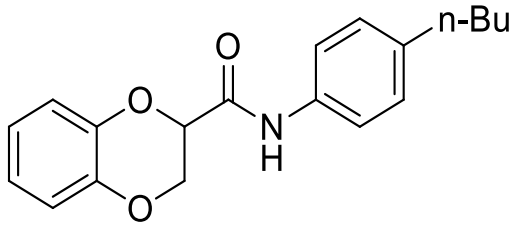

Figure 1.17. The structure of lead compound [26].

## 1.7. Integrated Small Molecule Drug Discovery and Development

Discovery and development of small molecule cancer drugs entails an exchange and network between many basic disciplines, such as genetics, bioinformatics, cell and molecular biology, tumor biology, pharmacology, pharmacokinetics and metabolism, medicinal chemistry, organic chemistry and experimental medicine. Preclinical small-molecule drug-development is represented as a linear process, starting from the target identification to lead generation, to highly optimized lead compound, to preclinical profiling, and finally to drug candidates for clinical assessment (Figure 1.18) [27].

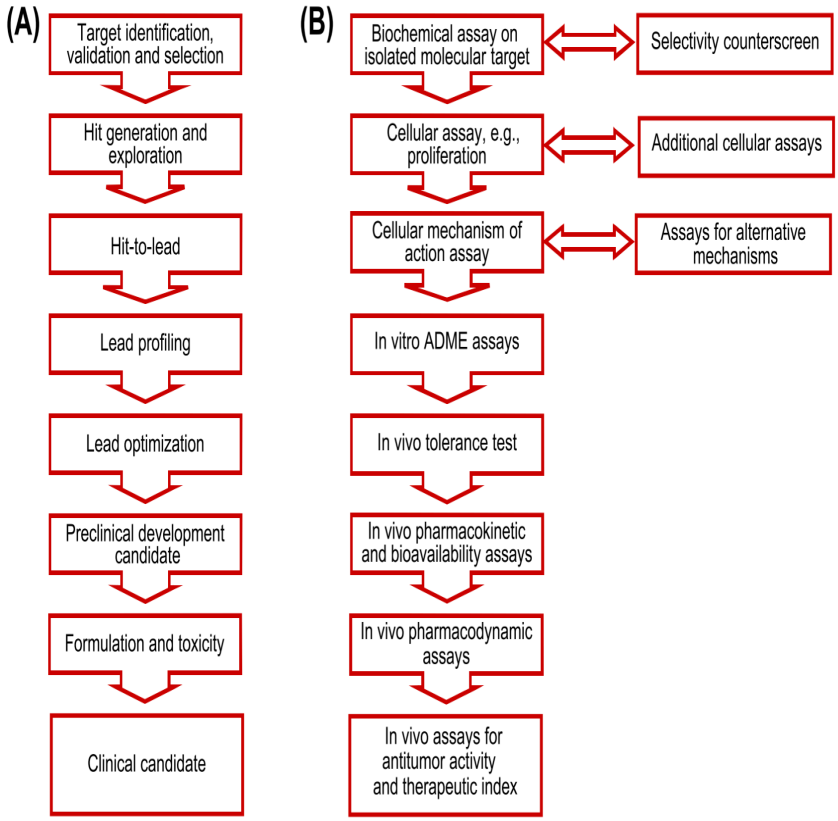


Figure 1.18. Schematic depiction of (A) the stages of drug discovery from target identification to clinical candidate; (B) a typical biological test cascade [27].

Although this scheme is practical and not completely inaccurate, a more comprehensive framework proposes an iterative and integrated diagram which is

contemporary with modern drug discovery. This integrated model proposes that structural biology and chemical biology interconnect with the multiple elements of the drug discovery process. Depicting the process as a loop instead of a linear scheme can strongly emphasize that different disciplines can build up a network, accelarating the path to the clinic with the advantages of feed-back and feed-forward between various stages.

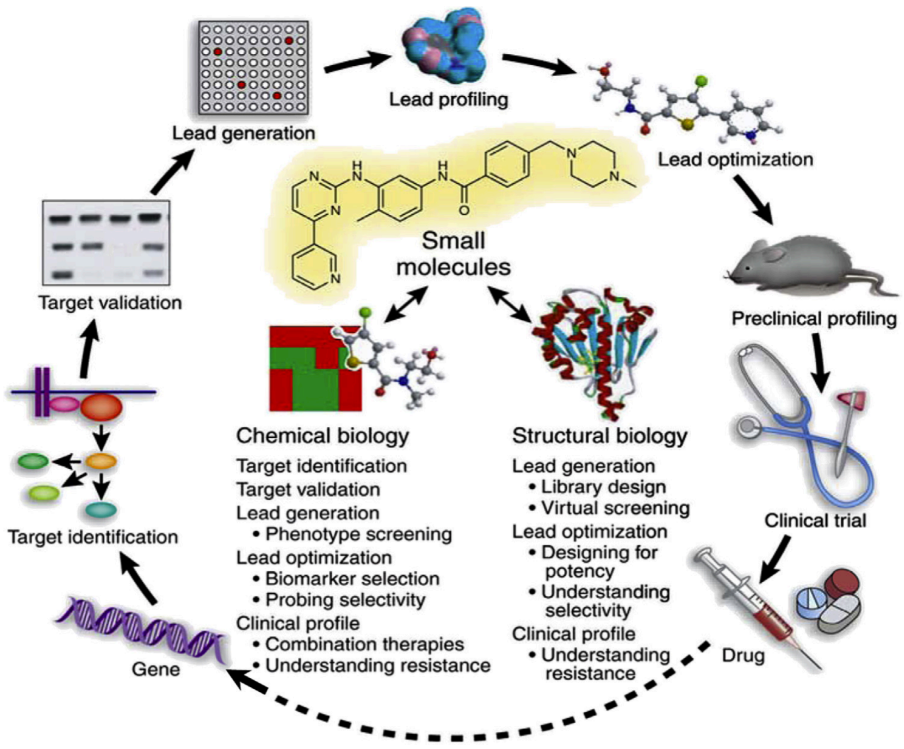


Figure 1.19. Integrated Small-Molecule Drug Design and Development [27].

### 1.7.1. Drug Optimization

A chemical compound introduced as a small-molecule lead requires a comprehensive modification in order to be optimized before being lauched as a clinical candidate. The optimization parameters include pharmaceutical properties; potency and specificity for the mechanism of action on the target biomolecule and in cells; relevant pharmacodynamic effects *in vivo* as well as tolerability and efficacy against tumors in appropriate *in vivo* models [16]. Overall preclinical discovery of a oncology drug typically requires 10-15 years, starting from target identification to its approval [27].

### 1.7.2. Structure-Based Drug Design

Structure-based drug design is based on insight of the three dimensional structure of the target protein acquired through X-Ray crystallography, NMR spectroscopy or computer-based modeling. If a crystal structure of a target is not determined, experimental structure of corresponding target can establish a homology model. Candidate drugs that are likely to bind with high affinity and selectivity to the target can be designed through employment of the structure of the biological target (Figure 1.20). There are basicly three categories for the prevalent methods for structure-based drug design. The first technique is called *virtual screening* and it involves the identification of new ligands for the corresponding receptor through the investigation of large database libraries with the three dimensional structures of small molecules. Then in order to detect the fitting to the binding pocket of the receptor using fast approximate docking programs. A second technique is known as *de novo design of new ligands*. This technique includes the development of ligand molecules within the restraining boundary of the binding pocket by assembling small fragments in a stepwise manner.. A third technique is the *optimization of known ligands* through assessment of proposed analogs within the binding cavity [28].

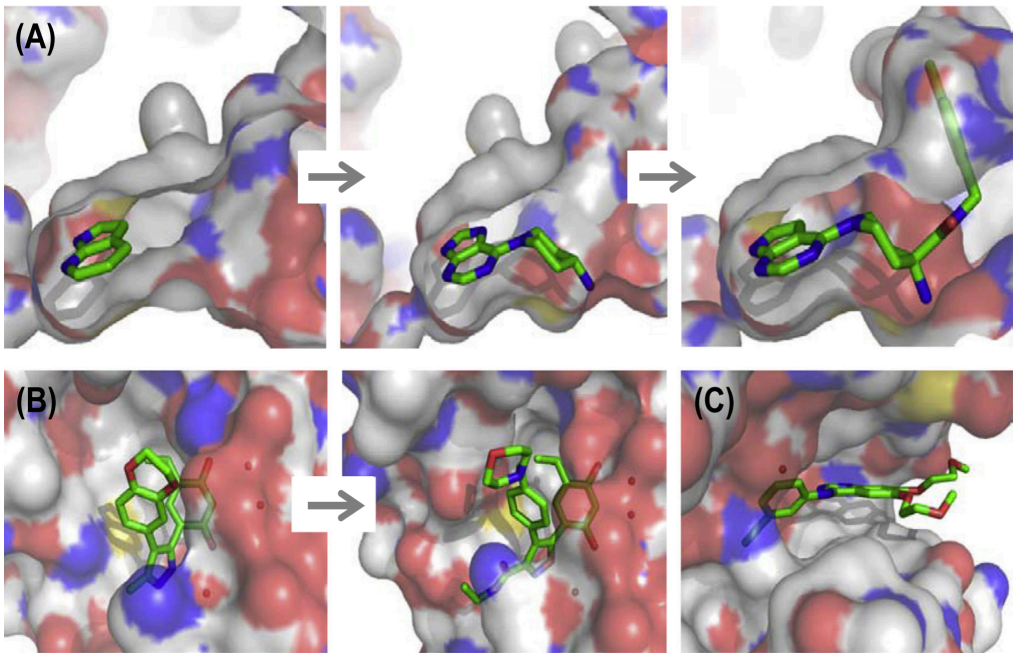


Figure 1.20. Examples of structure-based drug design [27].

## 1.8. CYP17A1: Inhibitory Studies

Prior to the present M.S. study, structure-based drug design (SBDD) approach was successfully applied using a computer-generated model structure of CYP17 enzyme in search of nonsteroidal CYP17 inhibitors. Since the crystal structure of CYP17 was not available when the project started, a homology model was developed [26].

23 candidates out of ~2,000,000 compounds were determined by an initial virtual screening provided by Ambinter SARL and they were subjected to the docking and binding energy calculations by the research group of Prof. Metin Türkay from Koç University. ADMET (adsorption, distribution, metabolism, elimination and toxicity) studies, Quantitative Structure Activity Relationship (QSAR) studies, IC50 measurements were also tested. Vectors with human CYP17 (pKU-1) were transfected into human embryonic kidney cell line (HEK 293T) *via* calcium-phosphate precipitation method [28]. The inhibitory effect of the candidate compounds were evaluated by Acetic Acid Release Assay method. Biological tests were performed by the research group of Assoc. Prof. İ. Halil Kavaklı from Koç University. Computational and biological tests introduced two compounds, N15 (nonsteroidal) and S3 (steroidal), with $IC_{50}$ values 35.65 μM and 46.30 μM, respectively (Figure 1.21).

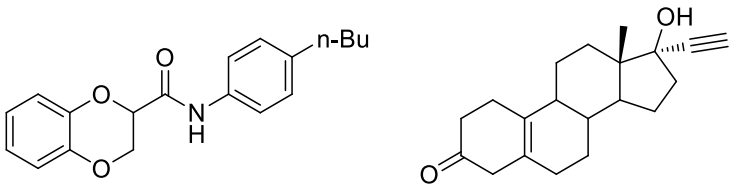


**N15** **S3**

Figure 1.21. Structures of non-steroidal (left) and steroidal (right) lead compounds.

As stated in literature, steroidal inhibitors have demonstrated comparably weaker efficacy than non-steroidal (steroidomimetic) ones due to their drawbacks. Therefore non-steroidal inhibitors are expected to be superior to steroidal ones. Consequently, N15 was selected as the lead molecule. Docking configuration of the lead compound is depicted in Figure 1.22.

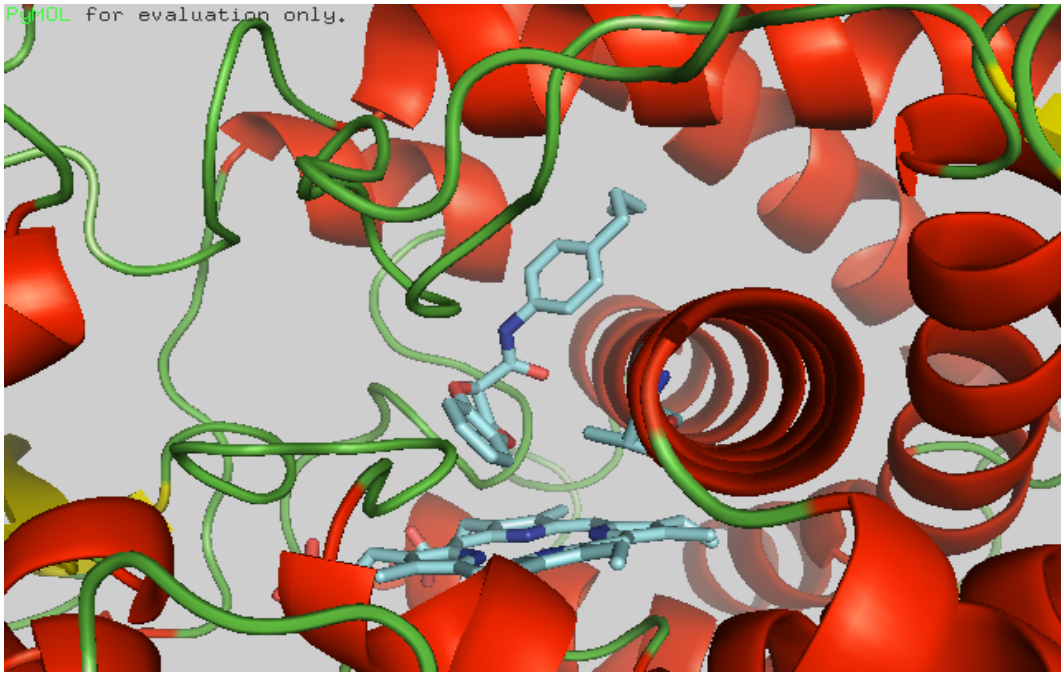


Docking Energy: -9.38 kcal/mol

Binding Energy: -7.45 kcal/mol

$IC_{50}$: 35 μM

Figure 1.22. The structure of lead compound for CYP17A1 inhibitory studies.

Throughout the project, several compounds which were synthesized upon this modification strategy demonstrated better binding and docking energies, and improved percent inhibition and $IC_{50}$ results. Table 1.1 summarizes the previously synthesized lead compound derivatives, their docking configurations and binding-docking energies. Remarkably, a novel compound (Table 1.1, bottom) with a isoquinoline fragment having amide juncture at its fifth position on the left-hand side exhibited 100% inhibition at 5μM concentration.

Table 1.1. Previosly reported lead compound derivatives.

| Structure | Docking Configuration | B.E. (kcal/mol) | D.E. (kcal/mol) |
|---|---|---|---|
| 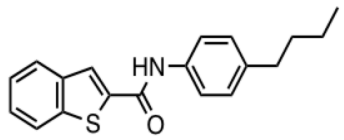 | 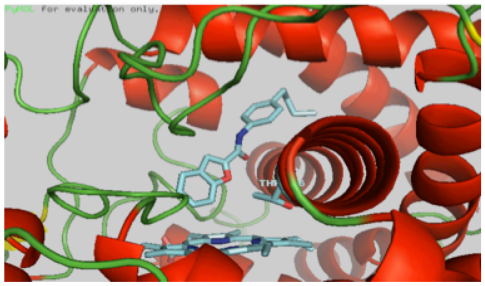 | -7.26 | -9.39 |
| 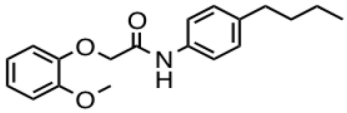 | 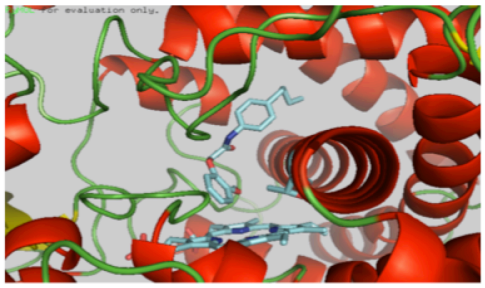 | -8.16 | -11.30 |
| 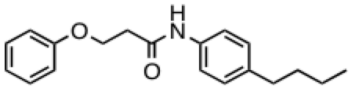 | 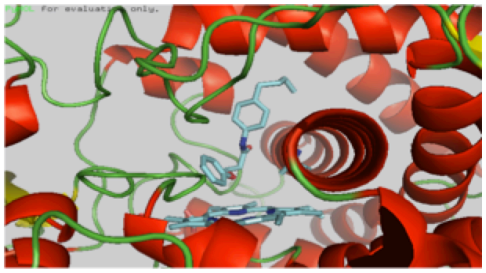 | -8.26 | -11.13 |
| 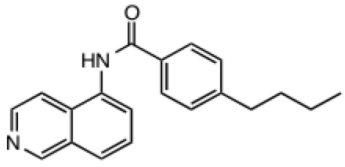 | 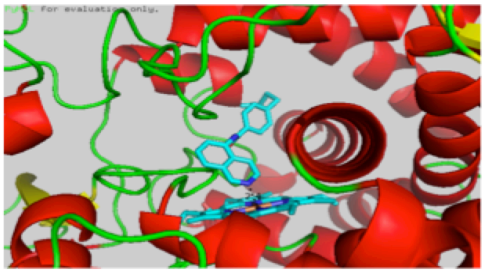 | -9.15 | -11.22 |

# 2. OBJECTIVES

In contemporary drug discovery and development, importance is given on the employment of multiparameter optimization as early as possible. This work aims to investigate the interaction of each fragment and each particular atom on the lead compound with the targeted enzyme in order to design and synthesize more potent and efficient derivatives. Throughout the study, the lead compound has been approached as a compound having two parts: left-hand side and right-hand side: 2,3-dihydro-1,4-dioxine ring as the left-hand side; *n*-butyl alkyl chain bearing phenyl unit as the right-hand side; and an amide group as a juncture of these two fragments. Figure 2.1 summarizes the fragments and atoms on the lead molecule.

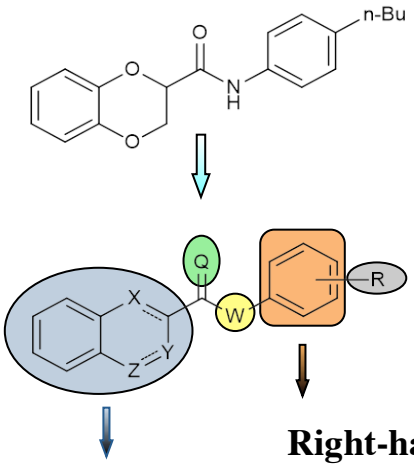


Where, X, Y, and Z : C, N, O
W : NH, O
Q : O, S
R : $C_1 - C_9$ alkyl or branching alkyl

Figure 2.1. Modification Strategy for lead compound.

*Left-Hand side* comprises of aromatic planar unit interacting with planar heme. In CYP enzymes, an iron atom is chelated by the quadridentate protoporphyrin whereas cysteine, the proximal ligand of iron, is coordinated to the whole heme. The sixth

coordination position is reserved; rendering here a reactive center. Therefore occupation of this specific position wih heme-coordinating ligands will presumably provide a competitive reversible inhibiton of the enzyme. In this respect, modification can be performed in several ways such as insertion of N, O, or S atoms into the aromatic ring at the various positions due to their coordinating ability to the heme iron. In this project, preceding modifications on lead molecule endeavored to synthesize compounds containing naphthalene, quinoline, isoquinoline, benzofuran, and benzothiophene fragments. As stated in recent literature, heterocycles containing $sp^2$ hybridized N atom were the most effective heme-coordinating groups [23]. Considering that the most active lead compound derivative (Table 1.1) involves an isoquinoline fragment, the modification will be mainly focused on the synthesis of isoquinoline derivatives.

*The right-hand side* can be modified by changing the chain lenght of n-butyl group or introducing branched alkyl chains. Other moieties such as methoxy- or floro- substituted naphthalene groups or ester substituted phenyl group may provide a key hydrogen bonding with hydroxyl group of Thr306 residue on I helix which is responsible for O-O bond cleavage.

Modification of *the amide functionality* of the lead compound is an alternative route. However, carbonyl oxygen and –NH- group are capable of acting as both H-donor and H-acceptor having a good ability to form hydrogen bonds. Moreover, since the amide group is stable and neutral, an in-depth analysis of Comprehensive Medicinal Chemistry database has revealed that carboxamide group appears in more than 25% of known drugs [29]. Thus, retainment of the amide group is preferential, but as an additional derivative carbonyl oxygen can be replaced with sulfur atom because of its potential heme-coordinating ability.

# 3. RESULTS AND DISCUSSION

In this work, syntheses of novel CYP17A1 inhibitors which are designed as the derivatives of lead compound previously reported are endeavored. The modification strategy is divided into three main categories which will be explained in detail in the following sections:

(i) Modification on hydrophobic tail: This strategy involves the modification of hydrophobic group on the right-hand side by replacing *n*-butyl tail with branched alkyl tail.
(ii) Modification on isoquinoline ring: This section comprises of the modification of left-hand side *via* altering the position of $sp^2$ hybridized N atom on isoquinoline ring,
(iii) Miscellaneous derivatives.

## 3.1. Modification of Hydrophobic Tail on the Right-Hand Side

In the preceding studies, docking energy and binding energy calculations of branched alkyl substituted naphthalene derivatives showed better results over linear alkyl substituted drug candidates [30]. Since the most-active lead compound derivative throughout the project involves a 5-isoquinoline ring as the left-hand side, the aim of the current modification strategy is to synthesize a lead derivative of 5-isoquinoline with a branched alkyl substituent on the right hand side. (Figure 3.1). Therefore, the synthesis of branched alkyl substituted phenyl ring was targeted which would then be completed by coupling with commercially available 5-isoquinolines.

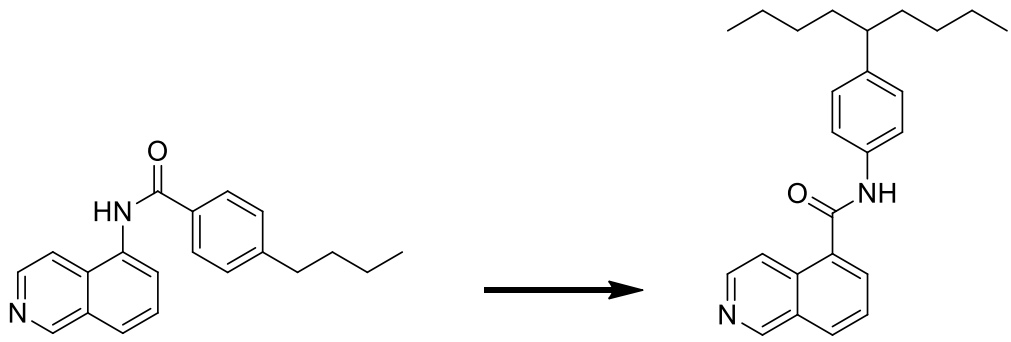


Figure 3.1. Modification strategy for the most-active lead compound derivative.

The general strategy followed in the synthesis of branched alkyl substituted phenyl rings previosly described in Turgay Yildirim's thesis [31]. The same procedure was applied for the synthesis of 4-(nonan-5-yl)aniline:

Ethyl 4-aminobenzoate **1** was used as the starting material. First, aromatic amine protection was done to prevent the side reactions in the next step. Protection of amine was achieved with $Ac_2O$ in water and white colored product **2** was obtained in 93% yield by pouring reactant in icy water and precipitating. Then n-butyl lithium (n-BuLi) was used as a nucleophile which attacks the carbonyl of the ethyl ester to make branching on the phenyl ring. n-BuLi is also a strong base therefore THF was used as solvent and reaction was carried out -78$^{o}$C to prevent any side reactions. n-BuLi amount used in this reaction was more than two-fold of ethyl ester due to the possibility of hydrogen abstraction from the amide. After the double addition of n-BuLi to the ethyl ester the tertiary benzyl alcohol **3** obtained. Then reduction of alcohol was carried out by $Et_3SiH$ and $Et_2O.BF_3$ in dry dichloromethane (DCM) as solvent. In the next stage deprotection reaction was carried out by refluxing at 70$^{o}$C with 30% sulfuric acid and methanol to produce compound **4** (Figure 3.2). Yield of this reaction was 78%.

Finally, obtained product was coupled with isoquinoline-5-carboxylic acid, which will be demonstrated in Section 3.2.

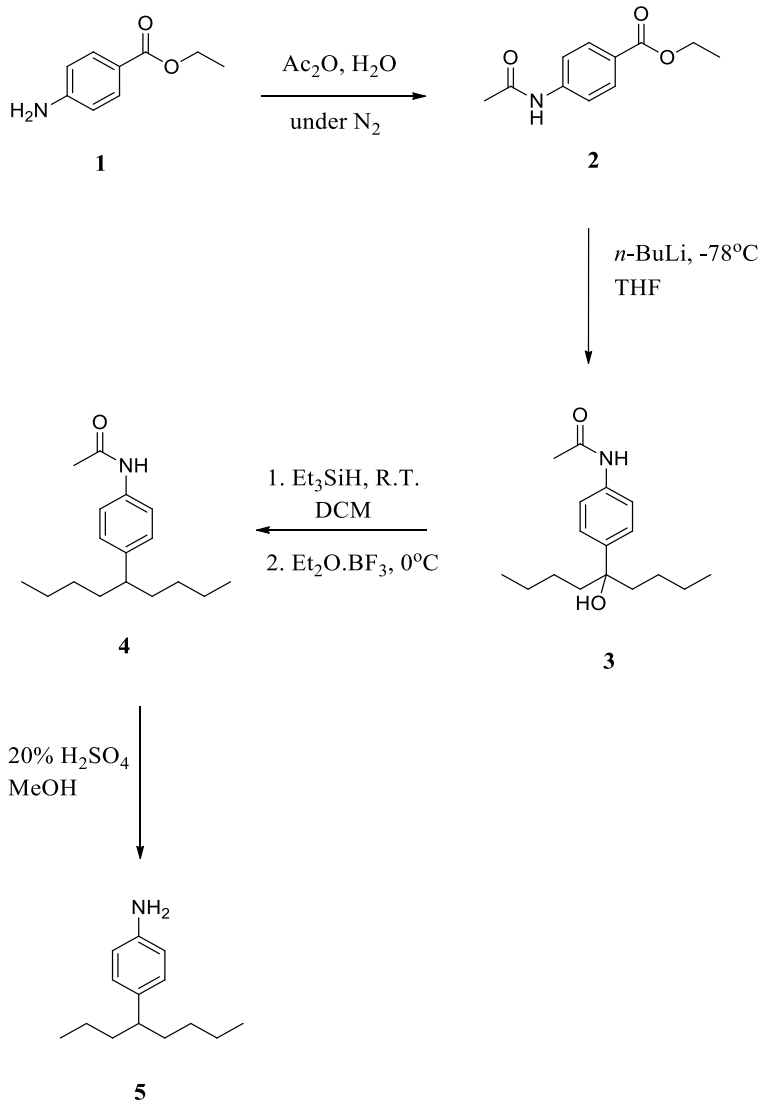


Figure 3.2. Synthetic strategy for synthesis of 4-(nonan-5-yl)aniline.

The docking configuration of the branched alkyl substituted compound (Figure 3.1, right) revealed that isoquinolines having substituted at its fifth position do not always coordinate the heme iron in the same binding mode (Figure 3.2). For *n*-butyl substituted lead compound derivative, $sp^2$ hybridized N atom coordinates the heme iron. However, for the branched alkyl substituted lead compound derivative, heme iron covalently binds to the carbonyl oxygen of amide.

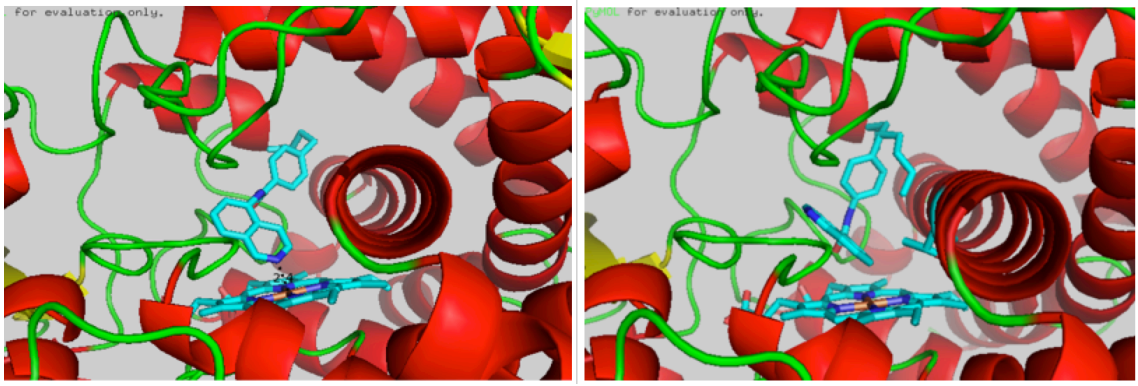

Figure 3.3. Comparison of docking configurations of n-butyl (left) and branching alkyl (right) substituted isoquinoline derivatives.

In order to understand the interaction of 5-isoquinolines with heme iron, a detailed docking study was performed by the research group of Prof. Metin Türkay from Koç University. More docking configurations for the branched alkyl substituted isoquinolines were obtained *via* AutoDock4 software. Carbonyl oxygen and heme interaction was captured from another pose (Figure 3.3). Surprisingly, $sp^2$ hybridized N atom was forming a hydrogen bond with residues located on hydrophobic I helix, altering the current modification strategy of the project.

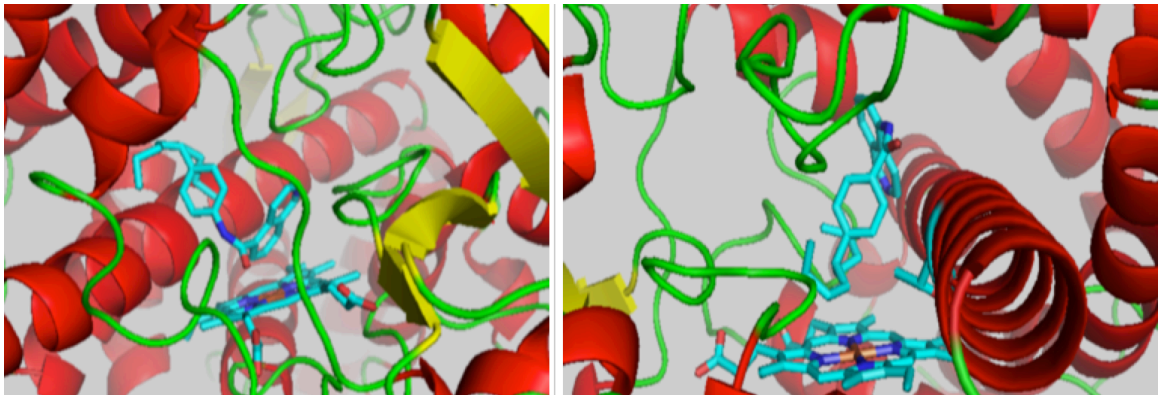

Figure 3.4. Carbonyl oxygen - heme interaction (left); $sp^2$ hybridized N atom of isoquinoline - I helix interaction (right).

### 3.2. Modification of Isoquinoline Ring

Variable docking configuration of 5-isoquinolines has brought about a novel perspective: In order to investigate the effect of each alternate position of $sp^2$ N atom on isoquinoline ring, lead derivatives involving 1-, 3-, 4- and 6-isoquinoline on the left-hand side with various right-hand side fragments were designed and synthesized. The docking data (Figure 3.4) for each compound revealed that 4-isoquinolines were very promising lead derivatives because both the amide juncture and the pyridine ring of isoquinoline fragment are on the same side, resulting in a binary interaction with heme iron. Moreover, the docking configuration of 6-isoquinoline derivative indicated the presence of a potential H-bonding with residues both on I helix and G-helix, leading to the design and synthesis of miscellaneous derivatives that will be presented later.

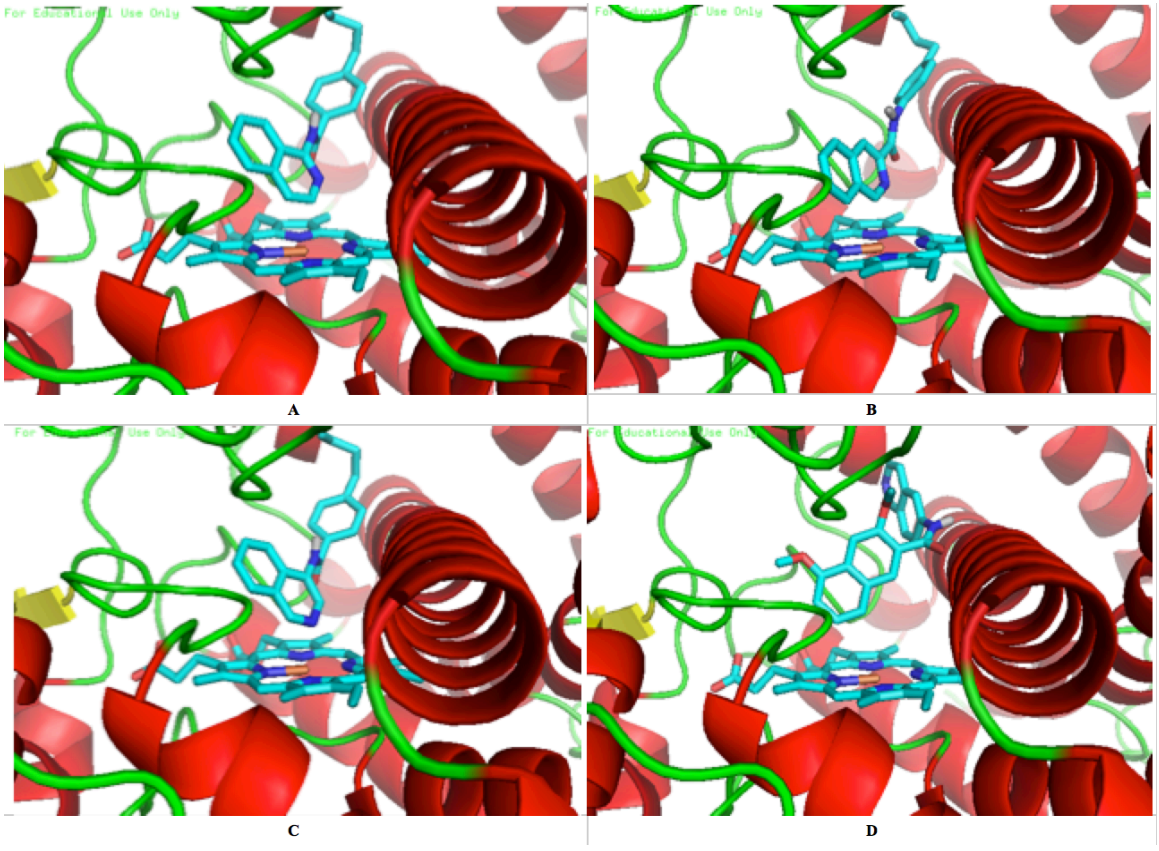


Figure 3.5. Docking configuration of 1-isoquinoline (A); 3-isoquinoline (B); 4-isoquinoline (C); 6-isoquinoline (D) with CYP17A1.

For this purpose, several commercially available isoquinolines with amino or acid substituents at alternating positions were coupled with different benzoic/naphthoic acids or anilines, respectively.

The synthesis of amide groups were accomplished through the coupling reaction of an carboxylic acid and amine/aniline. Amide or ester bond formation between an acid and an amine or an alcohol, respectively, is a condensation reaction. Although the esterification process is an equilibrium reaction, mixing an amine with a carboxylic acid primarily reveals an acid-base reaction, resulting in formation of a stable salt. Therefore the amide bond formation has to fight against adverse thermodynamics and shifts the side of hydrolysis rather than synthesis.

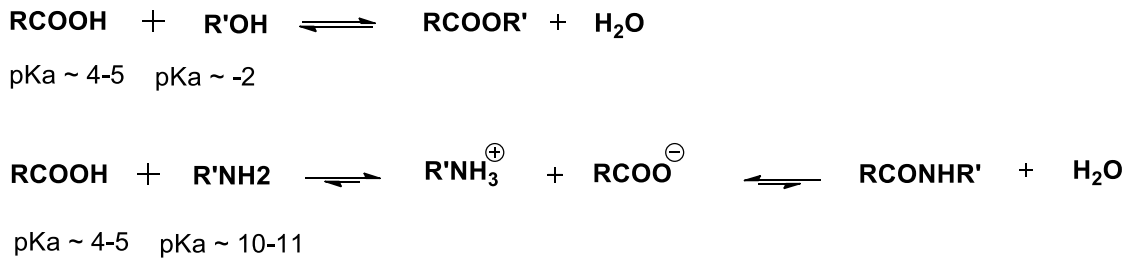


Figure 3.6. Ester bond formation versus amide bond formation.

The direct condensation of a stable salt requires high temperature (160-180°) which is quite incompatible with the presence of other functional groups. Therefore attachment of an activating group to the carboxylic acid in order to allow an attack by the amino is needed.

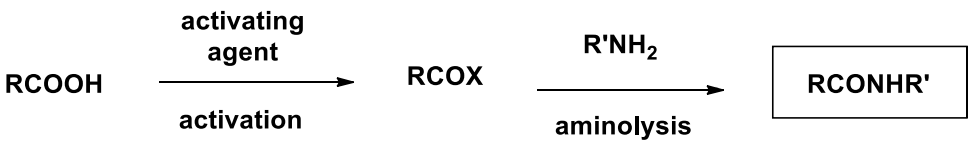


Figure 3.7. Acid activation and aminolysis step.

In this regard, a plethora of methods and strategies have been developed. EDC (1-ethyl-3-(3′-dimethylamino)carbodiimide HCl salt) is a frequently used versatile coupling agent for the synthesis of amides due to its several advantages such as ease of handling of the reagent, the enhanced solubility of EDC in water and especially in a variety of organic solvents (i.e. DCM, THF, DMF) and ease of purification of the late-stage intermediate or active-ingredient from the water-soluble products. This dissertation reports the syntheses several carboxamides *via* EDC coupling of aromatic amines with aromatic carboxylic acids. EDC coupling reactions were done according to the procedure indicated in Ahmet Köseoğlu's Ph.D. dissertation [32]. Figure 3.8-11 summarizes the synthetic approach used to synthesize all isoquinoline derivatives.

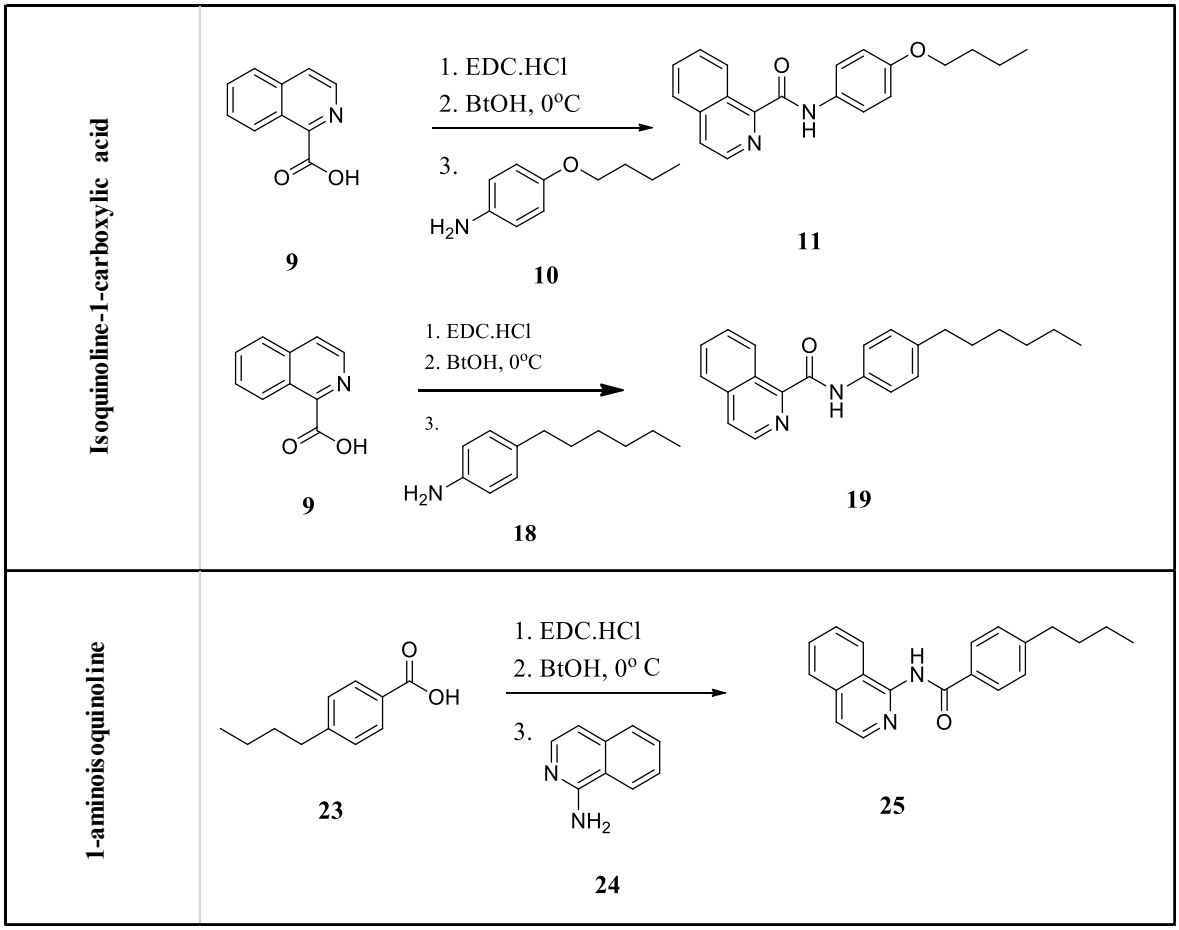


Figure 3.8. Isoquinoline-1-carboxylic acid (top); 1-aminoisoquinoline (bottom) left-hand sides.

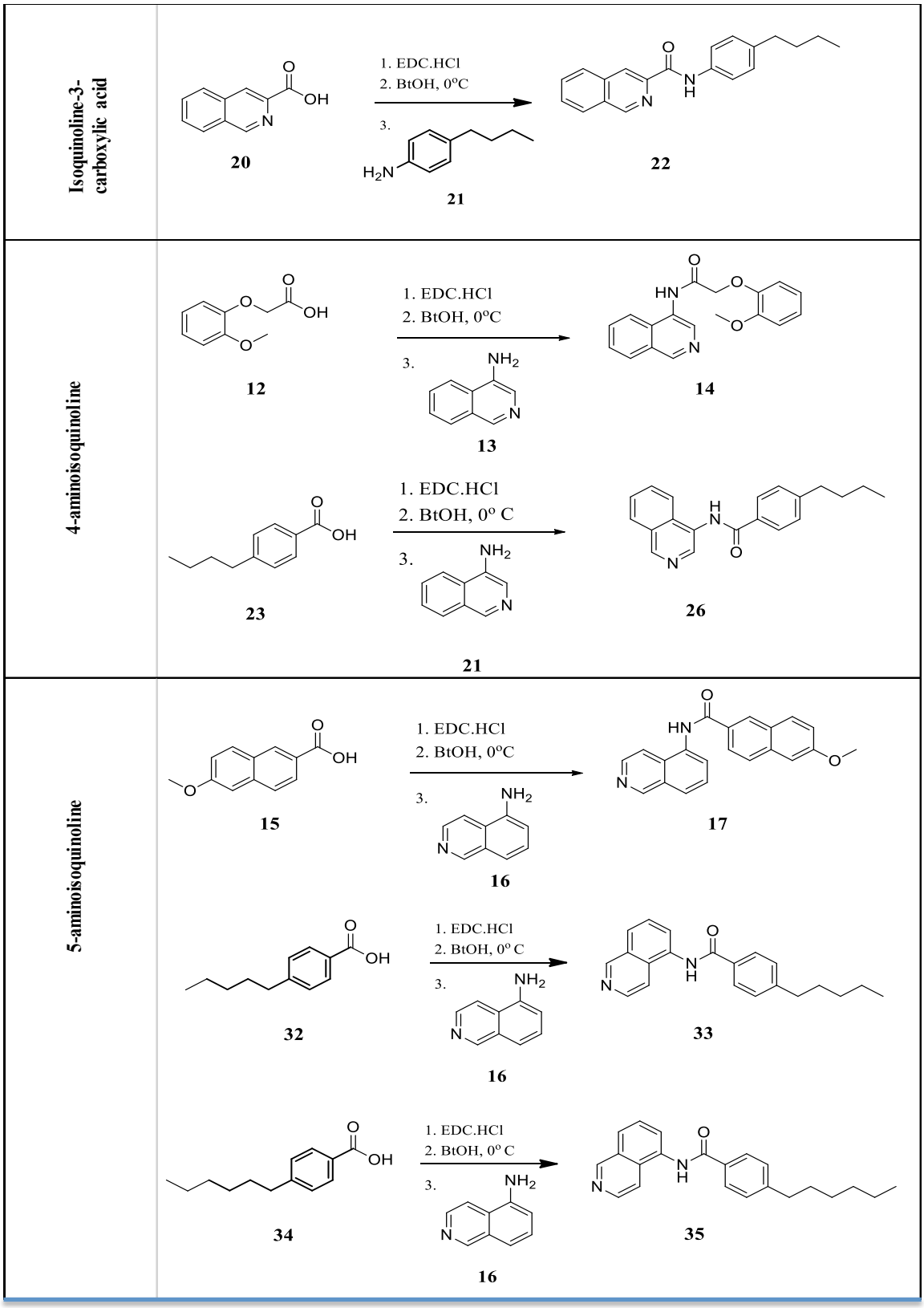


Figure 3.9. Isoquinoline-3-carboxylic acid (top); 4-aminoisoquinoline (middle); and 5-aminoisoquinoline (bottom) derivatives.

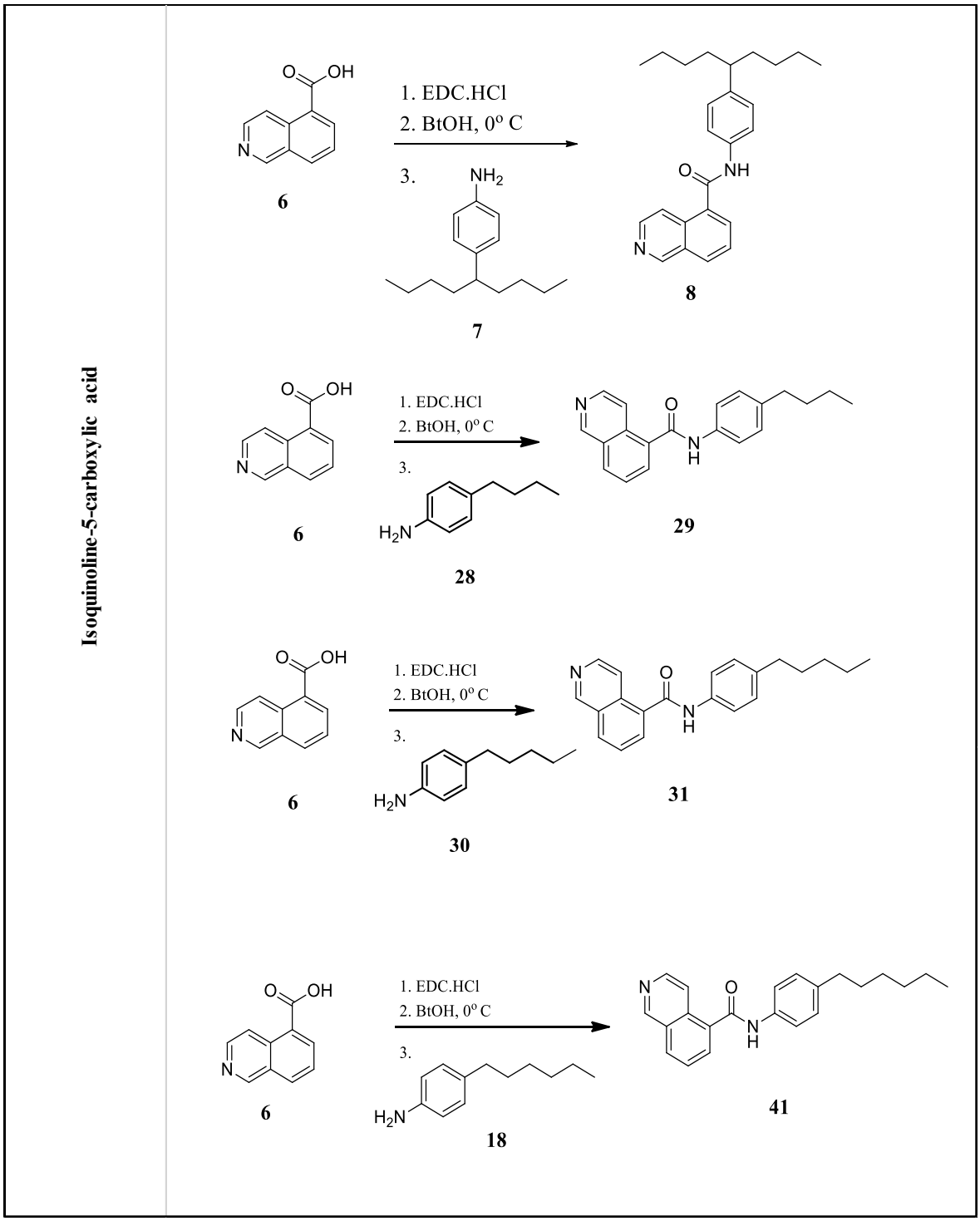


Figure 3.10. Isoquinoline-5-carboxylic acid derivatives.

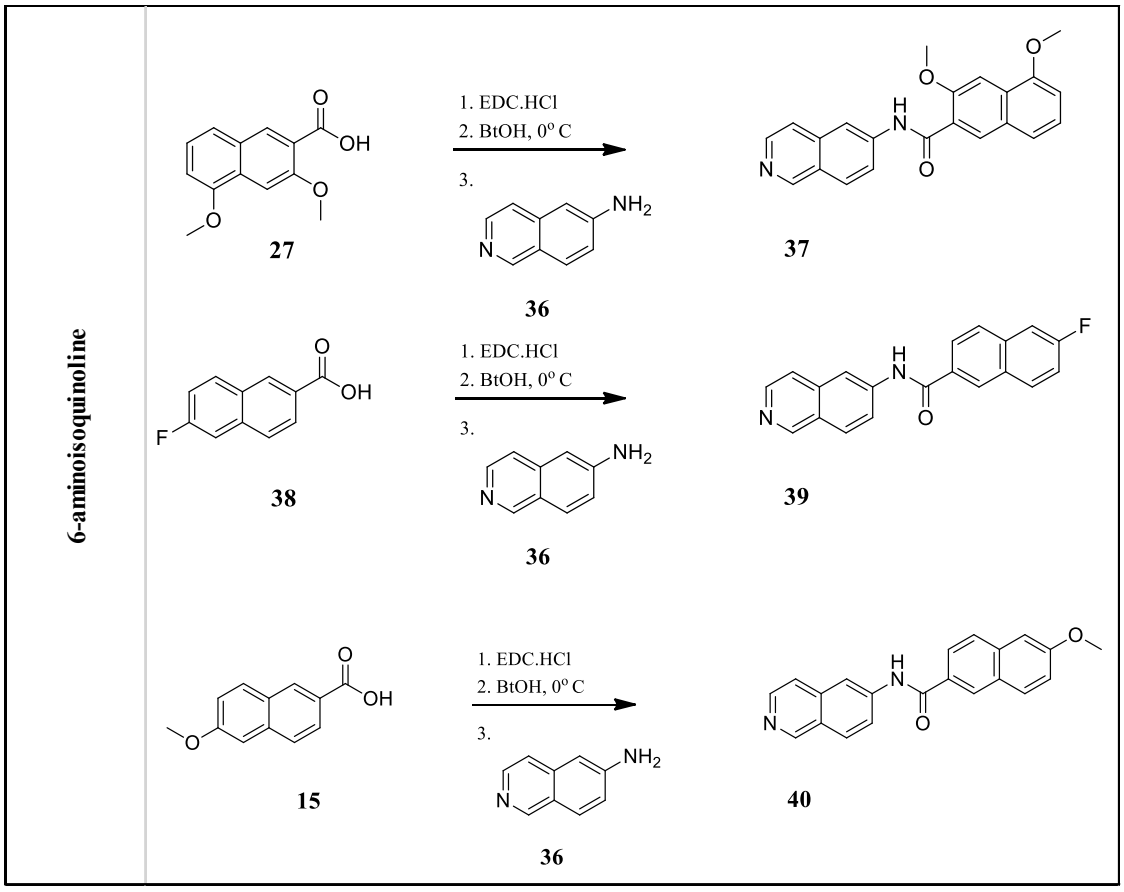


Figure 3.11. 6-aminoisoquinoline derivatives.

Several isoquinoline derivatives with different alkyl chain lengths or different substitution position were designed and synthesized and their biological activities were tested *in vitro*. Some of the final products, especially isoquinoline derivatives having substituted at the 5$^{th}$ position, showed a small amount of activity in preliminary test at 1 µM. More biological testing needs to be done at higher concentrations since the $IC_{50}$ value of the lead compound is 36.5 µM (Figure 3.12).

Binding and docking energies of the isoquinoline derivatives were also calculated by AutoDock4 software. Remarkably, the lead derivatives involving 5-isoquinolines as the left-hand side revealed promising results (Table 3.1).

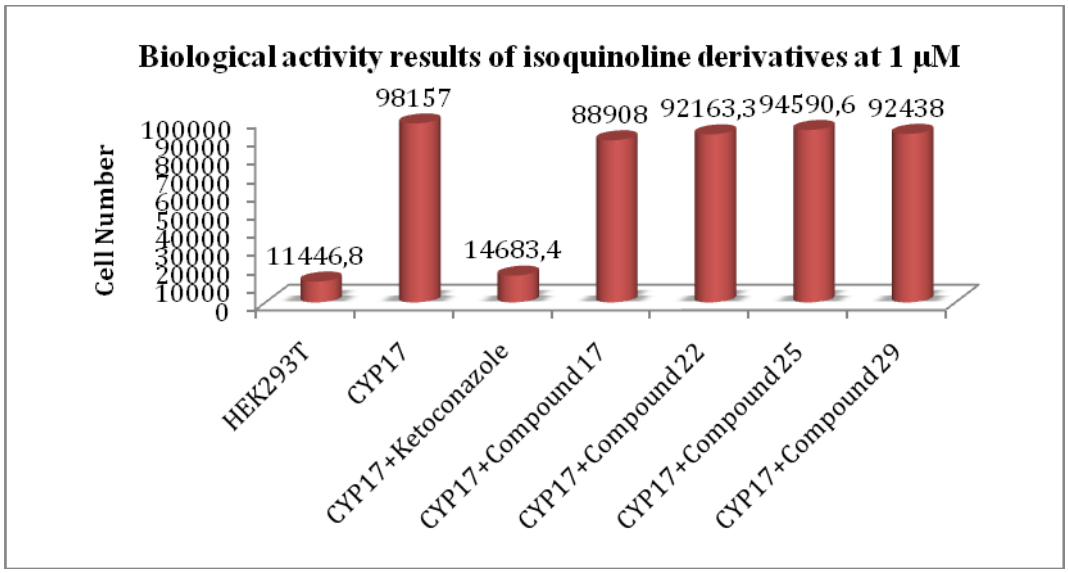


Figure 3.12. Biological activity results of isoquinoline derivatives at 1 µM.

Table 3.1. Binding and Docking Energies of Final Products with Isoquinoline-Left-Hand Side.

| Final Products | D.E. (kcal/ mol) | B.E. (kcal/ mol) | Final Products | D.E. (kcal/ mol) | B.E. (kcal/ mol) |
|---|---|---|---|---|---|
| 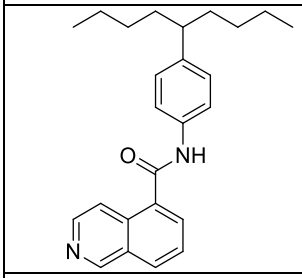 | -14.31 | -10.48 | 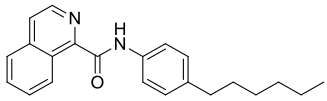 | -11.92 | -9.65 |
| 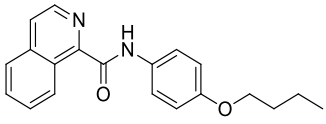 | -11.63 | -9.03 | 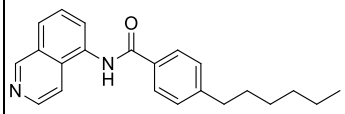 | -11.58 | -8.98 |
| 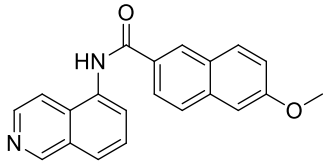 | -11.5 | -9.93 | 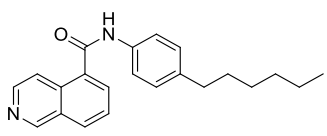 | -11.34 | -8.76 |

Table 3.1. Binding and Docking Energies of Final Products with Isoquinoline-Left-Hand Side (cont.).

| Final Products | D.E. (kcal/ mol) | B.E. (kcal/ mol) | Final Products | D.E. (kcal/ mol) | B.E. (kcal/ mol) |
|---|---|---|---|---|---|
| 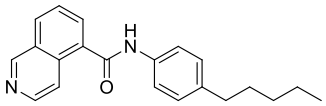 | -11.06 | -7.94 | 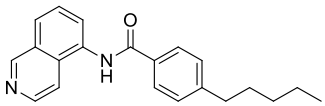 | -11.01 | -8.74 |
| 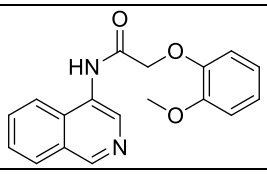 | -10.66 | -8.82 | 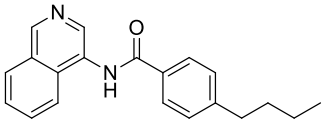 | -10.47 | -8.50 |
| 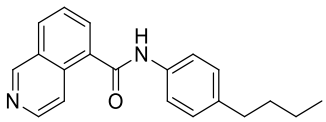 | -10.47 | -8.13 | 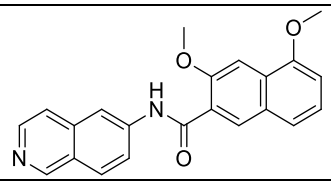 | -10.44 | -8.59 |
| 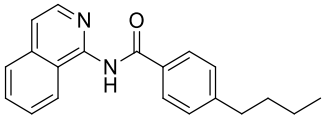 | -10.40 | -8.50 | 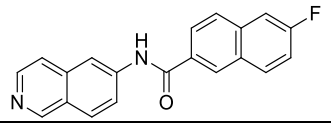 | -9.76 | -9.02 |
| 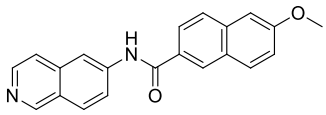 | -9.62 | -8.61 | 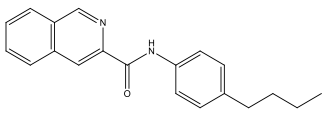 | -9.54 | -7.51 |

## 3.3. Miscellaneous Derivatives

### 3.3.1. 2-Benzofuran and 2-Benzothiophene Derivatives

Various other derivatives of the lead compound were designed and synthesized such as potentially active 2-benzofuran and 2-benzothiophene lef-hand side groups. Right-hand side was modified in two ways:

(i) Phenyl ring with different chain length

(ii) Phenyl ring with 4-ethyl benzoate substitution

As previosly stated in Ahmet Köseoğlu's Ph.D dissertation, benzofuran and benzothiophene derivatives with different alkyl chain lengths showed some activity in preliminary test at 5 µM. The $IC_{50}$ values of *n*-butyl substituted benzofuran derivative and *n*-butyl substituted benzothiophene derivative were found 25.5 µM and 15.4 µM, respectively. In this regard, small series of *n*-pentyl and *n*-hexyl substituted benzofuran and benzothiophene derivatives were synthesized and their biological activities were tested *in vitro,* which can be found in the above-mentioned thesis [32].

Although the ester group is hydrolytically unstable in human body, the reason for the latter modification is to investigate the H-bonding possibility with residues on I- or G-helices and the subsequent effects on *in vitro* tests. Consistent with the theory, docking configurations of 4-ethyl benzoate substituted derivatives revealed that the desired compounds were forming H-bonding with both I-helix and G-helix (Figure 3.13).

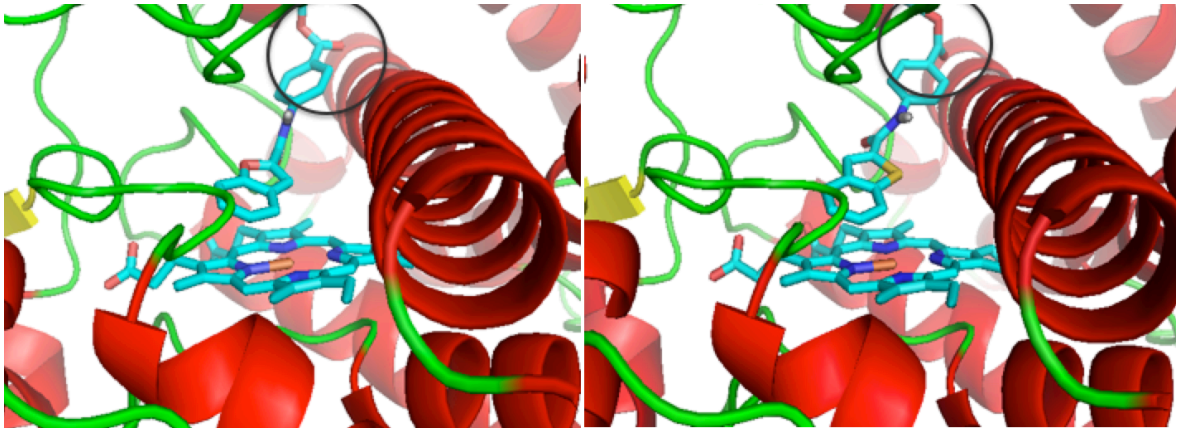

Figure 3.13. H-bonding network of 4-ethyl benzoate group with both I-helix and G-helix.

To synthesize the final products, 2-benzofurane and 2-benzothiophene were coupled with different anilines *via* EDC coupling. The synthetic strategies are shown in Figure 3.14 and Figure 3.15.

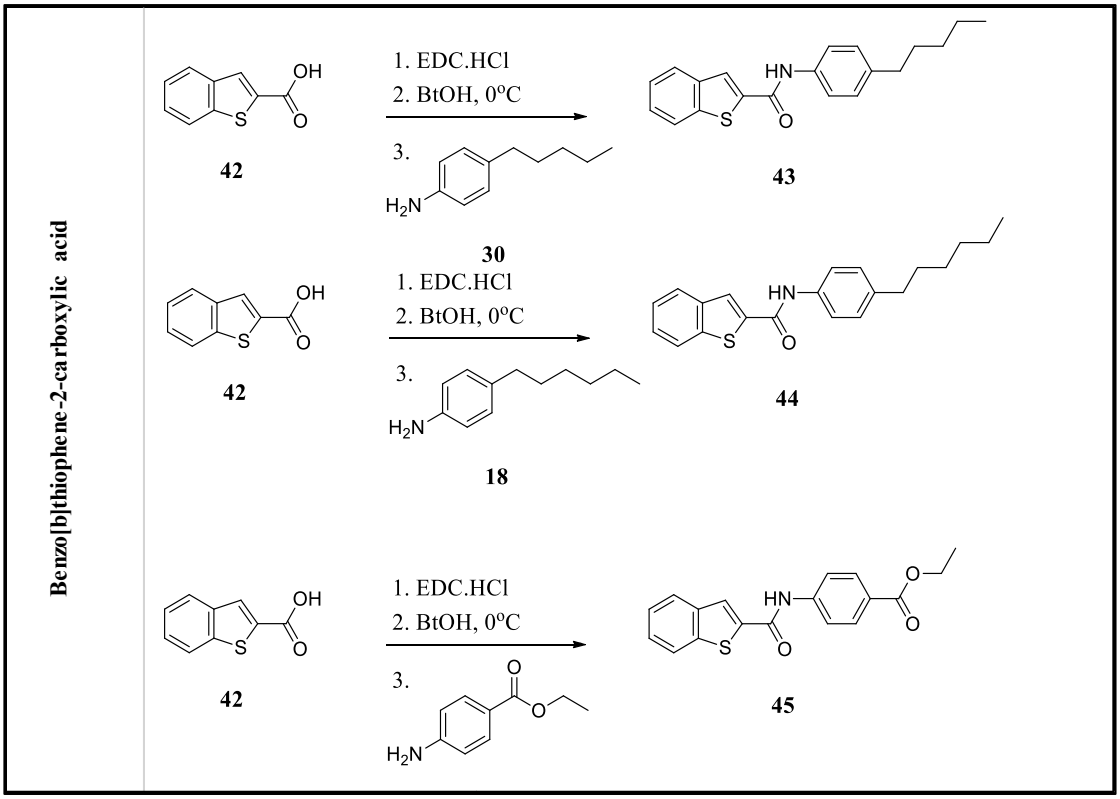


Figure 3.14. Benzo[b]thiophene-2-carboxylic acid derivatives.

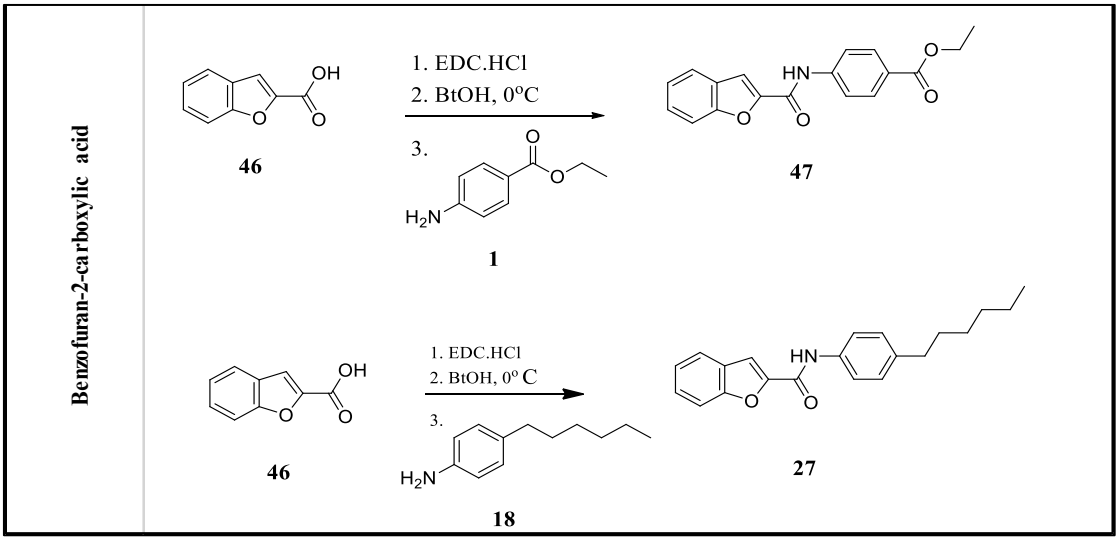


Figure 3.15. Benzofuran-2-carboxylic acid derivatives.

The binding and docking energies for 2-benzofuran and 2-benzothiophene derivatives are shown in Table 3.2. According to the energy calculations, 4-ethyl benzoate substituted lead derivatives are not promising compounds although they form key hydrogen bonding with residues on I- and G- helices. The weak coordination of sulphur and oxygen atom with heme-iron (Figure 3.13) may provide an explanation for this situation. Therefore, derivatives involving isoquinolines on the left-hand side and 4-ethyl benzoate substituted phenyl rings on the right-hand side may be designed and synthesized as a future work in order to eliminate the coordination problem with heme.

Table 3.2. The binding and docking energies for 2-benzofuran and 2-benzothiophene lead derivatives.

| **Final Products** | **D.E. (kcal/ mol)** | **B.E. (kcal/ mol)** | **Final Products** | **D.E. (kcal/ mol)** | **B.E. (kcal/ mol)** |
|---|---|---|---|---|---|
| 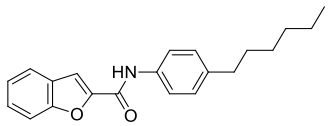 | -10.59 | -7.9 | 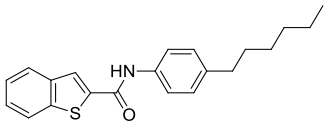 | -10.08 | -7.47 |
| 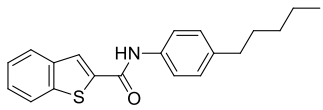 | -9.8 | -7.52 | 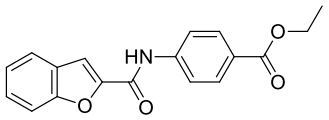 | -9.15 | -7.16 |
| 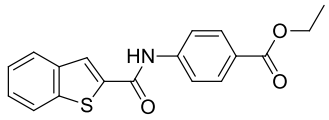 | -8.6 | -6.63 | | | |

### 3.3.2. Tetrazol Derivatives

From 2011 to 2012, Viamet Pharmaceuticals Inc. patented almost all derivatives of 1- or 4-triazole, 2-tetrazole or 4-pyrimidine substituted methylene naphthalenes or (iso)quinolines, and in January 2012, a compound among this set was announced to be the candidate for phase I/II clinical trial for the treatment of chemotheraphy naïve patients with CRPC [16]. Therefore, in order to examine the heme-coordinating capability of other $sp^2$ hybridized nitrogen bearing heterocycles, 4-(1H-tetrazol-5-yl)benzoic acid containing

novel drug candidates were designed and synthesized; however, their binding and docking energies were not promising. The biological tests for this set will be performed later on. In order to understand the energy gap, docking configurations of Viamet compounds as well as other drug candidates were obtained *via* AutoDock4 software. Comparison of these candidates with the tetrazol derivatives **50** and **51** revealed that key hydrogen bonding in G-helix is literally possible, as depicted in Figure 5.3. This hydrogen bonding may provide a broad perspective in future work in search for more active drug candidates to inhibite CYP17A1 (Figure 3.13).

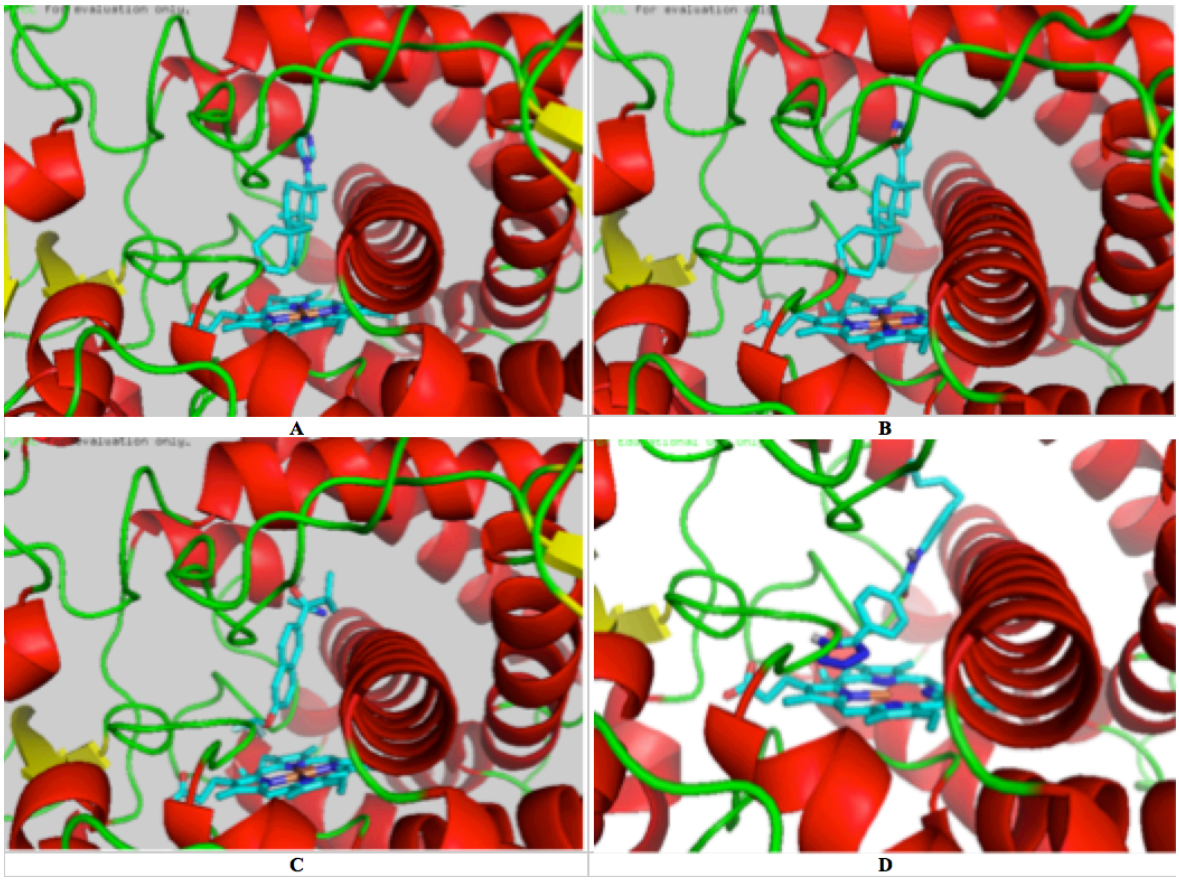


Figure 3.16. VN85-1 (A); L39 (B); Viamet-4 (C); Compound **50**.

To synthesize final products, 4-(1H-tetrazol-5-yl)benzoic acid were coupled with 4-butyl and 4-pentyl anilines *via* EDC coupling. The synthetic strategy for tetrazol derivatives is illustrated in Figure 3.17 and the energy calculations are tabulated in Table 3.3.

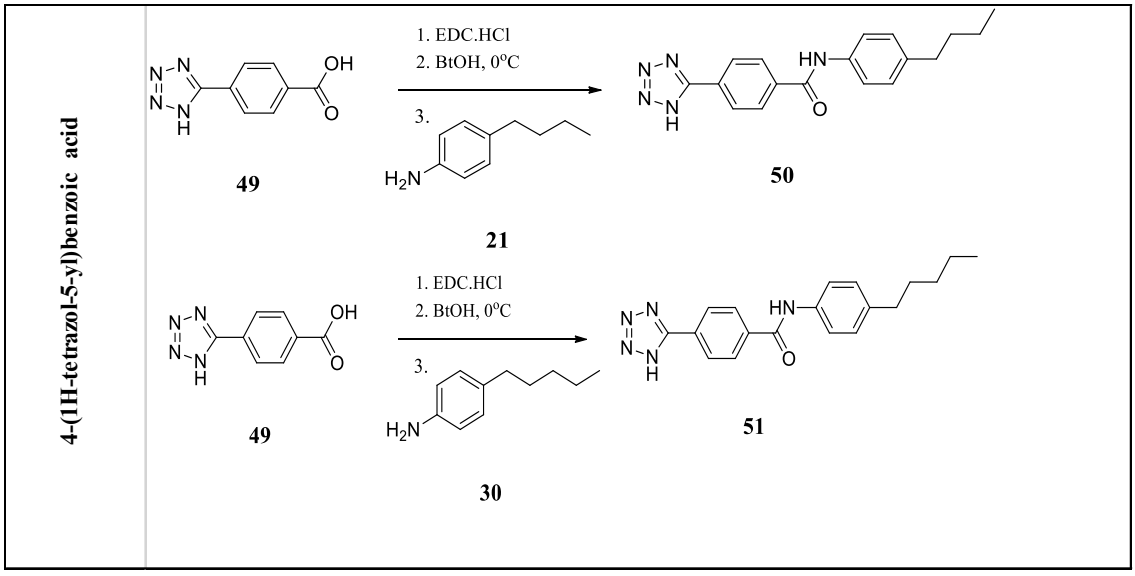


Figure 3.17. 4-(1H-tetrazol-5-yl)benzoic acid derivatives.

Table 3.3. Binding and Docking Energies of 4-(1H-tetrazol-5-yl)benzoic acid derivatives.

| Final Products | B.E. (kcal/ mol) | D.E. (kcal /mol) | Final Products | B.E. (kcal/ mol) | D.E. (kcal/ mol) |
|---|---|---|---|---|---|
| 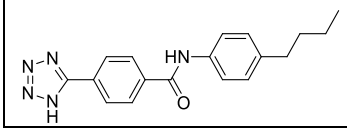 | -5.99 | -3.27 | 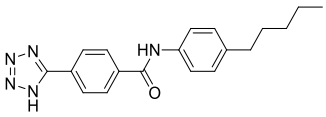 | -7.08 | -4.67 |

### 3.3.3. Conversion of Amides into Thioamides

Final miscellanous modification is the conversion reaction of carbonyl group into thionyl group in order to compare the heme-coordination capability of thioamides *versus* amides.

Lawesson's Reagent is a mild and convenient thionating agent for ketones, esters, and amides allowing the preparation of thioketones, thioesters and thioamides in good yields.

For thionation reaction, the procedure mentioned in Elif Zengin's M.Sc. thesis was applied [33]. Previously synthesized two 2-benzothiophene derivatives were selected for the thionation reactions. One equivalent carboxamide **43** or **44** was dissolved in 50 mL dry toluene and then 1 equivalent Lawesson's reagent was added. The reaction mixture was refluxed at 120°C, under $N_2$ for 24 hours. The resulting mixture was concentrated under reduced pressure and the crude product was purified to obtain compound **52** or **53**, respectively. The synthetic strategy (Figure 3.18) and the calculated energies ( Table 3.4) are as following:

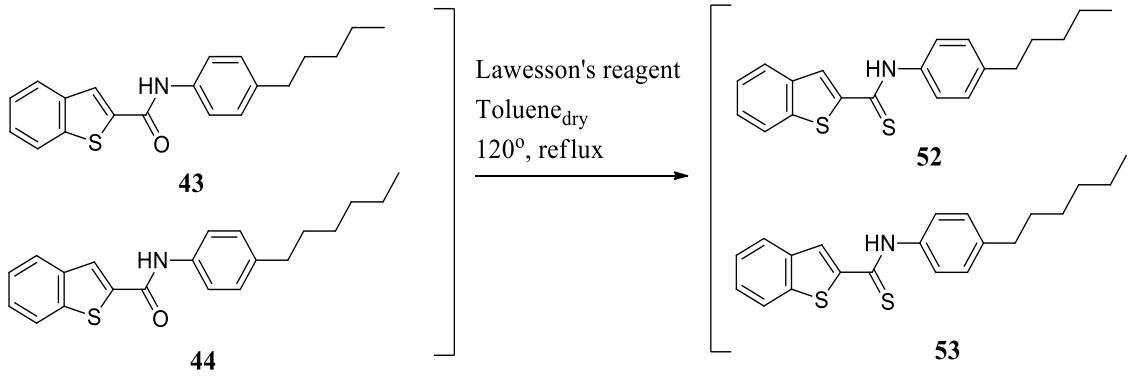


Figure 3.18. Thioamide derivatives.

Table 3.4. Binding and Docking Energies of Thionation Derivatives.

| Final Products | D.E. (kcal/ mol) | B.E. (kcal/ mol) | Final Products | D.E. (kcal/ mol) | B.E. (kcal/ mol) |
|---|---|---|---|---|---|
| 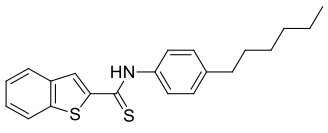 | -13.78 | -10.66 | 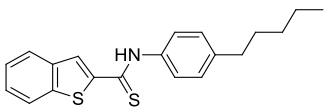 | -12.75 | -9.96 |

Remarkably, compound **53** demonstrated the lowest binding energy among all derivatives synthesized so far. Although the sulfur atom on heterocyclic group does not

seem to be well-coordinating group for heme iron, the H-bonding of amide with G-helix and the ease of leaning of *n*-hexyl group on I- helix may provide an explanation for low binding and docking energies.

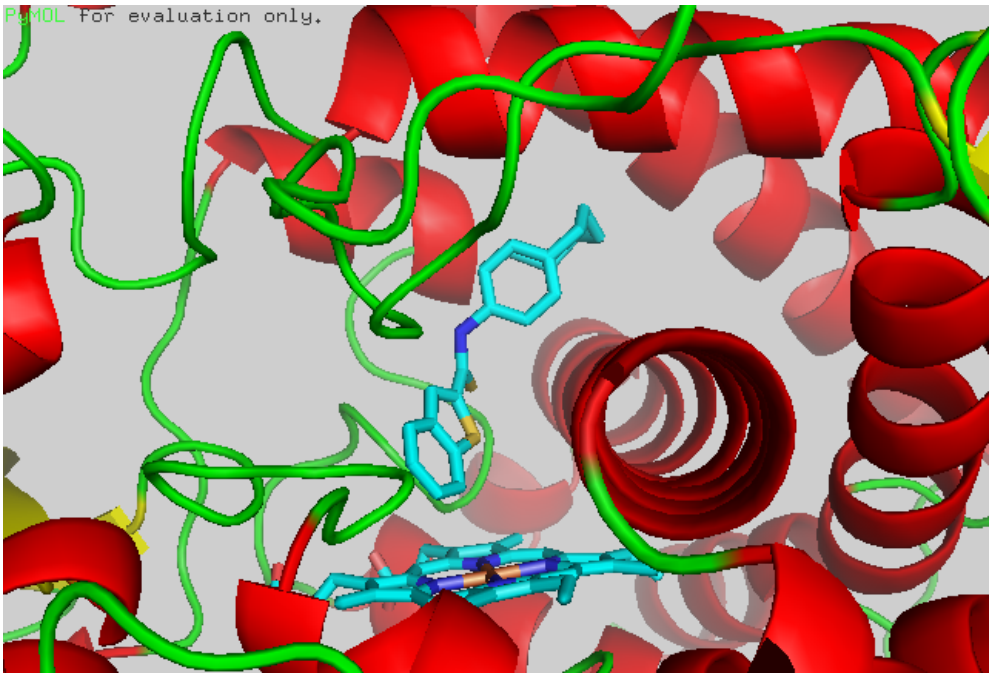


Figure 3.19. Docking configuration of compound 53 with CYP17A1 enzyme.

# 4. EXPERIMENTAL

## 4.1. Methods and Materials

All chemicals were used as received from the manufacturer (Merck, Aldrich, Alfa Aesar, and Riedel de Haen). Dry solvents ($CH_2Cl_2$, THF and Toluene) were obtained from ScimatCo Purification System; other solvents were dried of molecular sieves. Cooling to -78°C was carried out at Cryostat. Column chromatography was performed using silicagel-60 (43-60 nm). Thin layer chromatography was performed using silica gel plates (Kiesel gel 60 F254, 0,2mm, Merck) and aluminum oxide plates.

## 4.2. Instrumentation

Thin layer chromatography plates were viewed under 254 nm UV lamp. $^{1}$H-NMR and $^{13}$C-NMR spectra were recorded by using a Varian Gemini 400 MHz spectrometer Varian Associates, Palo Alto, CA) in $CDCl_3$ as solvent at the Advanced Technologies Research and Development Center at Bogazici University.

## 4.3. Syntheses of Branched Alkyl Substituted Phenyl Rings

The strategy followed in the synthesis of branched alkyl substituted phenyl rings (Figure 4.1) was done according to the method described in Turgay Yildirim's M.Sc. thesis [31]. The spectroscopic data of final product were compared with the above-mentioned thesis and the identical peaks were observed.

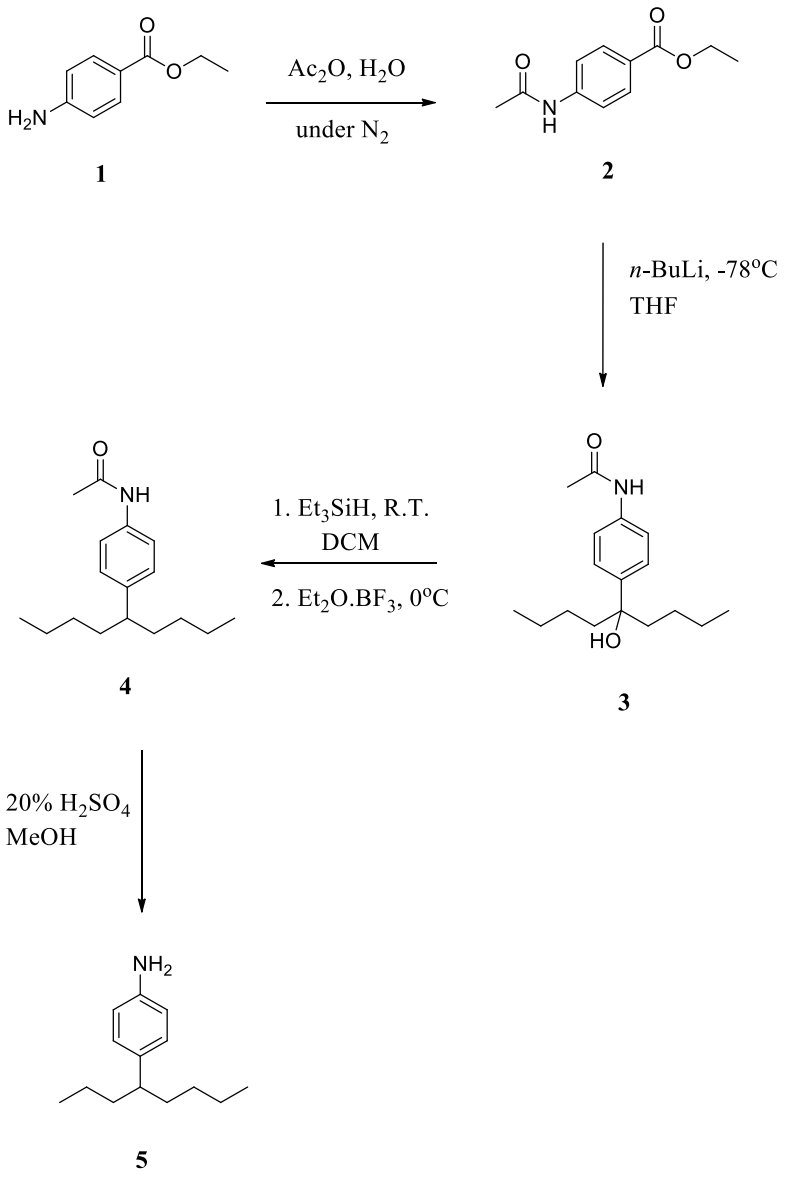


Figure 4.1. Synthetic strategy for synthesis of 4-(nonan-5-yl)aniline.

## 4.4. Synthesis of the Lead Compound Derivatives

### 4.4.1. Synthesis of *N*-(4-(nonan-5-yl)phenyl)isoquinoline-5-carboxamide

Compound **8** was synthesized through EDC coupling. Isoquinoline 5-carboxylic acid **6** (0.308 mmol, 53.5 mg) was dissolved in 3.5 ml:1.5 mL $DCM_{dry}/DMF_{dry}$ under $N_2$. To this solution, EDC.HCl reagent (0.308 mmol, 59.04 mg) was added and then BtOH (0.308 mmol, 41.61 mg) was added and mixed at $0^oC$ for 30 minutes. This step is followed

by the amine-addition step: 4-(nonan-5-yl)aniline **7** (0.154 mmol, 33.8 mg) was added and the reaction mixture was stirred for 24 hours. This mixture is dissolved in 15 mL EtOAc and extracted 3 times with 150 mL distilled water, 50 mL saturated $NaHCO_3$ and 50 mL brine, respectively. The organic layer was dried over $Na_2SO_4$, filtered and concentrated under reduced pressure. The crude product was impure and the purification was achieved by column chromatography using silica gel as the stationary phase and EtOAc/ Hexane (1:1) as the eluent phase. The final product was a yellow viscous liquid with 97% yield. **$^1$H NMR** (400 MHz, $CDCl_3$) δ 9.31 (s, 1H), 8.60 (d, 1H), 8.23 (d, *J* = 5.9 Hz, 1H), 8.10 (d, *J* = 8.2 Hz, 1H), 7.97 (d, *J* = 7.0 Hz, 1H), 7.71 (s, 1H), 7.68 – 7.63 (m, 1H), 7.60 (d, *J* = 8.3 Hz, 1H), 7.18 (d, *J* = 8.2 Hz, 1H), 2.55 – 2.42 (m, 1H), 1.68 – 1.50 (m, 2H), 1.31 – 1.22 (m, 1H), 0.84 (t, *J* = 7.2 Hz, 1H).

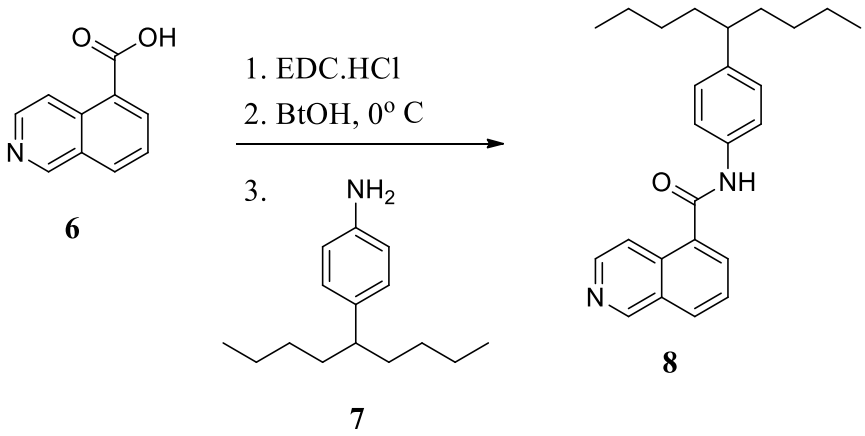


Figure 4.2. Synthesis of *N*-(4-(nonan-5-yl)phenyl)isoquinoline-5-carboxamide.

### 4.4.2. Synthesis of N-(4-butoxyphenyl)isoquinoline-1-carboxamide

Compound **11** was synthesized through EDC coupling. Isoquinoline-1-carboxylic acid **9** (1 mmol, 173 mg) was dissolved in 3.5 ml:1.5 mL $DCM_{dry}$/$DMF_{dry}$ under $N_2$. To this solution, EDC.HCl reagent (1 mmol, 191.7 mg) was added and then 1-hydroxybenzotriazole (BtOH) (1 mmol, 135.12 mg) was added and mixed at 0$^o$C for 30 minutes. This step is followed by the amine-addition step: 4-butoxyaniline **10** (0.66 mmol, 110 mg) was added and the reaction mixture was stirred for 24 hours. This mixture is dissolved in 15 mL EtOAc and extracted 3 times with 150 mL distilled water, 50 mL

saturated $NaHCO_3$ and 50 mL brine, respectively. The organic layer was dried over $Na_2SO_4$, filtered and concentrated under reduced pressure. The crude product was impure and the purification was achieved by column chromatography using silica gel as the stationary phase and EtOAc/ Hexane (1:1) as the eluent phase. The final product was a pale yellow solid with 72% yield **$^1$H NMR** (400 MHz, $CDCl_3$) δ 10.13 (s, 1H), 9.67 – 9.63 (m, 1H), 8.43 (d, *J* = 5.5 Hz, 1H), 7.80 (d, *J* = 1.7 Hz, 1H), 7.78 (s, 1H), 7.75 (d, *J* = 5.5 Hz, 1H), 7.66 – 7.62 (m, 1H), 6.86 (d, *J* = 7.0 Hz, 1H), 3.90 (t, *J* = 6.5 Hz, 1H), 1.70 (dt, *J* = 14.7, 6.6 Hz, 1H), 1.42 (dt, *J* = 14.6, 7.4 Hz, 1H), 0.91 (t, *J* = 7.4 Hz, 1H). **$^{13}$C NMR** (101 MHz, $CDCl_3$) δ 163.42 (s), 155.94 (s), 147.75 (s), 139.92 (s), 138.76 (d, *J* = 233.5 Hz), 140.16 – 130.67 (m), 134.78 (dd, *J* = 799.4, 140.7 Hz), 140.16 – 128.03 (m), 140.16 – 127.36 (m), 140.16 – 126.97 (m), 140.16 – 124.78 (m), 140.16 – 121.51 (m), 140.16 – 114.94 (m), 140.16 – 77.48 (m), 76.69 (s), 67.97 (s), 31.36 (s), 19.25 (s), 13.88 (s).

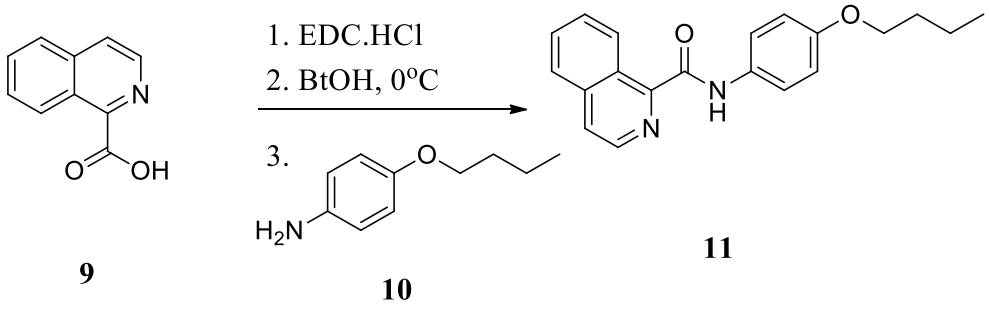


Figure 4.3. Synthesis of N-(4-butoxyphenyl)isoquinoline-1-carboxamide.

### 4.4.3. Synthesis of *N*-(isoquinolin-4-yl)-2-(2-methoxyphenoxy)acetamide

Compound **14** was synthesized through EDC coupling. 2-methoxyphenoxy acetic acid **12** (1 mmol, 182.17 mg) was dissolved in 3.5 ml:1.5 mL $DCM_{dry}$/$DMF_{dry}$ under $N_2$. To this solution, EDC.HCl reagent (1 mmol, 191.7 mg) was added and then BtOH (1 mmol, 135.12 mg) was added and mixed at 0°C for 30 minutes. This step is followed by the amine-addition step: 4-aminoisoquinoline **13** (0.66 mmol, 95.15 mg) was added and the reaction mixture was stirred for 24 hours. This mixture is dissolved in 15 mL EtOAc and extracted 3 times with 150 mL distilled water, 50 mL saturated $NaHCO_3$ and 50 mL brine, respectively. The organic layer was dried over $Na_2SO_4$, filtered and concentrated under reduced pressure. The crude product was impure and the purification was achieved by

column chromatography using silica gel as the stationary phase and EtOAc/ Hexane (1:1) as the eluent phase. The final product was a white solid with 64% yield. **$^1$H NMR** (400 MHz, $CDCl_3$) δ 9.37 (s, 5H), 9.20 (d, *J* = 8.1 Hz, 5H), 9.04 – 9.00 (m, 4H), 8.49 (d, *J* = 8.2 Hz, 5H), 8.11 (d, *J* = 7.8 Hz, 6H), 8.01 – 7.93 (m, 6H), 7.85 (ddd, *J* = 8.1, 7.1, 1.2 Hz, 6H), 7.71 (dd, *J* = 8.3, 4.4 Hz, 6H), 4.53 (s, 1H), 3.89 (s, 1H).

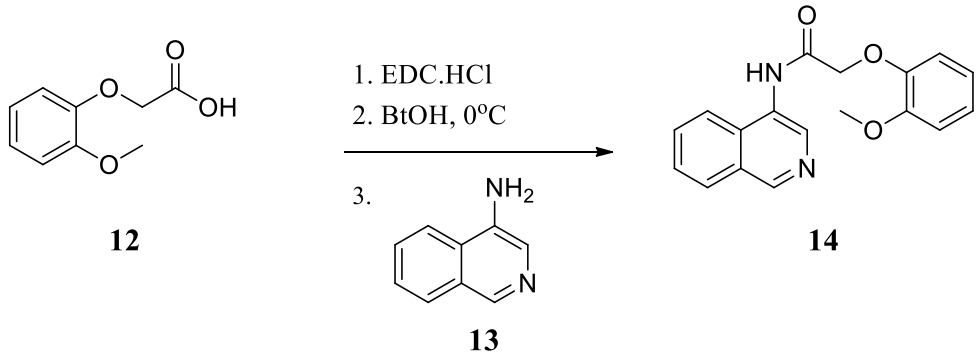


Figure 4.4. Synthesis of *N*-(isoquinolin-4-yl)-2-(2-methoxyphenoxy)acetamide.

### 4.4.4. Synthesis of *N*-(isoquinolin-5-yl)-6-methoxy-2-naphthamide

Compound **17** was synthesized through EDC coupling. 6-methoxy-2-naphtoic acid **15** (0.42 mmol, 85.4 mg) was dissolved in 3.5 ml:1.5 mL $DCM_{dry}/DMF_{dry}$ under $N_2$. To this solution, EDC.HCl reagent (0.42 mmol, 80.96 mg) was added and then BtOH (0.42 mmol, 57.0 mg) was added and mixed at 0°Cfor 30 minutes. This step is followed by the amine-addition step: 5-aminoisoquinoline **16** (0.28 mmol, 31.82 mg) was added and the reaction mixture was stirred for 24 hours. This mixture is dissolved in 15 mL EtOAc and extracted 3 times with 150 mL distilled water, 50 mL saturated $NaHCO_3$ and 50 mL brine, respectively. The organic layer was dried over $Na_2SO_4$, filtered and concentrated under reduced pressure. The crude product was impure and the purification was achieved by column chromatography using silica gel as the stationary phase and 100% EtOAc the eluent phase. The final product was a white solid with 51% yield. **$^1$H NMR** (400 MHz, $CDCl_3$) δ 8.82 (s, 1H), 8.17 (d, *J* = 8.6 Hz, 1H), 8.12 (d, *J* = 7.8 Hz, 1H), 7.95 (s, 1H), 7.92 (d, *J* = 6.3 Hz, 1H), 7.89 (s, 1H), 7.56 (s, 1H), 7.56 (s, 1H), 7.52 (t, *J* = 8.8 Hz, 1H), 7.47 (d, *J* = 7.9 Hz, 1H), 7.44 – 7.43 (m, 1H), 7.31 – 7.26 (m, 1H), 7.23 (s, 1H), 3.99 (s, 3H). **$^{13}$C NMR** (101 MHz, $CDCl_3$) δ 163.02 (s), 160.77 (s), 143.59 (s), 138.47 (s), 133.04 (s),

131.33 (s), 128.80 (d, *J* = 18.2 Hz), 127.76 (s), 125.81 (s), 124.82 (s), 120.57 (d, *J* = 1.7 Hz), 119.30 (s), 108.45 (s), 105.90 (s), 77.32 (s), 77.00 (s), 76.68 (s), 55.56 (s).

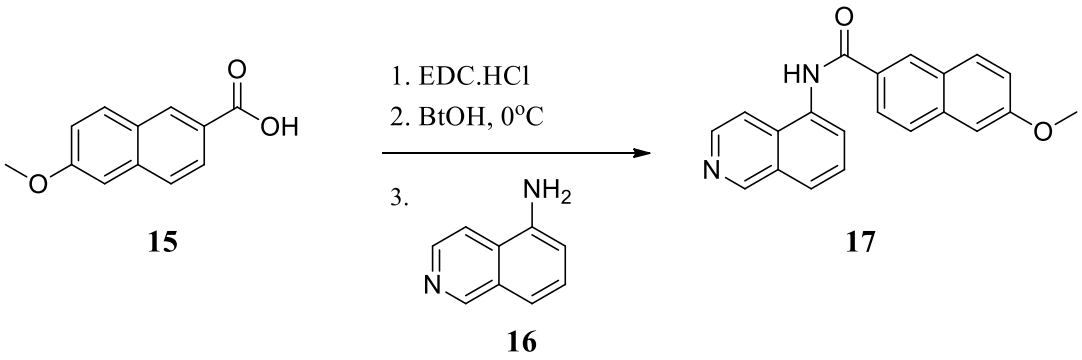


Figure 4.5. Synthesis of *N*-(isoquinolin-5-yl)-6-methoxy-2-naphthamide.

### 4.4.5. Synthesis of *N*-(4-hexylphenyl)isoquinoline-1-carboxamide

Compound **19** was synthesized through EDC coupling. Isoquinoline-1-carboxylic acid **9** (0.82 mmol, 142 mg) was dissolved in 3.5 ml:1.5 mL $DCM_{dry}$/$DMF_{dry}$ under $N_2$. To this solution, EDC.HCl reagent (0.82 mmol, 157 mg) was added and then BtOH (0.82 mmol, 111 mg) was added and mixed at 0°C for 30 minutes. This step is followed by the amine-addition step: 4-hexylaniline **18** (0.54 mmol, 96 mg) was added and the reaction mixture was stirred for 24 hours. This mixture is dissolved in 15 mL EtOAc and extracted 3 times with 150 mL distilled water, 50 mL saturated $NaHCO_3$ and 50 mL brine, respectively. The organic layer was dried over $Na_2SO_4$, filtered and concentrated under reduced pressure. The crude product was impure and the purification was achieved by column chromatography using silica gel as the stationary phase and EtOAc/ Hexane (1:7) as the eluent phase. The final product was a yellow viscous liquid with 95% yield. **$^1$H NMR** (400 MHz, $CDCl_3$) δ 10.28 (s, 1H), 9.74 (ddt, *J* = 7.6, 1.7, 0.8 Hz, 1H), 8.53 (d, *J* = 5.5 Hz, 1H), 7.90 – 7.86 (m, 1H), 7.87 – 7.84 (m, 1H), 7.77 (d, *J* = 1.6 Hz, 1H), 7.76 – 7.74 (m, 1H), 7.73 (t, *J* = 2.0 Hz, 1H), 7.71 (d, *J* = 2.3 Hz, 1H), 7.24 – 7.20 (m, 1H), 2.65 – 2.53 (m, 1H), 1.62 (dt, *J* = 15.4, 7.6 Hz, 1H), 1.35 – 1.28 (m, 2H), 0.94 – 0.86 (m, 1H).

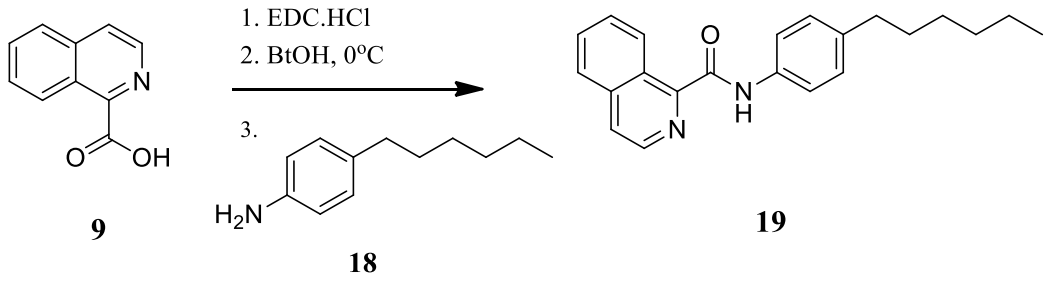


**9** **18** **19**

Figure 4.6. Synthesis of *N*-(4-hexylphenyl)isoquinoline-1-carboxamide.

### 4.4.6. Synthesis of N-(4-butylphenyl)isoquinoline-3-carboxamide

Compound **22** was synthesized through EDC coupling. Isoquinoline-3-carboxylic acid **20** (0.82 mmol, 141.9 mg) was dissolved in 3.5 ml:1.5 mL $DCM_{dry}/DMF_{dry}$ under $N_2$. To this solution, EDC.HCl reagent (0.82 mmol, 157 mg) was added and then BtOH (0.82 mmol, 111 mg) was added and mixed at 0°C for 30 minutes. This step is followed by the amine-addition step: 4-butylaniline **21** (0.54 mmol, 80.6 mg) was added and the reaction mixture was stirred for 24 hours. This mixture is dissolved in 15 mL EtOAc and extracted 3 times with 150 mL distilled water, 50 mL saturated $NaHCO_3$ and 50 mL brine, respectively. The organic layer was dried over $Na_2SO_4$, filtered and concentrated under reduced pressure. The crude product was impure and the purification was achieved by column chromatography using silica gel as the stationary phase and EtOAc/ Hexane (1:4) as the eluent phase. The final product was a pale yellow solid with 97% yield. **$^1$H NMR** (400 MHz, $CDCl_3$) δ 10.18 (s, 1H), 9.22 (s, 1H), 8.72 (s, 1H), 8.07 (d, *J* = 8.0 Hz, 1H), 8.02 (d, *J* = 8.2 Hz, 1H), 7.80 (ddd, *J* = 8.2, 6.9, 1.3 Hz, 1H), 7.22 (d, *J* = 8.4 Hz, 1H), 2.64 – 2.54 (m, 1H), 1.70 – 1.53 (m, 1H), 1.37 (dq, *J* = 14.5, 7.3 Hz, 1H), 0.94 (t, *J* = 7.3 Hz, 1H).

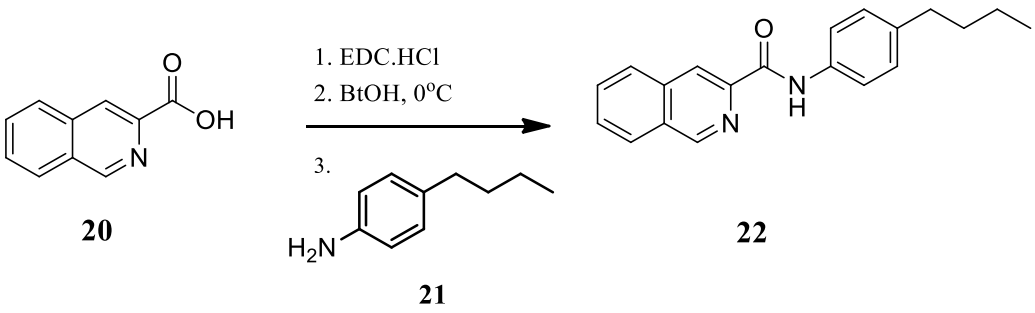


Figure 4.7. Synthesis of N-(4-butylphenyl)isoquinoline-3-carboxamide.

### 4.4.7. Synthesis of 4-butyl-N-(isoquinolin-4-yl)benzamide

Compound **25** was synthesized through EDC coupling. 4-butylbenzoic acid **23** (0.82 mmol, 146.1 mg) was dissolved in 3.5 ml:1.5 mL $DCM_{dry}/DMF_{dry}$ under $N_2$. To this solution, EDC.HCl reagent (0.82 mmol, 157 mg) was added and then BtOH (0.82 mmol, 111 mg) was added and mixed at 0°C for 30 minutes. This step is followed by the amine-addition step: 1-aminoisoquinoline **24** (0.54 mmol, 77.8 mg) was added and the reaction mixture was stirred for 24 hours. This mixture is dissolved in 15 mL EtOAc and extracted 3 times with 150 mL distilled water, 50 mL saturated $NaHCO_3$ and 50 mL brine, respectively. The organic layer was dried over $Na_2SO_4$, filtered and concentrated under reduced pressure. The crude product was impure and the purification was achieved by column chromatography using silica gel as the stationary phase and EtOAc/ Hexane (1:3) as the eluent phase. The final product was a pale orange solid with 42% yield. **$^1$H NMR** (400 MHz, $CDCl_3$) δ 8.20 – 8.15 (m, 1H), 8.10 – 8.06 (m, 1H), 7.93 (d, *J* = 8.1 Hz, 1H), 7.77 (d, *J* = 8.2 Hz, 1H), 7.56 – 7.52 (m, 1H), 7.48 – 7.43 (m, 1H), 7.41 – 7.38 (m, 1H), 7.26 (s, 1H), 7.19 (d, *J* = 8.1 Hz, 1H), 2.77 – 2.72 (m, 1H), 1.73 – 1.56 (m, 1H), 1.40 – 1.32 (m, 1H), 0.95 (dd, *J* = 10.1, 4.6 Hz, 1H).

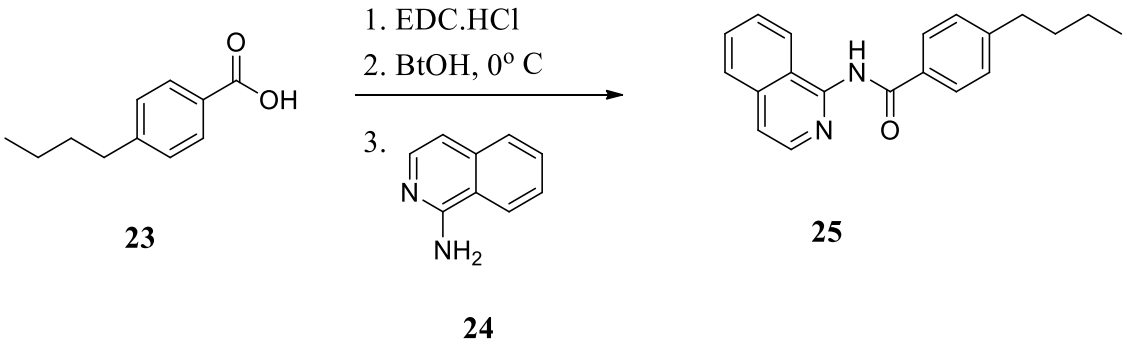


Figure 4.8. Synthesis of 4-butyl-N-(isoquinolin-1-yl)benzamide.

### 4.4.8. Synthesis of 4-butyl-N-(isoquinolin-4-yl)benzamide

Compound **26** was synthesized through EDC coupling. 4-butylbenzoic acid **23** (0.82 mmol, 146.1 mg) was dissolved in 3.5 ml:1.5 mL $DCM_{dry}/DMF_{dry}$ under $N_2$. To this solution, EDC.HCl reagent (0.82 mmol, 157 mg) was added and then BtOH (0.82 mmol, 111 mg) was added and mixed at $0^oC$ for 30 minutes. This step is followed by the amine-addition step: 4-aminoisoquinoline **21** (0.54 mmol, 77.8 mg) was added and the reaction mixture was stirred for 24 hours. This mixture is dissolved in 15 mL EtOAc and extracted 3 times with 150 mL distilled water, 50 mL saturated $NaHCO_3$ and 50 mL brine, respectively. The organic layer was dried over $Na_2SO_4$, filtered and concentrated under reduced pressure. The crude product was impure and the purification was achieved by column chromatography using silica gel as the stationary phase and EtOAc/ Hexane (1:3) as the eluent phase. The final product was a pale pink solid with 53% yield. **$^1$H NMR** (400 MHz, $CDCl_3$) δ 9.17 (s, 1H), 8.97 (d, *J* = 7.1 Hz, 1H), 8.09 (s, 1H), 8.04 (d, *J* = 8.1 Hz, 1H), 7.94 – 7.90 (m, 1H), 7.76 (ddd, *J* = 8.4, 6.9, 1.3 Hz, 1H), 7.66 (ddd, *J* = 8.1, 6.9, 1.1 Hz, 1H), 7.35 (d, *J* = 8.4 Hz, 1H), 2.77 – 2.68 (m, 1H), 1.71 – 1.61 (m, 1H), 1.39 (dq, *J* = 14.6, 7.4 Hz, 1H), 0.96 (t, *J* = 7.3 Hz, 1H). **$^{13}$C NMR** (101 MHz, $CDCl_3$) δ 166.57 (s), 150.32 (s), 147.80 (s), 138.87 (s), 131.31 (s), 130.95 (s), 130.70 (s), 129.97 (s), 128.83 (d, *J* = 11.9 Hz), 128.53 – 128.02 (m), 127.43 (d, *J* = 4.1 Hz), 120.92 (s), 35.65 (d, *J* = 13.3 Hz), 33.32 (s), 29.69 (s), 22.31 (d, *J* = 3.5 Hz), 13.92 (s).

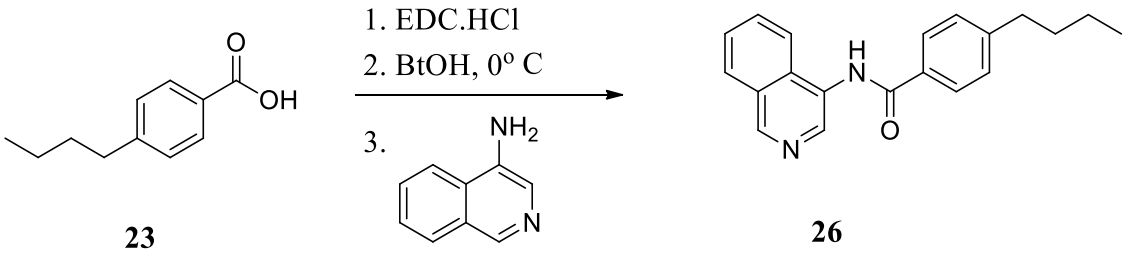


**23** **21** **26**

Figure 4.9. Synthesis of 4-butyl-N-(isoquinolin-4-yl)benzamide.

### 4.4.9. Synthesis of N-(4-butylphenyl)isoquinoline-5-carboxamide

Compound **29** was synthesized through EDC coupling. Isoquinoline-5-carboxylic acid **6** (0.28 mmol, 50 mg) was dissolved in 3.5 ml:1.5 mL $DCM_{dry}/DMF_{dry}$ under $N_2$. To this solution, EDC.HCl reagent (0.28 mmol, 54 mg) was added and then BtOH (0.28 mmol, 38 mg) was added and mixed at $0^oC$ for 30 minutes. This step is followed by the amine-addition step: e **21** (0.14 mmol, 20 mg) was added and the reaction mixture was stirred for 24 hours. This mixture is dissolved in 15 mL EtOAc and extracted 3 times with 150 mL distilled water, 50 mL saturated $NaHCO_3$ and 50 mL brine, respectively. The organic layer was dried over $Na_2SO_4$, filtered and concentrated under reduced pressure. The crude product was impure and the purification was achieved by column chromatography using silica gel as the stationary phase and 100% DCM as the eluent phase. The final product was a light brown viscous liquid with 24% yield. **$^1$H NMR** (400 MHz, $CDCl_3$) δ 8.55 (d, *J* = 11.5 Hz, 1H), 8.28 (d, *J* = 1.8 Hz, 1H), 7.76 (s, 1H), 7.39 – 7.34 (m, 1H), 7.08 (t, *J* = 9.1 Hz, 2H), 6.94 – 6.89 (m, 1H), 2.51 (dq, *J* = 12.4, 6.4 Hz, 2H), 1.63 (s, 1H), 1.54 – 1.46 (m, 2H), 1.27 (dqd, *J* = 14.6, 7.3, 3.3 Hz, 2H), 0.86 – 0.79 (m, 2H).

.

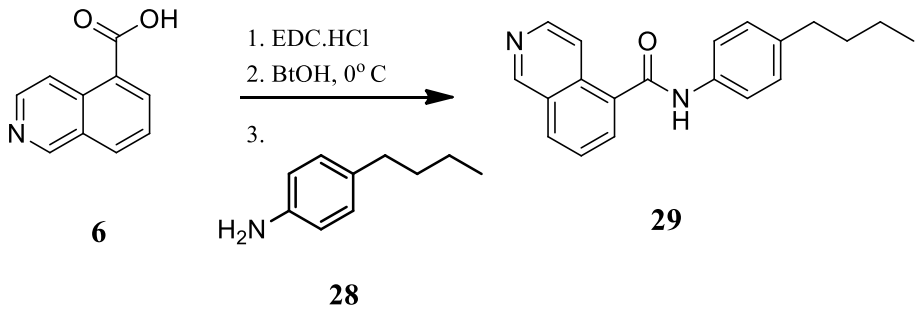


**6** **28** **29**

Figure 4.10. Synthesis of N-(4-butylphenyl)isoquinoline-5-carboxamide.

### 4.4.10. Synthesis of N-(4-pentylphenyl)isoquinoline-5-carboxamide

Compound **31** was synthesized through EDC coupling. Isoquinoline-5-carboxylic acid **6** (0.28 mmol, 50 mg) was dissolved in 3.5 ml:1.5 mL $DCM_{dry}/DMF_{dry}$ under $N_2$. To this solution, EDC.HCl reagent (0.28 mmol, 54 mg) was added and then BtOH (0.28 mmol, 38 mg) was added and mixed at $0^oC$ for 30 minutes. This step is followed by the amine-addition step: 4-butylaniline **30** (0.14 mmol, 22.8 mg) was added and the reaction mixture was stirred for 24 hours. This mixture is dissolved in 15 mL EtOAc and extracted 3 times with 150 mL distilled water, 50 mL saturated $NaHCO_3$ and 50 mL brine, respectively. The organic layer was dried over $Na_2SO_4$, filtered and concentrated under reduced pressure. The crude product was impure and the purification was achieved by column chromatography using silica gel as the stationary phase and EtOAc/ Hexane (1:1) as the eluent phase. The final product was a light brown viscous liquid with 21% yield. **$^1$H NMR** (400 MHz, $CDCl_3$) δ 9.24 (s, 1H), 8.54 (d, *J* = 6.1 Hz, 1H), 8.18 – 7.84 (m, 4H), 7.64 (s, 1H), 7.62 – 7.56 (m, 1H), 7.52 (d, *J* = 8.1 Hz, 2H), 7.16 (d, *J* = 7.8 Hz, 2H), 6.85 (dd, *J* = 8.0, 1.8 Hz, 1H), 2.44 – 2.39 (m, 2H), 2.12 (dt, *J* = 13.7, 5.0 Hz, 2H), 1.29 – 1.21 (m, 11H), 0.84 (t, *J* = 5.6 Hz, 4H).

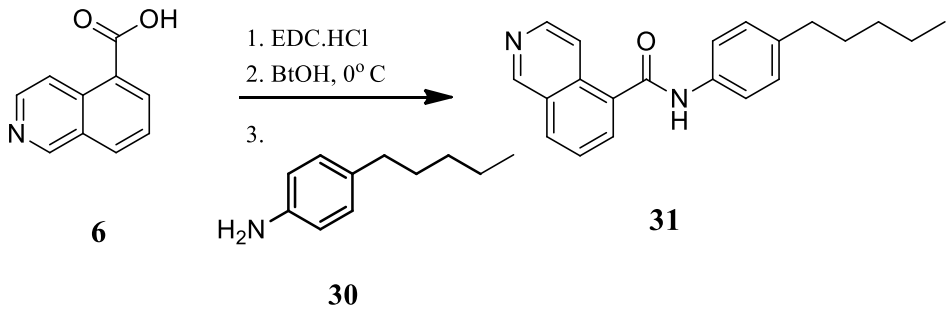


**6** **30** **31**

Figure 4.11. Synthesis of N-(4-pentylphenyl)isoquinoline-5-carboxamide.

### 4.4.11. Synthesis of N-(isoquinolin-5-yl)-4-pentylbenzamide

Compound **33** was synthesized through EDC coupling. 4-pentylbenzoic acid **32** (0.35 mmol, 67.28 mg) was dissolved in 3.5 ml:1.5 mL $DCM_{dry}/DMF_{dry}$ under $N_2$. To this solution, EDC.HCl reagent (0.35 mmol, 67.095 mg) was added and then BtOH (0.35 mmol, 47.3 mg) was added and mixed at 0°C for 30 minutes. This step is followed by the amine-addition step: 4-aminoisoquinoline **16** (0.17 mmol, 24.5 mg) was added and the reaction mixture was stirred for 24 hours. This mixture is dissolved in 15 mL EtOAc and extracted 3 times with 150 mL distilled water, 50 mL saturated $NaHCO_3$ and 50 mL brine, respectively. The organic layer was dried over $Na_2SO_4$, filtered and concentrated under reduced pressure. The crude product was impure and the purification was achieved by column chromatography using silica gel as the stationary phase and EtOAc/ Hexane (1:5) as the eluent phase. The final product was a yellow solid with 56% yield. **$^1$H NMR** (400 MHz, $CDCl_3$) δ 8.20 – 8.16 (m, 1H), 8.10 – 8.07 (m, 1H), 8.01 (d, *J* = 8.3 Hz, 1H), 7.55 (d, *J* = 0.9 Hz, 1H), 7.53 (dt, *J* = 2.2, 1.1 Hz, 1H), 7.52 (d, *J* = 1.0 Hz, 1H), 7.48 – 7.46 (m, 1H), 7.46 – 7.44 (m, 1H), 7.43 (dd, *J* = 1.6, 1.2 Hz, 1H), 7.42 – 7.38 (m, 1H), 7.27 – 7.24 (m, 1H), 2.78 – 2.63 (m, 1H), 1.83 – 1.51 (m, 1H), 1.40 – 1.18 (m, 1H), 1.01 – 0.78 (m, 1H).

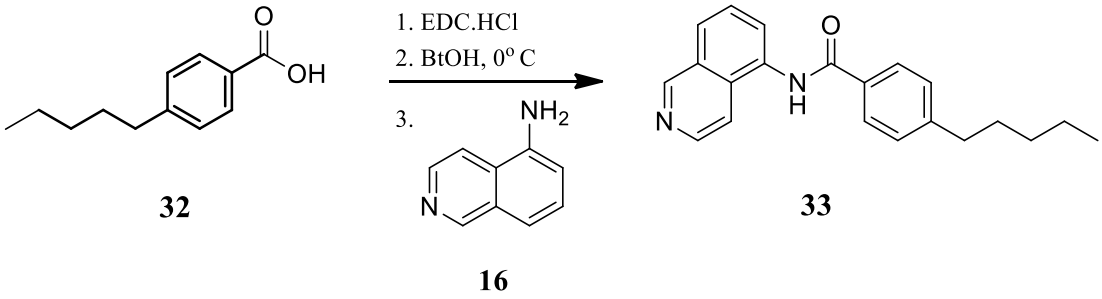


**32** **16** **33**

Figure 4.12. Synthesis of N-(isoquinolin-5-yl)-4-pentylbenzamide.

### 4.4.12. Synthesis of N-(isoquinolin-5-yl)-4-hexylbenzamide

Compound **35** was synthesized through EDC coupling. 4-hexylbenzoic acid **34** (0.35 mmol, 72.2 mg) was dissolved in 3.5 ml:1.5 mL $DCM_{dry}/DMF_{dry}$ under $N_2$. To this solution, EDC.HCl reagent (0.35 mmol, 67.095 mg) was added and then BtOH (0.35 mmol, 47.3 mg) was added and mixed at $0^oC$ for 30 minutes. This step is followed by the amine-addition step: 5-aminoisoquinoline **16** (0.17 mmol, 24.5 mg) was added and the reaction mixture was stirred for 24 hours. This mixture is dissolved in 15 mL EtOAc and extracted 3 times with 150 mL distilled water, 50 mL saturated $NaHCO_3$ and 50 mL brine, respectively. The organic layer was dried over $Na_2SO_4$, filtered and concentrated under reduced pressure. The crude product was impure and the purification was achieved by column chromatography using silica gel as the stationary phase and EtOAc/ Hexane (1:5) as the eluent phase. The final product was a yellow solid with 51% yield. **$^1$H NMR** (400 MHz, $CDCl_3$) δ 8.14 – 8.10 (m, 1H), 8.04 (dt, *J* = 8.4, 0.9 Hz, 1H), 7.50 (d, *J* = 0.9 Hz, 1H), 7.48 (dd, *J* = 1.6, 1.0 Hz, 1H), 7.47 (d, *J* = 1.0 Hz, 1H), 7.41 (t, *J* = 1.0 Hz, 1H), 7.39 (dd, *J* = 2.1, 1.1 Hz, 1H), 7.39 – 7.37 (m, 1H), 7.35 (dd, *J* = 6.2, 4.8 Hz, 1H), 2.73 – 2.64 (m, 1H), 1.61 (dt, *J* = 15.3, 7.5 Hz, 1H), 1.35 – 1.20 (m, 2H), 0.86 – 0.80 (m, 1H).

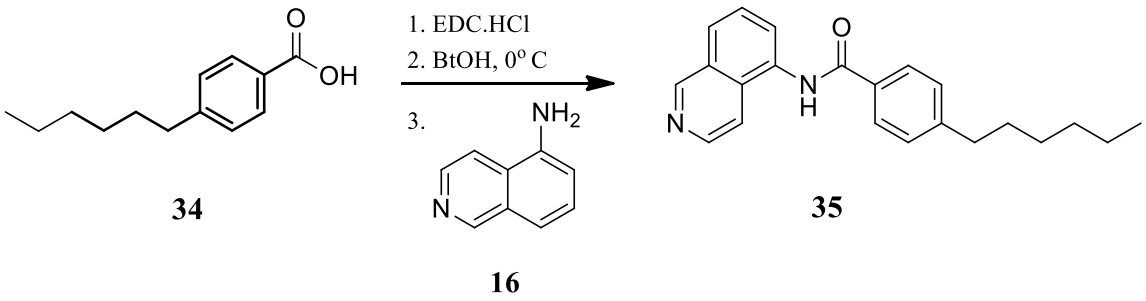


Figure 4.13. Synthesis of N-(isoquinolin-5-yl)-4-hexylbenzamide.

### 4.4.13. Synthesis of N-(isoquinolin-6-yl)-3,5-dimethoxy-2-naphthamide

Compound **37** was synthesized through EDC coupling. 3,5-dimethoxy-2-naphthoic acid **27** (0.35 mmol, 78.9 mg) was dissolved in 3.5 ml:1.5 mL $DCM_{dry}/DMF_{dry}$ under $N_2$. To this solution, EDC.HCl reagent (0.35 mmol, 67.095 mg) was added and then BtOH (0.35 mmol, 47.3 mg) was added and mixed at 0°C for 30 minutes. This step is followed by the amine-addition step: 6-aminoisoquinoline **36** (0.17 mmol, 24.5 mg) was added and the reaction mixture was stirred for 24 hours. This mixture is dissolved in 15 mL EtOAc and extracted 3 times with 150 mL distilled water, 50 mL saturated $NaHCO_3$ and 50 mL brine, respectively. The organic layer was dried over $Na_2SO_4$, filtered and concentrated under reduced pressure. The crude product was impure and the purification was achieved by column chromatography using silica gel as the stationary phase and EtOAc/ Hexane (1:3) as the eluent phase. The final product was a pink solid with 93% yield. **$^1$H NMR** (400 MHz, $CDCl_3$) δ 10.26 (s, 1H), 9.11 (s, 1H), 8.78 (s, 1H), 8.46 (d, $J$ = 21.4 Hz, 1H), 7.89 (s, 1H), 7.63 (d, $J$ = 24.7 Hz, 1H), 7.48 (s, 1H), 7.30 (s, 1H), 7.19 (s, 1H), 6.86 (s, 1H), 4.17 (s, 1H), 3.97 (s, 1H).

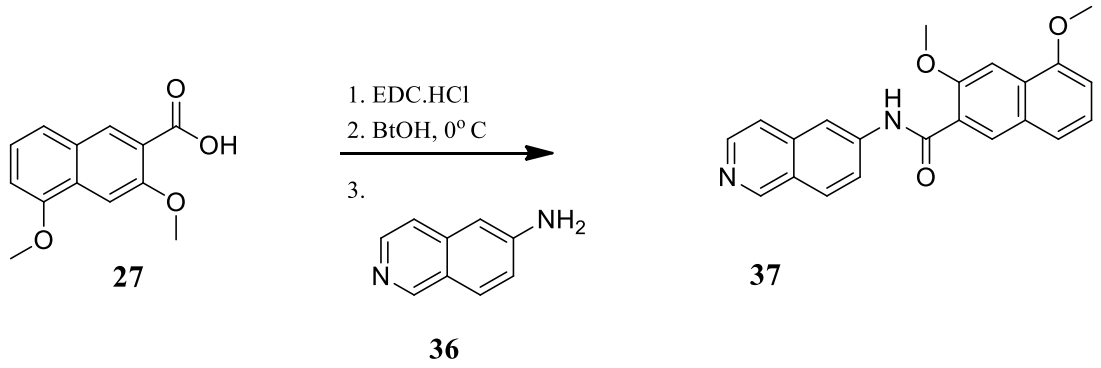


Figure 4.14. Synthesis of N-(isoquinolin-6-yl)-3,5-dimethoxy-2-naphthamide.

### 4.4.14. Synthesis of 6-fluoro-N-(isoquinolin-6-yl)-2-naphthamide

Compound **39** was synthesized through EDC coupling. 6-fluoro-2-naphthoic acid **38** (0.27 mmol, 51.4 mg) was dissolved in 3.5 ml:1.5 mL $DCM_{dry}/DMF_{dry}$ under $N_2$. To this solution, EDC.HCl reagent (0.27 mmol, 36.48 mg) was added and then BtOH (0.35 mmol, 47.3 mg) was added and mixed at $0^oC$ for 30 minutes. This step is followed by the amine-addition step: 6-aminoisoquinoline **36** (0.135 mmol, 19.46 mg) was added and the reaction mixture was stirred for 24 hours. This mixture is dissolved in 15 mL EtOAc and extracted 3 times with 150 mL distilled water, 50 mL saturated $NaHCO_3$ and 50 mL brine, respectively. The organic layer was dried over $Na_2SO_4$, filtered and concentrated under reduced pressure. The crude product was impure and the purification was achieved by column chromatography using silica gel as the stationary phase and EtOAc/ Hexane (1:1) as the eluent phase. The final product was a white solid with 87% yield. **$^1$H NMR** (400 MHz, $CDCl_3$) δ 8.84 (s, 1H), 8.17 (d, *J* = 8.7 Hz, 1H), 8.06 (dd, *J* = 8.4, 0.7 Hz, 1H), 8.00 (dd, *J* = 9.0, 5.5 Hz, 1H), 7.92 (d, *J* = 8.7 Hz, 1H), 7.52 (dd, *J* = 6.9, 5.0 Hz, 2H), 7.49 (s, 1H), 7.45 (s, 1H), 7.43 – 7.41 (m, 1H), 7.41 – 7.38 (m, 1H), 7.36 (dd, *J* = 8.7, 2.5 Hz, 1H).

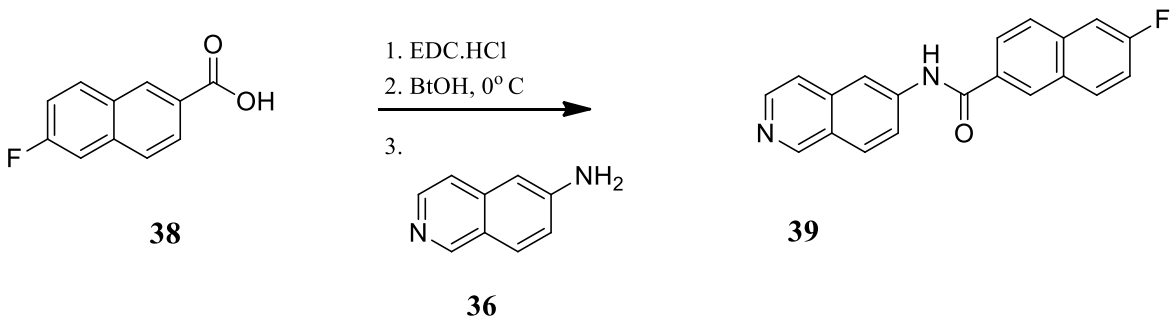


**38** **36** **39**

Figure 4.15. Synthesis of 6-fluoro-N-(isoquinolin-6-yl)-2-naphthamide.

### 4.4.15. Synthesis of N-(isoquinolin-6-yl)-6-methoxy-2-naphthamide

Compound **40** was synthesized through EDC coupling. 6-methoxy-2-naphthoic acid **15** (0.33 mmol, 66.72 mg) was dissolved in 3.5 ml:1.5 mL $DCM_{dry}/DMF_{dry}$ under $N_2$. To this solution, EDC.HCl reagent (0.33 mmol, 63.26 mg) was added and then BtOH (0.33 mmol, 44.58 mg) was added and mixed at $0^oC$ for 30 minutes. This step is followed by the amine-addition step: 6-aminoisoquinoline **36** (0.16 mmol, 23.4 mg) was added and the reaction mixture was stirred for 24 hours. This mixture is dissolved in 15 mL EtOAc and extracted 3 times with 150 mL distilled water, 50 mL saturated $NaHCO_3$ and 50 mL brine, respectively. The organic layer was dried over $Na_2SO_4$, filtered and concentrated under reduced pressure. The crude product was impure and the purification was achieved by column chromatography using silica gel as the stationary phase and EtOAc/ Hexane (1:1) as the eluent phase. The final product was a white solid with 85% yield. **$^1$H NMR** (400 MHz, $CDCl_3$) δ 8.74 (s, 1H), 8.09 (d, *J* = 8.6 Hz, 1H), 8.05 (d, *J* = 8.4 Hz, 1H), 7.87 (s, 1H), 7.84 (d, *J* = 5.8 Hz, 1H), 7.81 (s, 1H), 7.48 (d, *J* = 6.8 Hz, 1H), 7.45 (s, 1H), 7.21 (d, *J* = 9.0 Hz, 1H), 7.19 (s, 1H), 7.15 (s, 1H), 3.96 – 3.86 (m, 4H).

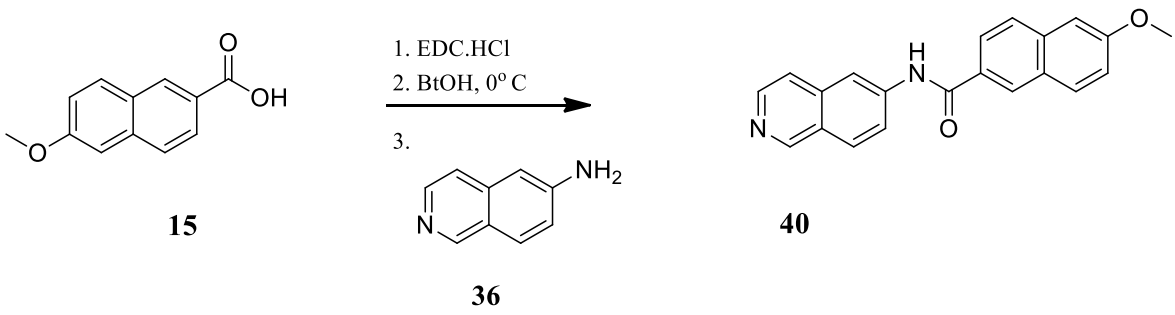


Figure 4.16. Synthesis of N-(isoquinolin-6-yl)-6-methoxy-2-naphthamide.

### 4.4.16. Synthesis of N-(4-hexylphenyl)isoquinoline-5-carboxamide

Compound **41** was synthesized through EDC coupling. Isoquinoline-5-carboxylic acid **16** (0.28 mmol, 49.8 mg) was dissolved in 3.5 ml:1.5 mL $DCM_{dry}/DMF_{dry}$ under $N_2$. To this solution, EDC.HCl reagent (0.28 mmol, 53.67 mg) was added and then BtOH (0.28 mmol, 37.8 mg) was added and mixed at $0^oC$ for 30 minutes. This step is followed by the amine-addition step: 4-hexylaniline **18** (0.14 mmol, 25.5 mg) was added and the reaction mixture was stirred for 24 hours. This mixture is dissolved in 15 mL EtOAc and extracted 3 times with 150 mL distilled water, 50 mL saturated $NaHCO_3$ and 50 mL brine, respectively. The organic layer was dried over $Na_2SO_4$, filtered and concentrated under reduced pressure. The crude product was impure and the purification was achieved by column chromatography using silica gel as the stationary phase and EtOAc/ Hexane (1:1) as the eluent phase. The final product was a pale yellow solid with 74% yield. **$^1$H NMR** (400 MHz, $CDCl_3$) δ 9.01 (d, *J* = 0.8 Hz, 1H), 8.38 (s, 1H), 8.33 (d, *J* = 6.0 Hz, 1H), 7.97 (d, *J* = 6.0 Hz, 1H), 7.82 (d, *J* = 8.2 Hz, 1H), 7.75 (d, *J* = 6.9 Hz, 1H), 7.50 (d, *J* = 8.2 Hz, 1H), 7.40 (dd, *J* = 8.1, 7.2 Hz, 1H), 7.10 (d, *J* = 8.3 Hz, 1H), 2.55 – 2.47 (m, 1H), 1.53 (dd, *J* = 14.7, 7.1 Hz, 1H), 1.31 – 1.17 (m, 3H), 0.82 – 0.76 (m, 1H).

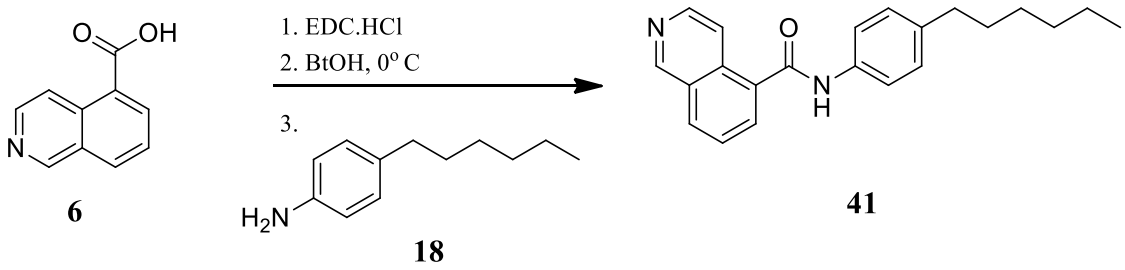


Figure 4.17. Synthesis of N-(4-hexylphenyl)isoquinoline-5-carboxamide.

## 4.5. Syntheses of 2-Benzofuran, 2-Benzo[b]thiophene and 3-(1H-Tetrazol-5-yl) Benzoic Acid Left Hand-Side Derivatives

### 4.5.1. Synthesis of 1-(Benzo[b]thiophen-2-yl)-2-(4-pentylphenyl)ethanone

Compound **43** was synthesized through EDC coupling. Benzo[b]thiophene-2-carboxylic acid **42** (0.82 mmol, 146.13 mg) was dissolved in 3.5 ml:1.5 mL $DCM_{dry}/DMF_{dry}$ under $N_2$. To this solution, EDC.HCl reagent (0.82 mmol, 155.27 mg) was added and then BtOH (0.82 mmol, 110.79 mg) was added and mixed at $0^oC$ for 30 minutes. This step is followed by the amine-addition step: 4-pentylaniline **30** (0.54 mmol, 88.16 mg) was added and the reaction mixture was stirred for 24 hours. This mixture is dissolved in 15 mL EtOAc and extracted 3 times with 150 mL distilled water, 50 mL saturated $NaHCO_3$ and 50 mL brine, respectively. The organic layer was dried over $Na_2SO_4$, filtered and concentrated under reduced pressure. The crude product was impure and the purification was achieved by column chromatography using silica gel as the stationary phase and DCM/ Hexane (1:1) as the eluent phase. The final product was a beige solid 98% yield. **$^1$H NMR** (400 MHz, $CDCl_3$) δ 7.92 – 7.72 (m, 49H), 7.58 – 7.50 (m, 25H), 7.43 (pd, 25H), 7.26 (s, 7H), 7.18 (d, 25H), 2.64 – 2.55 (m, 26H), 1.70 – 1.44 (m, 44H), 1.42 – 1.17 (m, 56H), 0.89 (t, 37H), 0.79 – 0.68 (m, 1H).

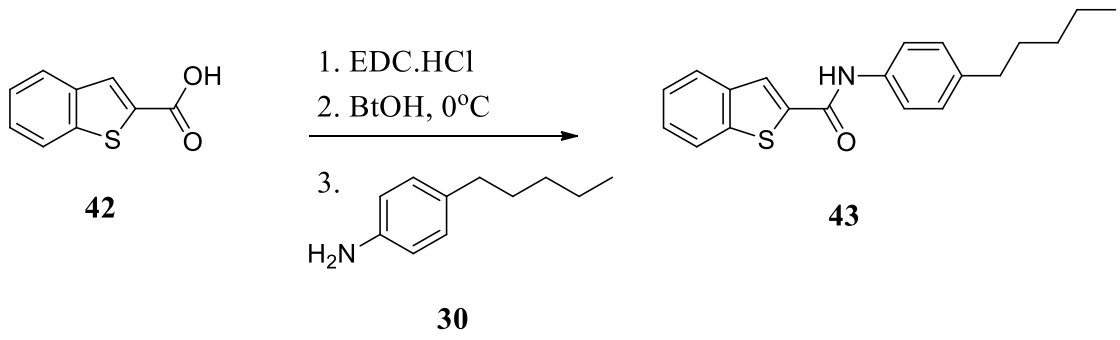


**42** **30** **43**

Figure 4.18. Synthesis of 1-(Benzo[b]thiophen-2-yl)-2-(4-pentylphenyl)ethanone.

### 4.5.2. Synthesis of 1-(Benzo[b]thiophen-2-yl)-2-(4-hexylphenyl)ethanone

Compound **44** was synthesized through EDC coupling. Benzo[b]thiophene-2-carboxylic acid **42** (0.82 mmol, 146.13 mg) was dissolved in 3.5 ml:1.5 mL DCMdry/$DMF_{dry}$ under $N_2$. To this solution, EDC.HCl reagent (0.82 mmol, 155.27 mg) was added and then BtOH (0.82 mmol, 110.79 mg) was added and mixed at $0^oC$ for 30 minutes. This step is followed by the amine-addition step: 4-hexylaniline **18** (0.54 mmol, 95.73 mg) was added and the reaction mixture was stirred for 24 hours. This mixture is dissolved in 15 mL EtOAc and extracted 3 times with 150 mL distilled water, 50 mL saturated $NaHCO_3$ and 50 mL brine, respectively. The organic layer was dried over $Na_2SO_4$, filtered and concentrated under reduced pressure. The crude product was impure and the purification was achieved by column chromatography using silica gel as the stationary phase and DCM/ Hexane (1:1) as the eluent phase. The final product was a beige solid with 96% yield. **$^1$H NMR** (400 MHz, $CDCl_3$) δ 7.81 (dt, *J* = 5.3, 2.4 Hz, 53H), 7.68 (s, 23H), 7.48 (d, *J* = 8.5 Hz, 37H), 7.44 – 7.31 (m, 38H), 7.22 – 7.09 (m, 89H), 2.58 – 2.49 (m, 38H), 2.15 – 2.07 (m, 71H), 1.52 (d, *J* = 15.7 Hz, 144H), 1.29 – 1.10 (m, 118H), 0.90 – 0.74 (m, 57H). **$^{13}$C NMR** (101 MHz, $CDCl_3$) δ 141.01 (s), 139.69 (s), 139.06 (s), 135.00 (s), 129.00 (s), 126.53 (s), 125.53 (s), 125.08 (d, *J* = 10.5 Hz), 122.73 (s), 120.30 (s), 35.40 (s), 31.71 (s), 31.44 (s), 28.91 (s), 22.61 (s), 14.10 (s).

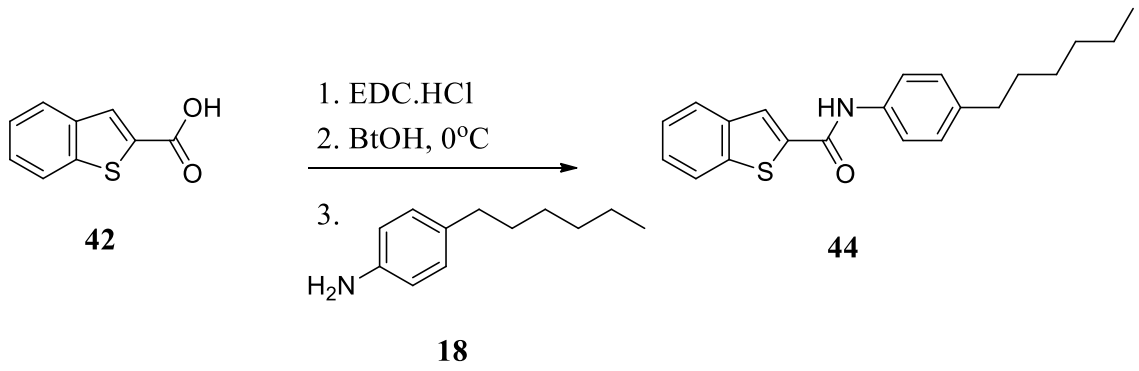


Figure 4.19. Synthesis of 1-(Benzo[b]thiophen-2-yl)-2-(4-hexylphenyl)ethanone.

### 4.5.3. Synthesis of Ethyl 4-(benzo[b]thiophene-2-carboxamido)benzoate

Compound **45** was synthesized through EDC coupling. Benzo[b]thiophene-2-carboxylic acid **42** (1 mmol, 178.2 mg) was dissolved in 3.5 ml:1.5 mL $DCM_{dry}/DMF_{dry}$ under $N_2$. To this solution, EDC.HCl reagent (1 mmol, 191.7 mg) was added and then BtOH (1 mmol, 135.12 mg) was added and mixed at 0°C for 30 minutes. This step is followed by the amine-addition step: Ethyl-4-aminobenzoate **1** (0.82 mmol, 135.45 mg) was added and the reaction mixture was stirred for 24 hours. This mixture is dissolved in 15 mL EtOAc and extracted 3 times with 150 mL distilled water, 50 mL saturated $NaHCO_3$ and 50 mL brine, respectively. The organic layer was dried over $Na_2SO_4$, filtered and concentrated under reduced pressure. The crude product was impure and the purification was achieved by column chromatography using silica gel as the stationary phase and EtOAc/ Hexane (2:1) as the eluent phase. The final product was a white solid with 93% yield. **$^1$H NMR** (400 MHz, $CDCl_3$) δ 8.48 (s, 65H), 8.09 (d, *J* = 8.2 Hz, 122H), 7.81 (d, *J* = 8.5 Hz, 125H), 7.72 (d, *J* = 7.8 Hz, 61H), 7.60 (d, *J* = 19.6 Hz, 81H), 7.50 (dd, *J* = 24.1, 16.8 Hz, 102H), 7.38 – 7.13 (m, 116H), 7.19 – 7.13 (m, 2H), 4.38 (d, *J* = 7.0 Hz, 135H), 2.17 (s, 5H), 1.58 (s, 128H), 1.40 (t, *J* = 7.0 Hz, 188H), 1.25 (s, 6H).

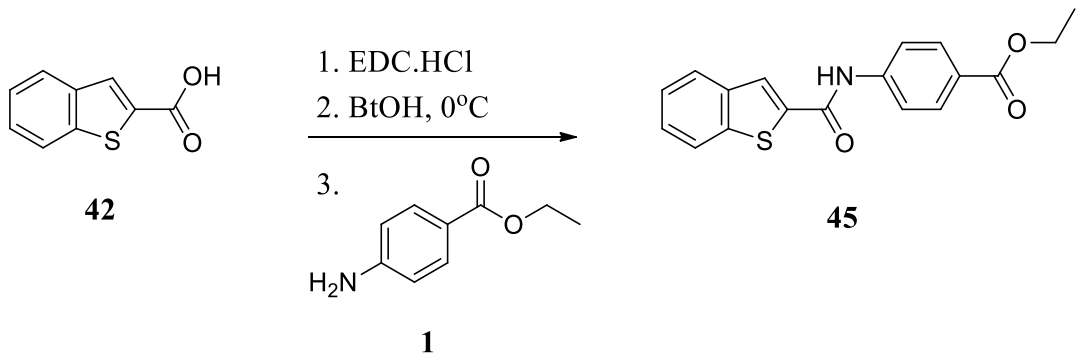


Figure 4.20. Synthesis of Ethyl 4-(benzo[b]thiophene-2-carboxamido)benzoate.

### 4.5.4. Synthesis of Ethyl 4-(benzofuran-2-carboxamido)benzoate

Compound **47** was synthesized through EDC coupling. Benzofuran-2-carboxylic acid **46** (1 mmol, 162.14 mg) was dissolved in 3.5 ml:1.5 mL $DCM_{dry}/DMF_{dry}$ under $N_2$. To this solution, EDC.HCl reagent (1 mmol, 191.7 mg) was added and then BtOH (1 mmol, 135.12 mg) was added and mixed at $0^oC$ for 30 minutes. This step is followed by the amine-addition step: Ethyl-4-aminobenzoate **1**(0.82 mmol, 135.45 mg) was added and the reaction mixture was stirred for 24 hours. This mixture is dissolved in 15 mL EtOAc and extracted 3 times with 150 mL distilled water, 50 mL saturated $NaHCO_3$ and 50 mL brine, respectively. The organic layer was dried over $Na_2SO_4$, filtered and concentrated under reduced pressure. The crude product was impure and the purification was achieved by column chromatography using silica gel as the stationary phase and DCM/ Hexane (1:1) as the eluent phase. The final product was a yellow viscous liquid with 97% yield. **$^1$H NMR** (400 MHz, $CDCl_3$) δ 8.15 – 8.04 (m, 23H), 8.03 – 7.85 (m, 46H), 7.81 – 7.70 (m, 24H), 7.46 (dqd, *J* = 14.6, 7.1, 1.2 Hz, 24H), 7.30 – 7.23 (m, 25H), 4.38 (dt, *J* = 10.0, 5.7 Hz, 24H), 2.17 (s, 1H), 1.55 (d, *J* = 11.6 Hz, 37H), 1.46 – 1.36 (m, 35H), 1.25 (s, 3H).

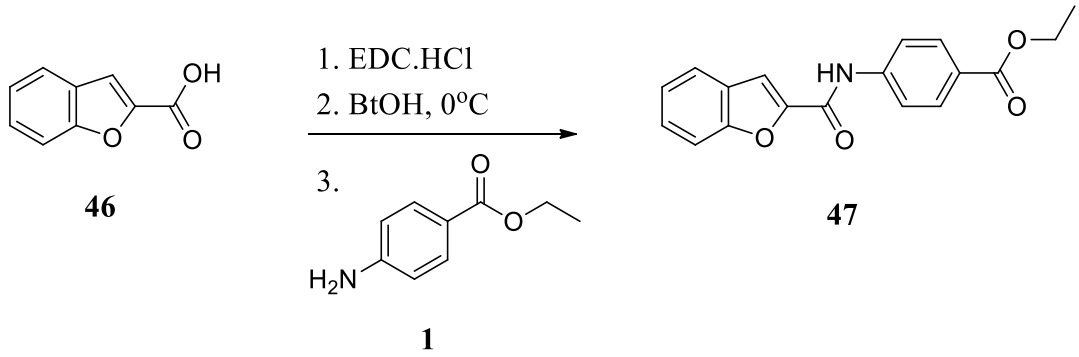


**46** **1** **47**

Figure 4.21. Synthesis of Ethyl 4-(benzofuran-2-carboxamido)benzoate.

### 4.5.5. Synthesis of N-(4-hexylphenyl)benzofuran-2-carboxamide

Compound **48** was synthesized through EDC coupling. Benzofuran-2-carboxylic acid **46** (1 mmol, 162.14 mg) was dissolved in 3.5 ml:1.5 mL $DCM_{dry}/DMF_{dry}$ under $N_2$. To this solution, EDC.HCl reagent (1 mmol, 191.7 mg) was added and then BtOH (1 mmol, 135.12 mg) was added and mixed at $0^oC$ for 30 minutes. This step is followed by the amine-addition step: 4-hexylaniline **18** (0.66 mmol, 117.01 mg) was added and the reaction mixture was stirred for 24 hours. This mixture is dissolved in 15 mL EtOAc and extracted 3 times with 150 mL distilled water, 50 mL saturated $NaHCO_3$ and 50 mL brine, respectively. The organic layer was dried over $Na_2SO_4$, filtered and concentrated under reduced pressure. The crude product was impure and the purification was achieved by column chromatography using silica gel as the stationary phase and DCM/ Hexane (2:1) as the eluent phase. The final product was a pale yellow solid with 91% yield. **$^1$H NMR** (400 MHz, $CDCl_3$) δ 8.30 (s, 3H), 7.70 (d, *J* = 7.8 Hz, 3H), 7.67 – 7.52 (m, 11H), 7.45 (dd, *J* = 8.4, 7.2 Hz, 3H), 7.37 – 7.16 (m, 16H), 2.65 – 2.55 (m, 6H), 1.83 – 1.54 (m, 15H), 1.31 (s, 20H), 0.88 (dd, *J* = 7.2, 5.9 Hz, 9H).

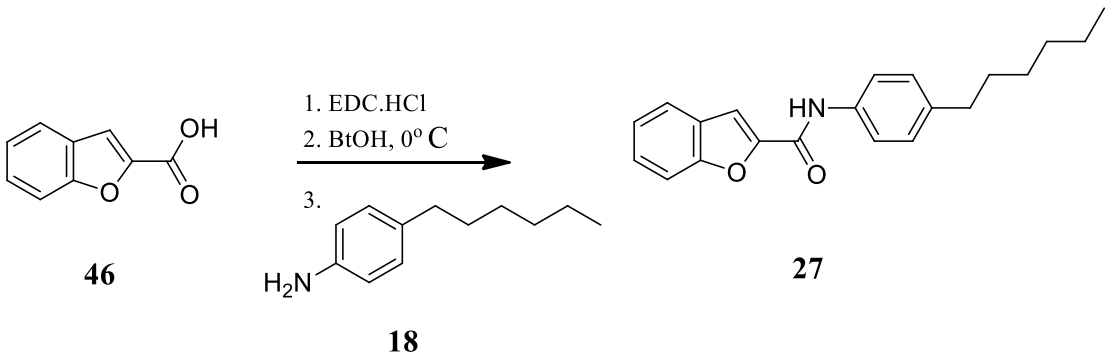


Figure 4.22. Synthesis of N-(4-hexylphenyl)benzofuran-2-carboxamide.

### 4.5.6. Synthesis of N-(4-butylphenyl)-4-(1H-tetrazol-5-yl)benzamide

Compound **50** was synthesized through EDC coupling. 4-(1H-tetrazol-5-yl)benzoic acid **49** (0.82 mmol, 155.93 mg) was dissolved in 3.5 ml:1.5 mL $DCM_{dry}/DMF_{dry}$ under $N_2$. To this solution, EDC.HCl reagent (0.82 mmol, 157.2 mg) was added and then BtOH (0.82, 110.8 mg) was added and mixed at $0^oC$ for 30 minutes. This step is followed by the amine-addition step: 4-butylaniline **21** (0.54 mmol, 80.58 mg) was added and the reaction mixture was stirred for 24 hours. This mixture is dissolved in 15 mL EtOAc and extracted 3 times with 150 mL distilled water, 50 mL saturated $NaHCO_3$ and 50 mL brine, respectively. The organic layer was dried over $Na_2SO_4$, filtered and concentrated under reduced pressure. The crude product was impure and the purification was achieved by column chromatography using silica gel as the stationary phase and EtOAc/ Hexane (1:3) as the eluent phase. The final product was a brown liquid with 37% yield. **$^1$H NMR** (400 MHz, $CDCl_3$) δ 8.55 (d, *J* = 11.5 Hz, 81H), 8.29 (d, *J* = 1.7 Hz, 71H), 7.96 (s, 10H), 7.53 – 7.48 (m, 42H), 7.36 (d, *J* = 8.5 Hz, 152H), 7.22 – 7.15 (m, 114H), 7.09 (t, *J* = 8.7 Hz, 398H), 6.96 – 6.88 (m, 189H), 6.70 (d, *J* = 8.6 Hz, 28H), 5.99 (d, *J* = 7.0 Hz, 20H), 2.57 – 2.46 (m, 342H), 2.39 (s, 23H), 2.09 (d, *J* = 5.7 Hz, 13H), 1.82 (s, 12H), 1.57 – 1.41 (m, 503H), 1.41 – 1.11 (m, 592H), 0.90 – 0.77 (m, 593H), -0.00 (s, 13H).

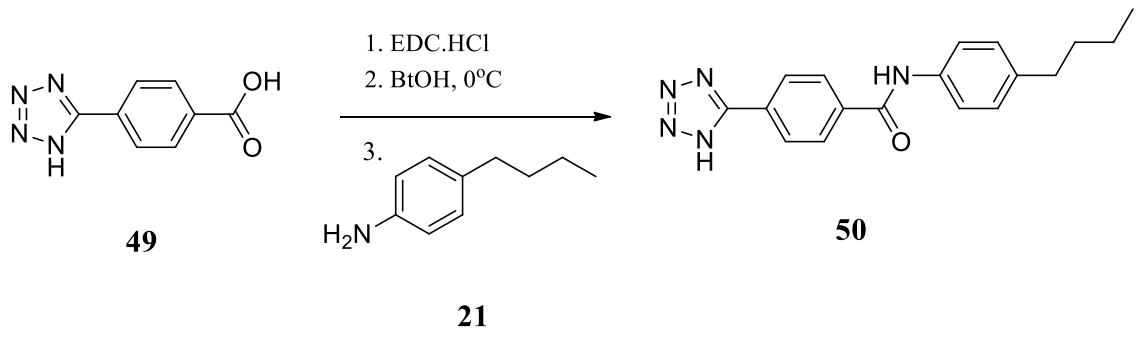


Figure 4.23. Synthesis of N-(4-butylphenyl)-4-(1H-tetrazol-5-yl)benzamide.

### 4.5.7. Synthesis of N-(4-pentylphenyl)-4-(1H-tetrazol-5-yl)benzamide

Compound **51** was synthesized through EDC coupling. 4-(1H-tetrazol-5-yl)benzoic acid **49** (0.82 mmol, 155.93 mg) was dissolved in 3.5 ml:1.5 mL $DCM_{dry}$/$DMF_{dry}$ under $N_2$. To this solution, EDC.HCl reagent (0.82 mmol, 157.2 mg) was added and then BtOH (0.82, 110.8 mg) was added and mixed at 0°C for 30 minutes. This step is followed by the amine-addition step: 4-penylaniline **30** (0.54 mmol, 88.16 mg) was added and the reaction mixture was stirred for 24 hours. This mixture is dissolved in 15 mL EtOAc and extracted 3 times with 150 mL distilled water, 50 mL saturated $NaHCO_3$ and 50 mL brine, respectively. The organic layer was dried over $Na_2SO_4$, filtered and concentrated under reduced pressure. The crude product was impure and the purification was achieved by column chromatography using silica gel as the stationary phase and EtOAc/ Hexane (1:1) as the eluent phase. The final product was a brown liquid with 69% yield. **$^1$H NMR** (400 MHz, $CDCl_3$) δ 8.55 (d, *J* = 11.5 Hz, 29H), 8.28 (d, *J* = 1.8 Hz, 25H), 7.71 (s, 26H), 7.52 – 7.37 (m, 9H), 7.37 – 7.30 (m, 50H), 7.23 – 7.03 (m, 160H), 7.00 – 6.70 (m, 85H), 6.59 – 6.10 (m, 23H), 2.52 – 2.49 (m, 4H), 1.58 – 1.47 (m, 6H), 1.32 – 1.17 (m, 13H), 0.81 (dd, *J* = 4.3, 2.7 Hz, 6H).

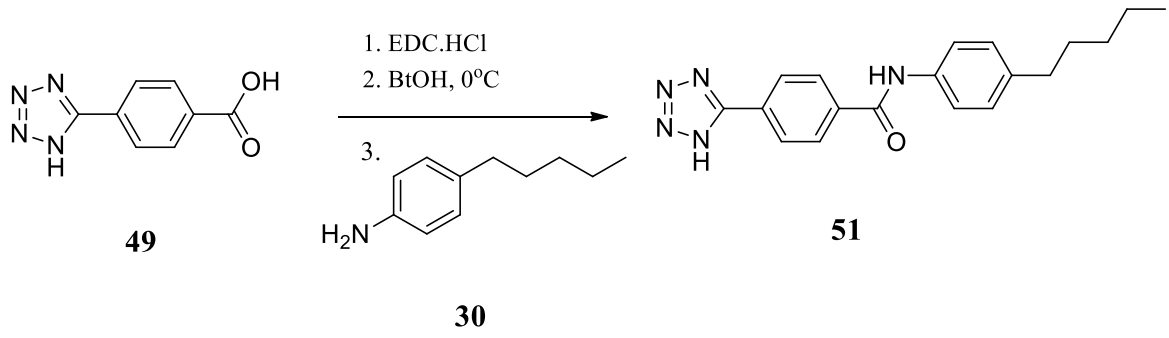


Figure 4.24. Synthesis of N-(4-pentylphenyl)-4-(1H-tetrazol-5-yl)benzamide.

## 4.6. Conversion of Amides into Thioamides

Conversion of amides into thioamide experiments was conducted according to the method represented in Elif Zengin's M.Sc. Thesis [33]. Both compounds were yellow solids with percent yields of 74% and 70%, respectively. **$^1$H NMR** for Compound **52** (400 MHz, $CDCl_3$) δ 9.01 (s, 56H), 7.92 (s, 8H), 7.74 (t, *J* = 8.9 Hz, 149H), 7.52 (t, *J* = 22.8 Hz, 139H), 7.40 – 7.27 (m, 121H), 7.22 – 7.16 (m, 133H), 7.04 (s, 18H), 2.60 – 2.51 (m, 119H), 2.09 (s, 3H), 1.64 – 1.37 (m, 169H), 1.37 – 0.99 (m, 259H), 0.87 (s, 7H), 0.83 (dd, *J* = 9.0, 5.0 Hz, 175H), 0.67 (s, 5H), -0.00 (s, 6H).

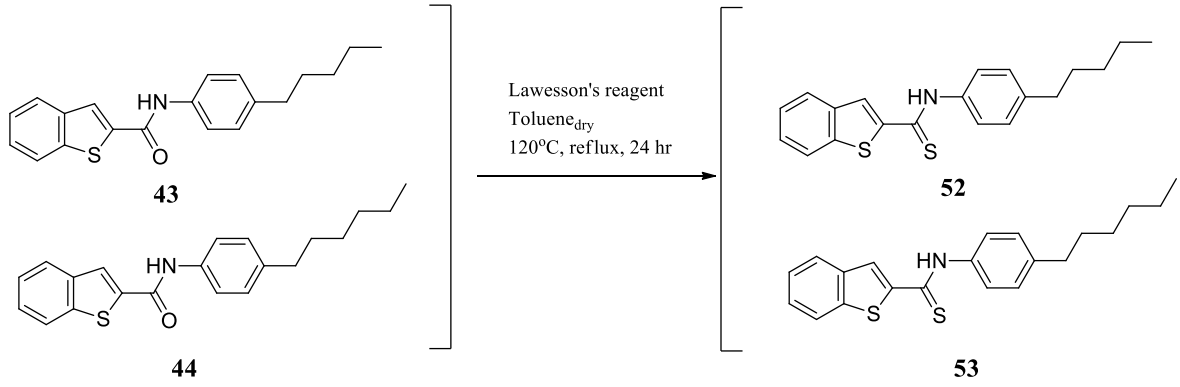


Figure 4.25. Conversion of amides into thioamides.

# 5. CONCLUSION

In this study, mainly the synthesis of isoquinoline derivatives as inhibitors of CYP17 were reported. Several potentially active heteroaromatic derivatives of the lead compound including benzothiophene, benzofuran and tetrazol rings were also designed and synthesized. The characterization of the synthesized drug candidates were done by $^{1}$H-NMR and $^{13}$C-NMR. The biological tests were to be done at the time the present thesis was written.

A detailed docking study was performed in order to investigate the interactions of isoquinoline derivatives with heme iron, leading to a better understanding of the nature of CYP17A1 enzyme. Due to the ease of leaning of hydrophobic right-hand side on I helix, isoquinoline derivatives having substituted at the 4$^{th}$ or 5$^{th}$ positions were observed as promising heme-coordinating groups. The docking configuration of 6-isoquinoline derivatives indicated the presence of a potential H-bonding with residues both on I helix and G-helix, eventuating the synthesis of miscellecenaous derivatives. Some isoquinoline derivatives, especially the ones having substituted at the 5$^{th}$ position, showed a small amount of activity in preliminary test at 1 μM. More biological testing needs to be done at higher concentrations since the $IC_{50}$ value of the lead compound is 36.5 μM.

In order to confirm the H-bonding network within the binding cavity, 2-benzofuran and 2-benzothiophene derivatives with 4-ethyl benzoate substituted right-hand side fragment were synthesized and their docking conformations were examined. Consistent with the theory, docking configurations of 4-ethyl benzoate substituted derivatives revealed that the ester group was forming H-bonding with both I-helix and G-helix, indicating that it would be worth to focus on these derivatives in future work.

Heme-coordinating capability of other sp$^2$ hybridized nitrogen bearing heterocycles were examined through tetrazol derivatives. Comparison of docking configuration of tetrazol derivatives with some CYP17A1 inhibitors currently under clinical trial was again confirmed the presence of H-bonding residues.

Heme-coordinating capability of amides *versus* thioamides were also evaluated. A carbothioamide compound made of 2-benzothiophene and n-hexyl substituted phenyl ring showed the lowest binding and docking energy among all derivatives synthesized so far.

# APPENDIX A: DOCKING CONFIGURATION DATA

This section reports the docking configurations of synthesized compounds with CYP17A1 *via* AutoDock4.

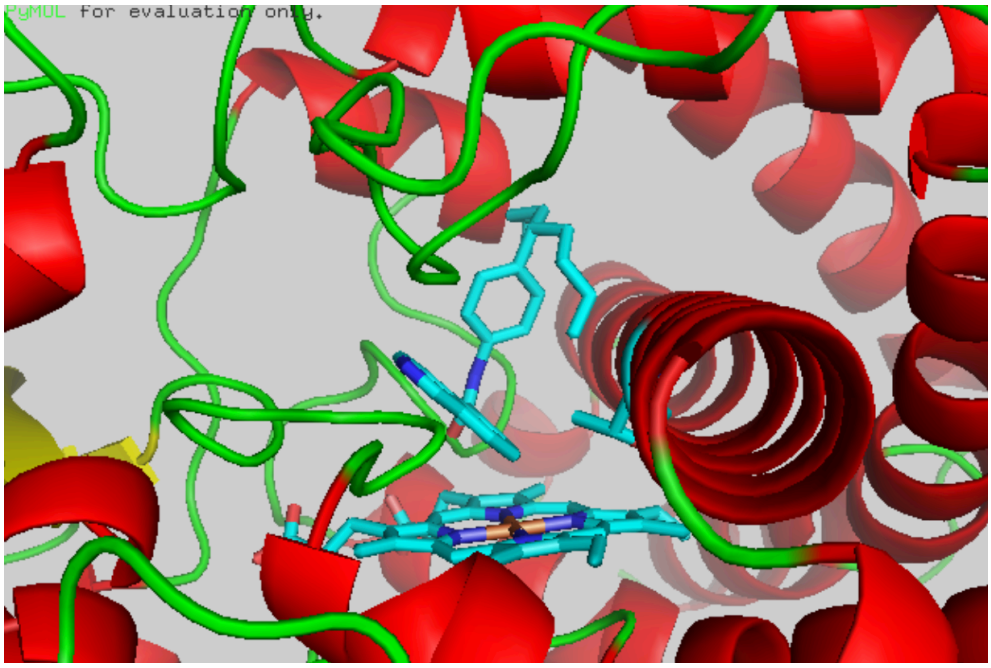


Figure A.1. Docking configuration of *N*-(4-(nonan-5-yl)phenyl)isoquinoline-5-carboxamide.

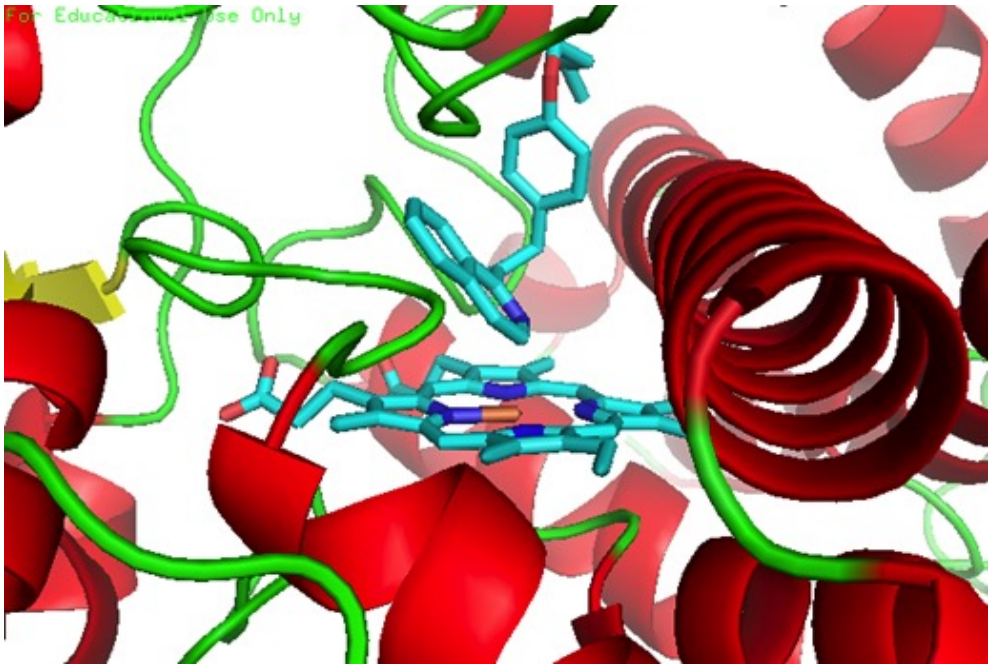


Figure A.2. Docking configuration of N-(4-butoxyphenyl)isoquinoline-1-carboxamide.

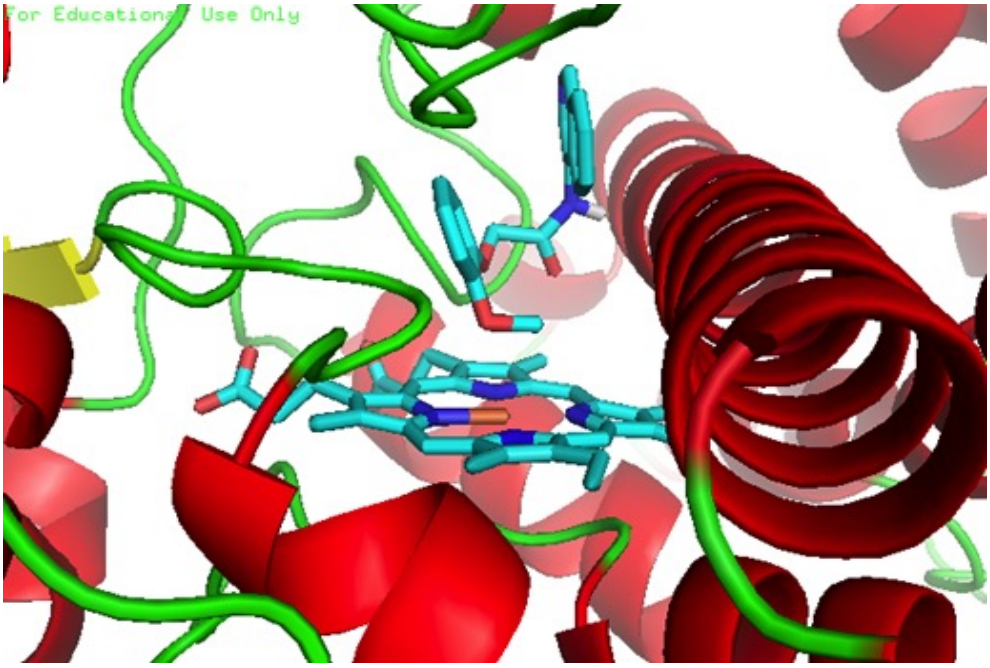


Figure A.3. Docking configuration of *N*-(isoquinolin-4-yl)-2-(2-methoxyphenoxy)acetamide.

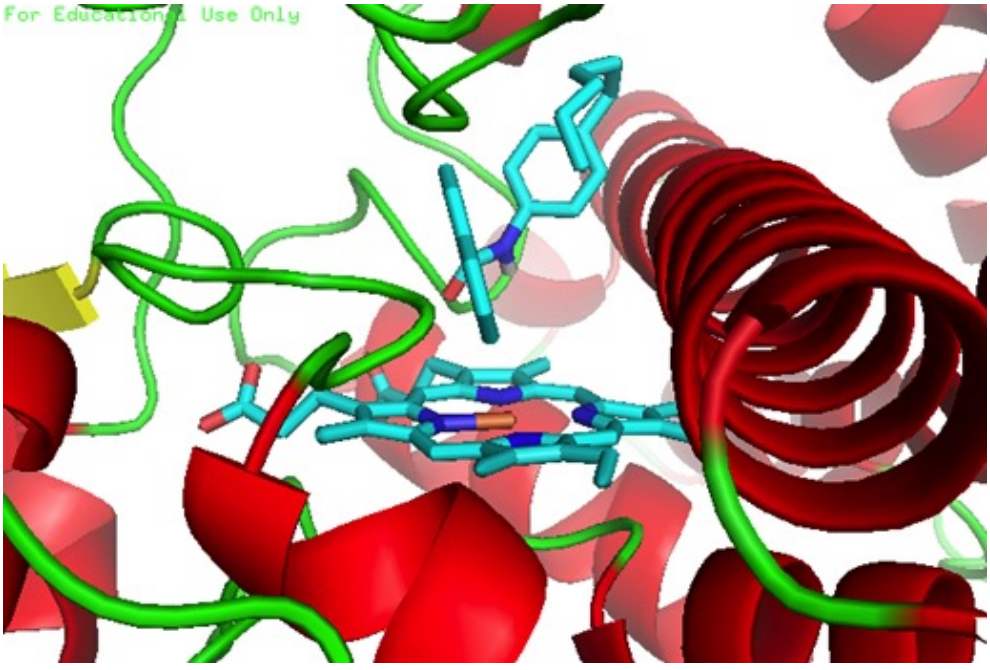


Figure A.4. Docking configuration of *N*-(4-hexylphenyl)isoquinoline-1-carboxamide.

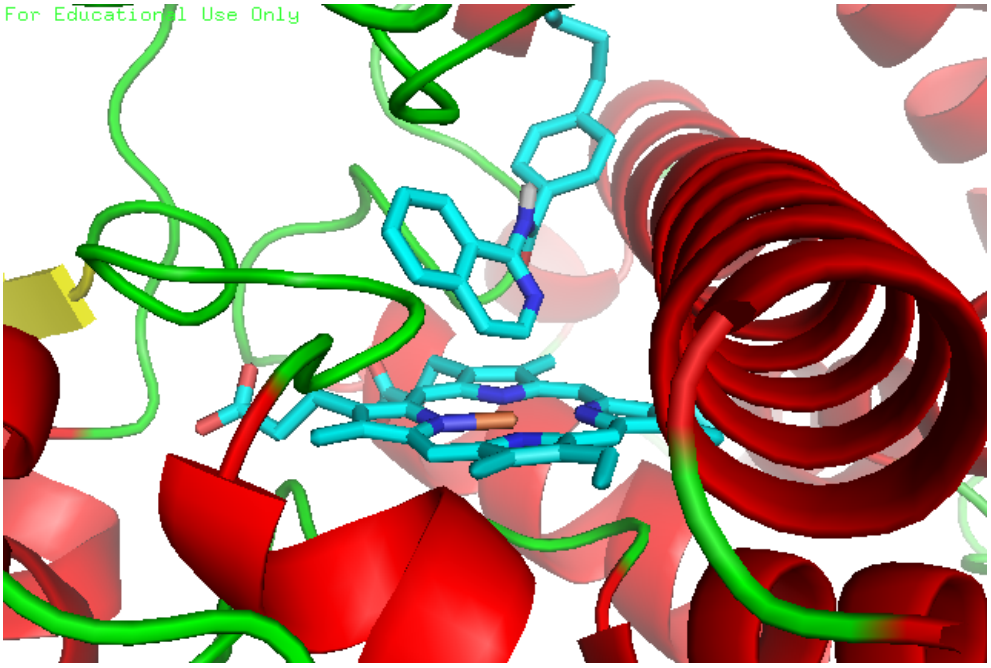


Figure A.5. Docking configuration of 4-butyl-N-(isoquinolin-1-yl)benzamide.

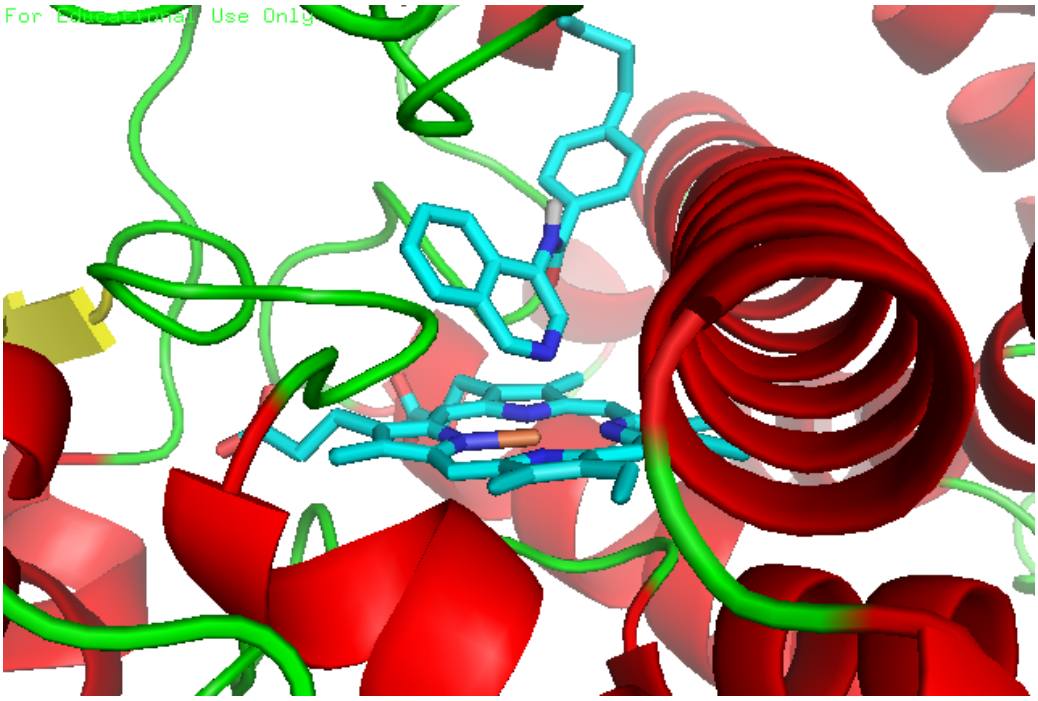


Figure A.6. Docking configuration of -butyl-N-(isoquinolin-4-yl)benzamide.

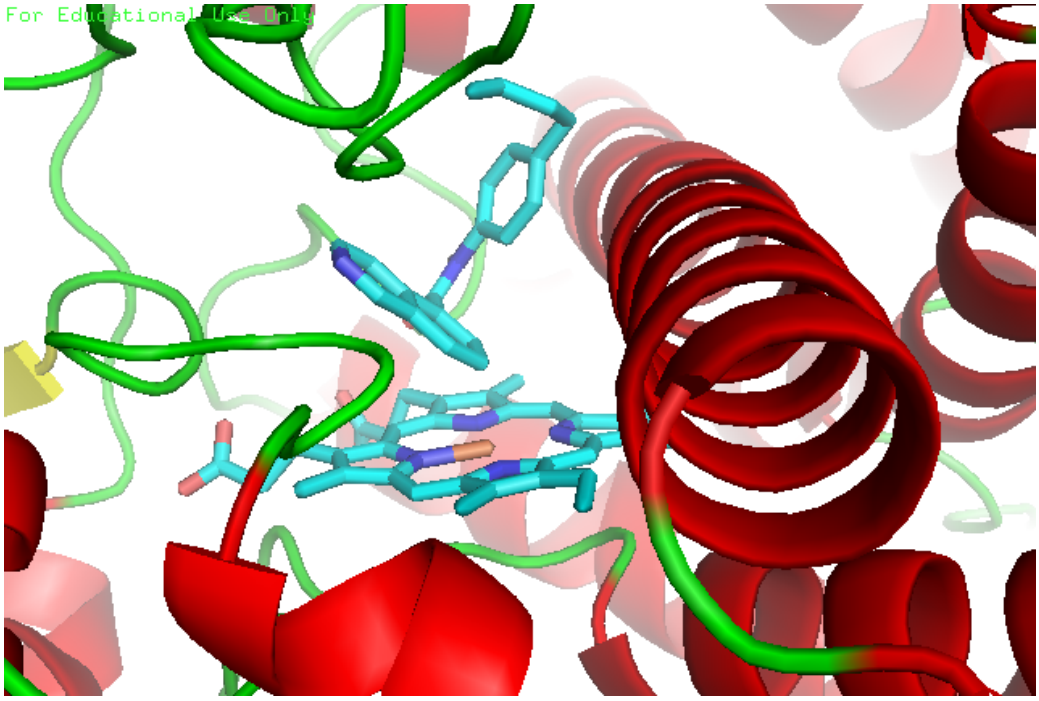

Figure A. 7. Docking configuration of N-(4-butylphenyl)isoquinoline-5-carboxamide.

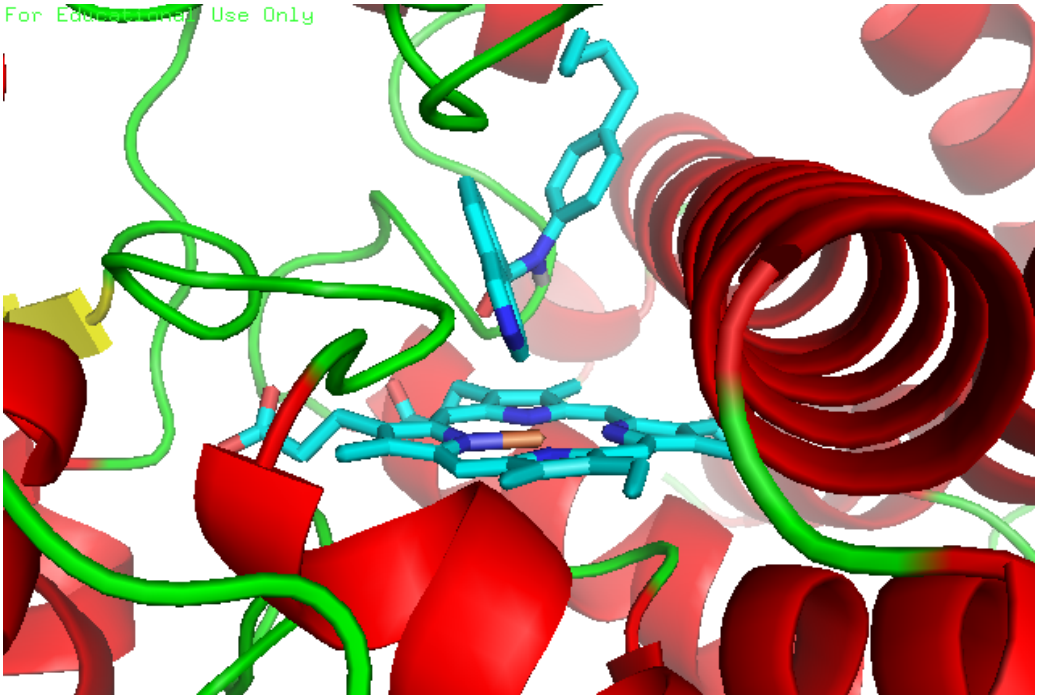

Figure A. 8. Docking configuration of N-(4-pentylphenyl)isoquinoline-5-carboxamide.

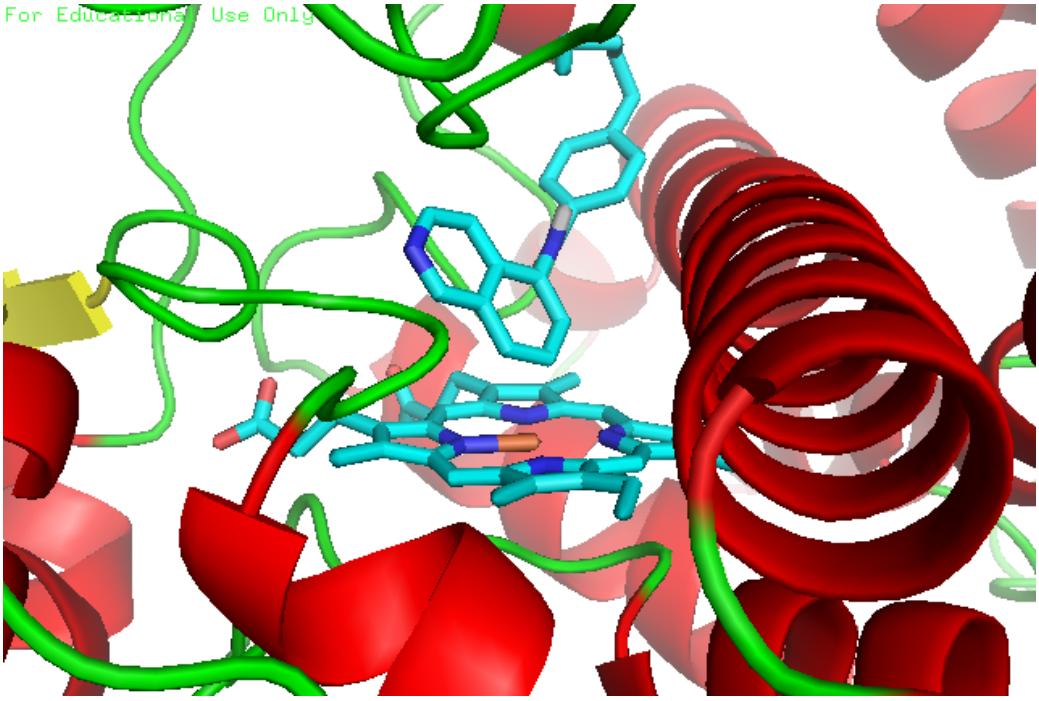


Figure A.9. Docking configuration of N-(isoquinolin-5-yl)-4-pentylbenzamide.

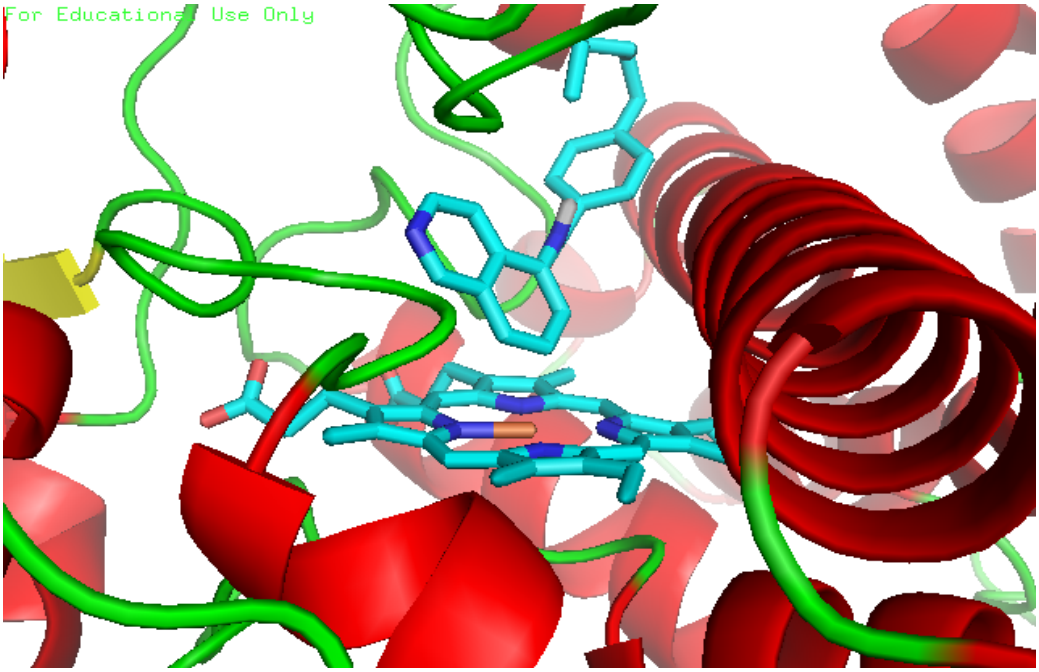


Figure A.10. Docking configuration of N-(isoquinolin-5-yl)-4-hexylbenzamide.

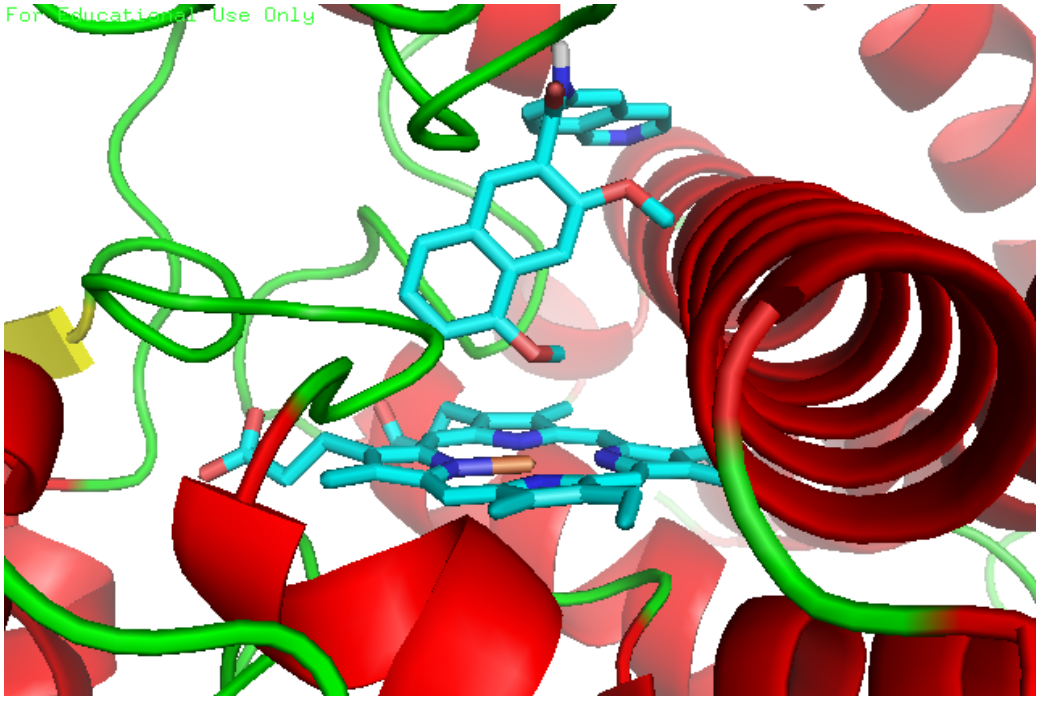


Figure A.11. Docking configuration of N-(isoquinolin-6-yl)-3,5-dimethoxy-2-naphtamide.

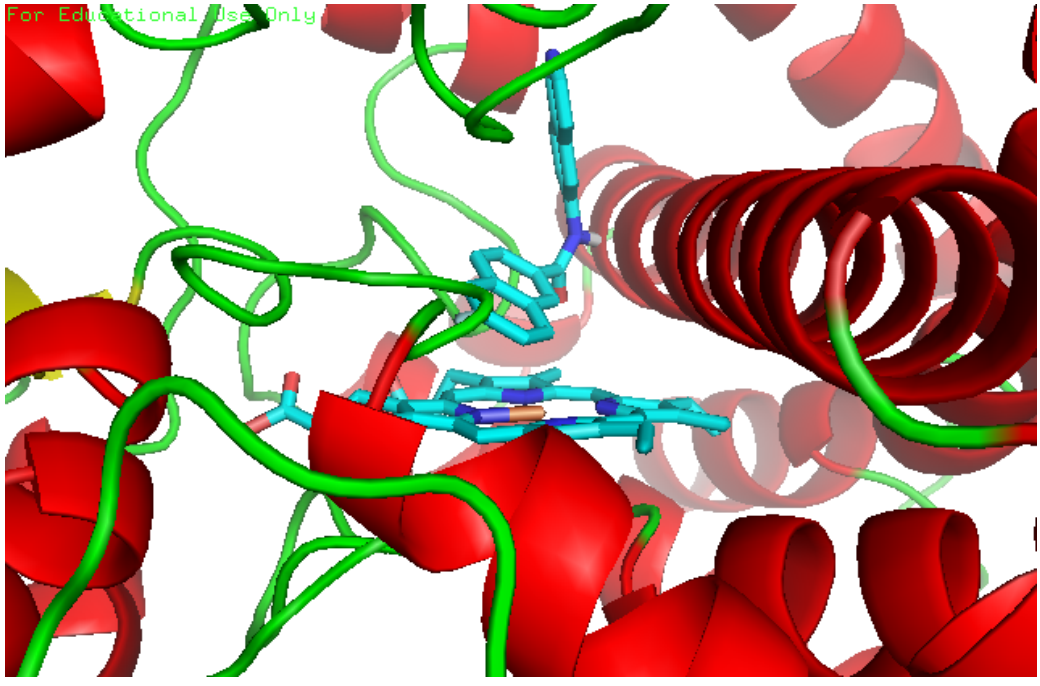


Figure A.12. Docking configuration of 6-fluoro-N-(isoquinolin-6-yl)-2-naphthamide.

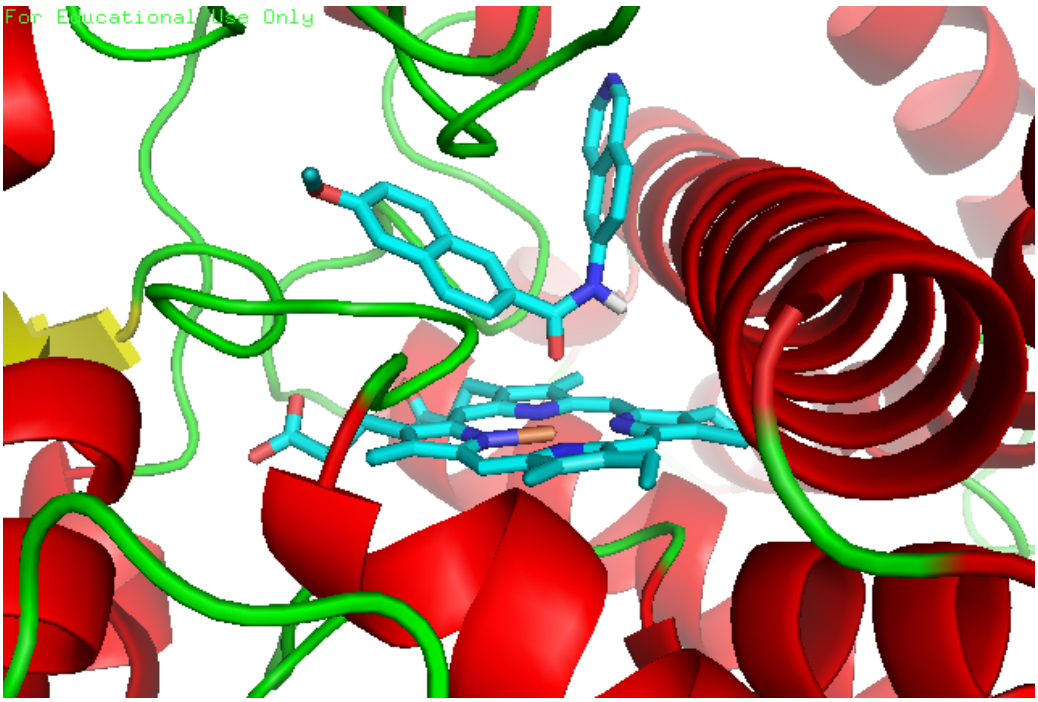


Figure A.12. Docking configuration of N-(isoquinolin-6-yl)-6-methoxy-2-naphthamide.

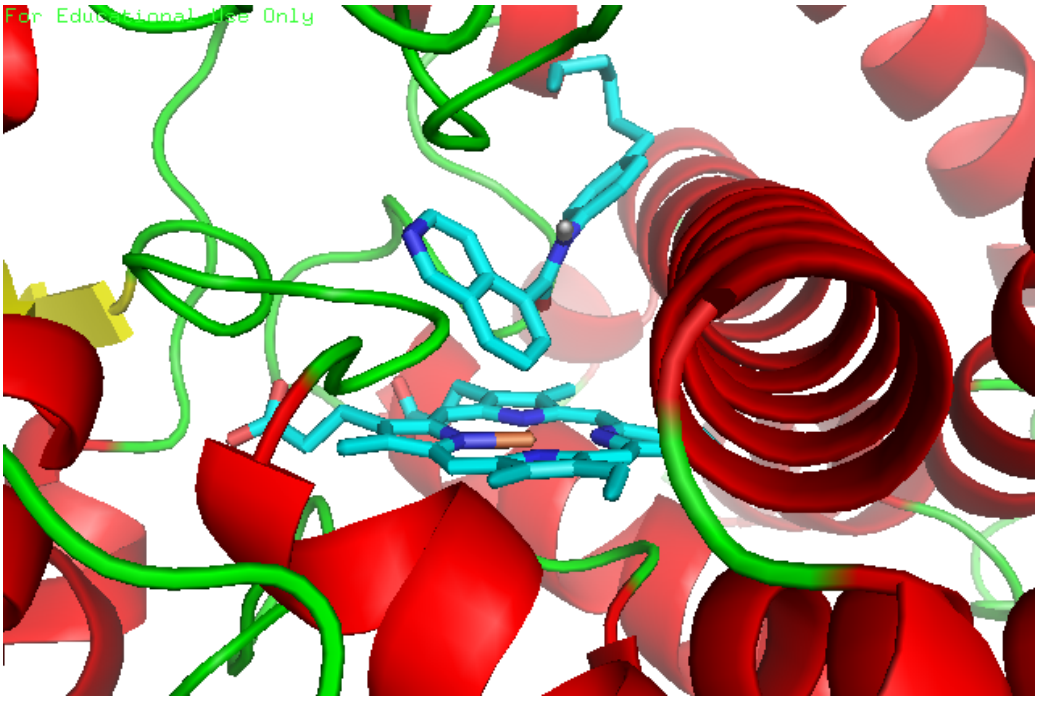


Figure A.13. Docking configuration of N-(4-hexylphenyl)isoquinoline-5-carboxamide.

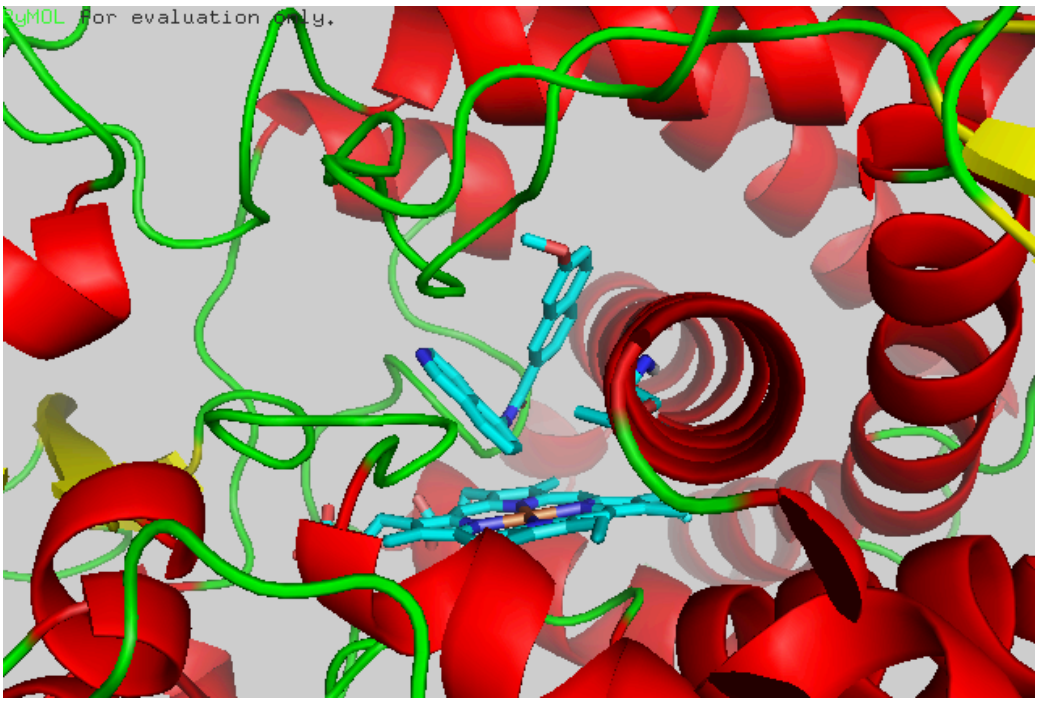


Figure A.14. Docking configuration of *N*-(isoquinolin-5-yl)-6-methoxy-2-naphthamide.

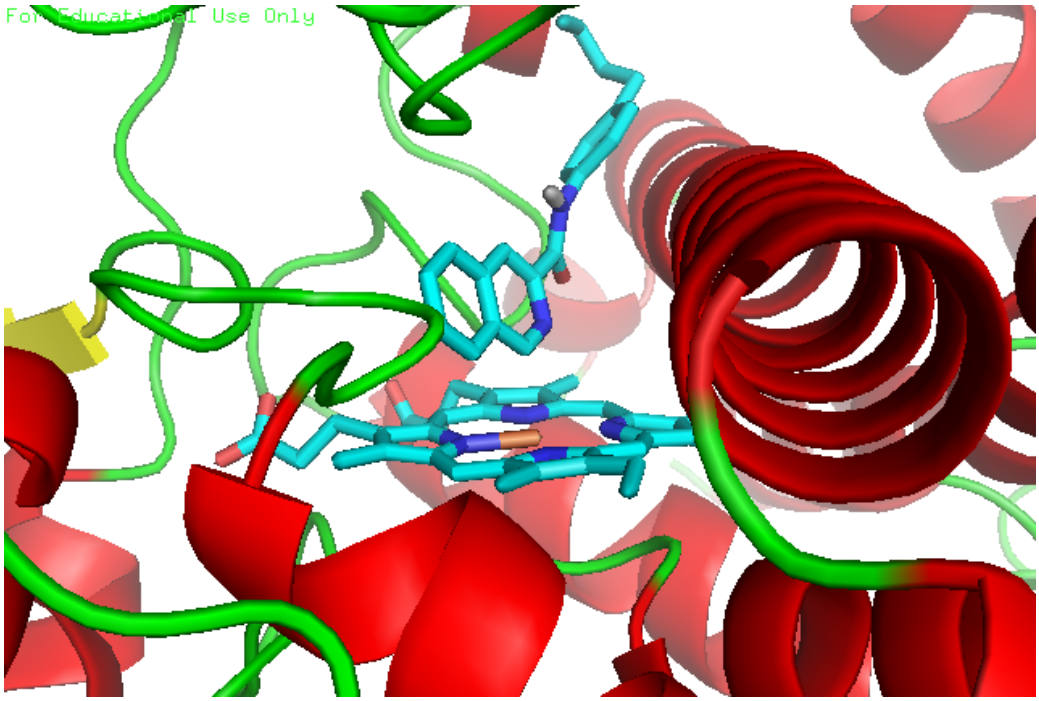


Figure A.15. Docking configuration of N-(4-butylphenyl)isoquinoline-3-carboxamide.

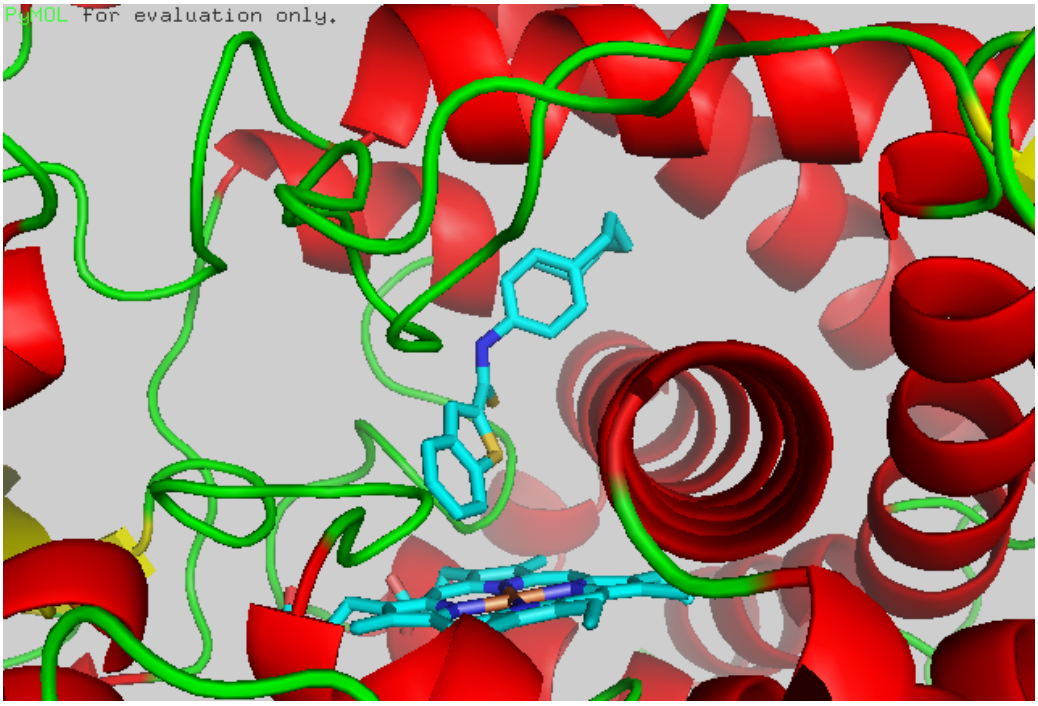


Figure A.16. Docking configuration of *N*-(4-hexylphenyl)benzo[*b*]thiophene-2-carbothioamide.

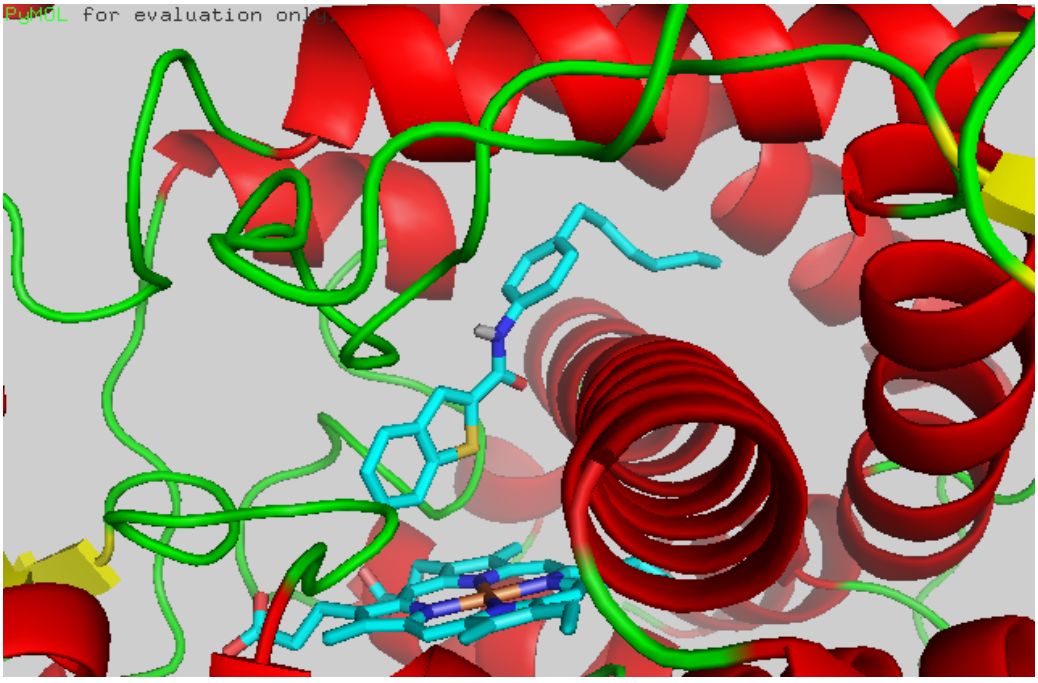


Figure A.17. Docking configuration of 1-(Benzo[b]thiophen-2-yl)-2-(4-hexylphenyl)ethanone.

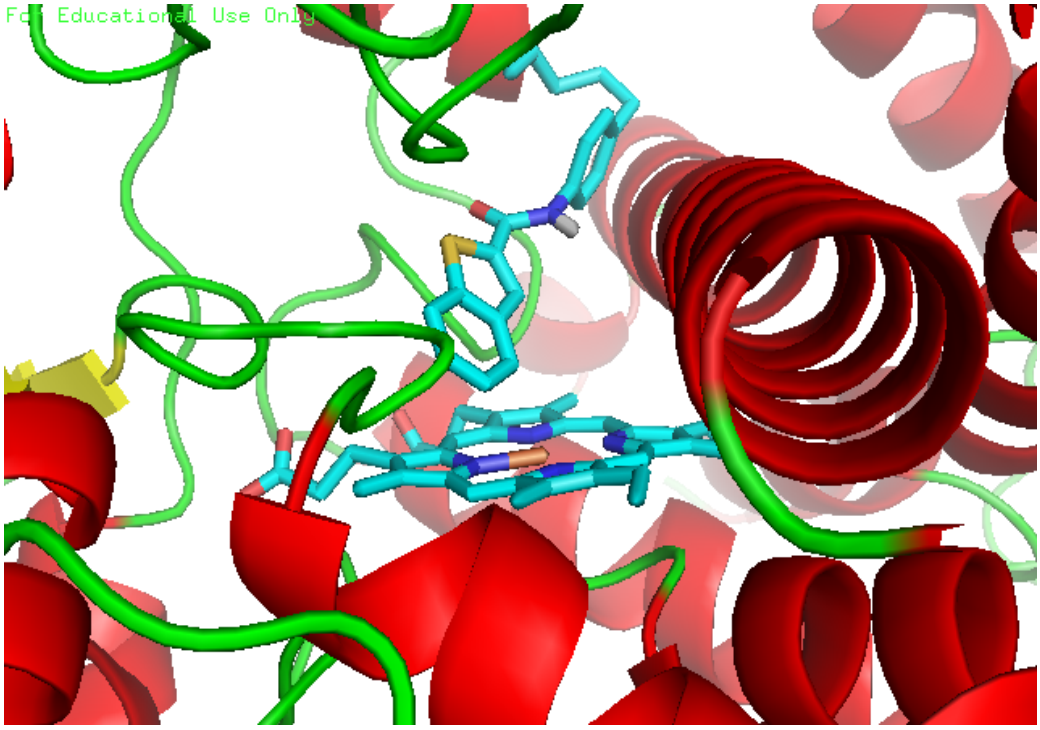


Figure A.18. Docking configuration of 1-(Benzo[b]thiophen-2-yl)-2-(4-pentylphenyl)ethanone.

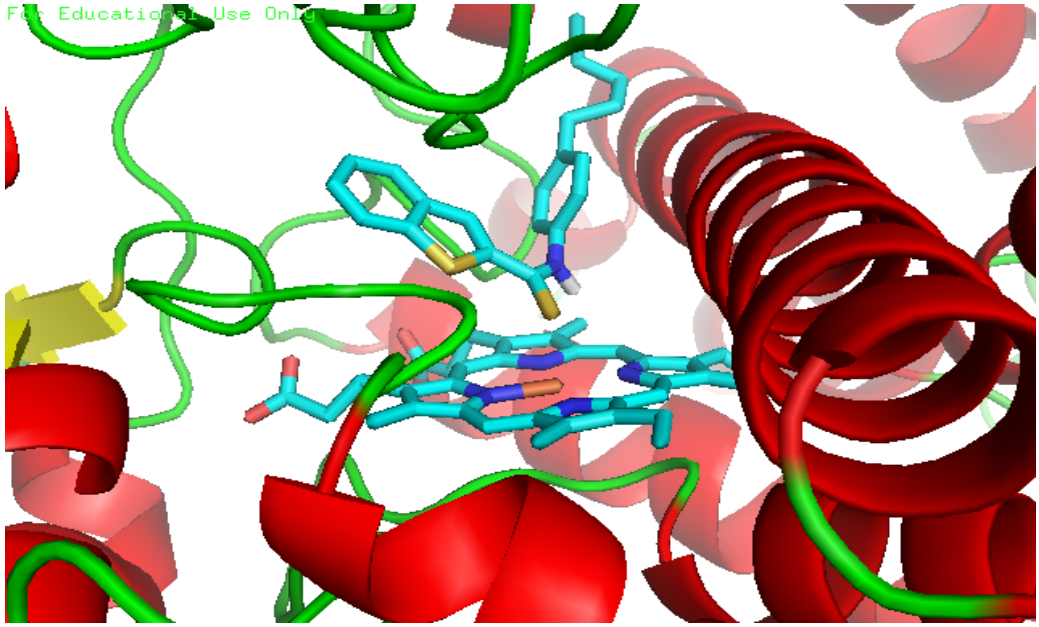


Figure A.19. Docking configuration of *N*-(4-pentylphenyl)benzo[*b*]thiophene-2-carbothioamide.

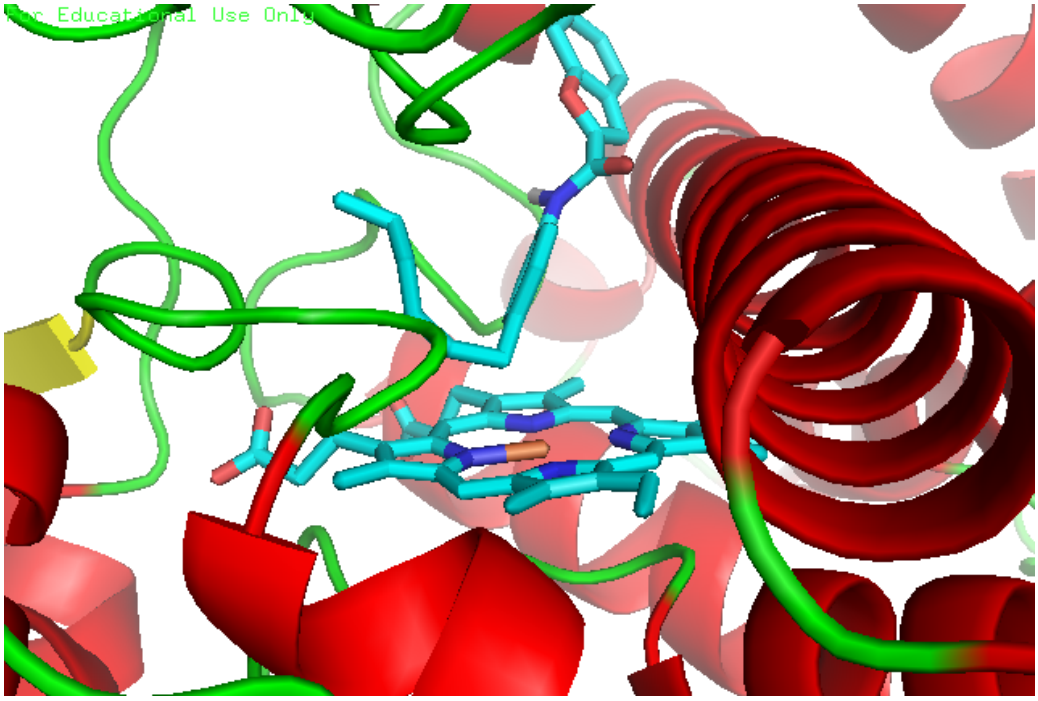

Figure A.20. Docking configuration of N-(4-hexylphenyl)benzofuran-2-carboxamide.

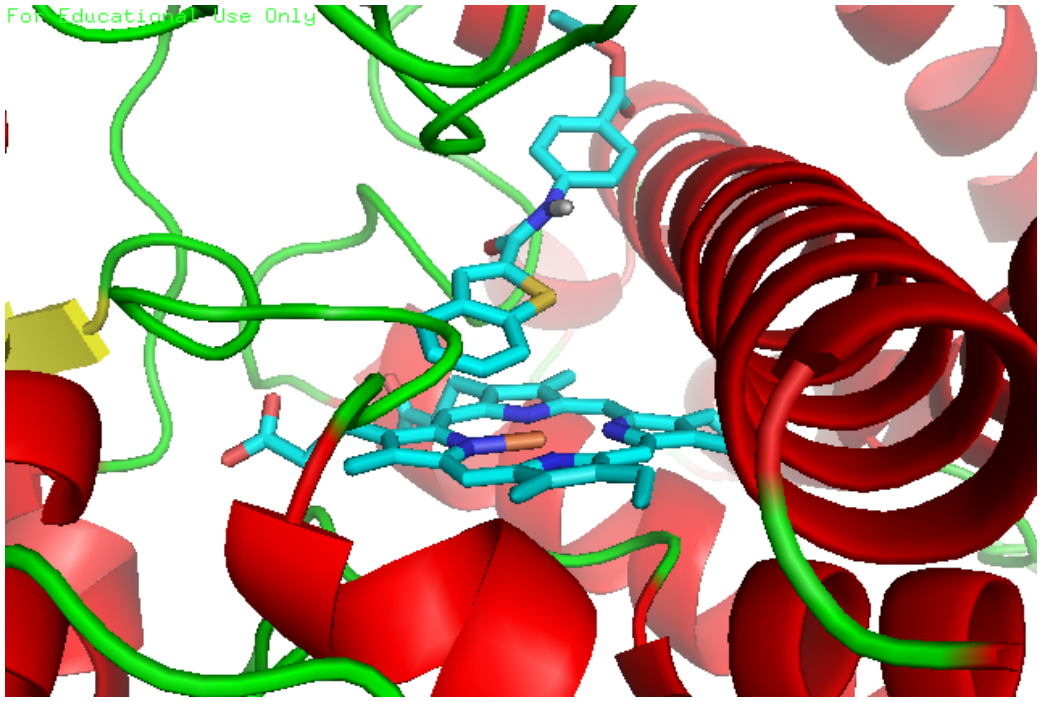

Figure A.21. Docking configuration of Ethyl 4-(benzo[b]thiophene-2-carboxamido)benzoate.

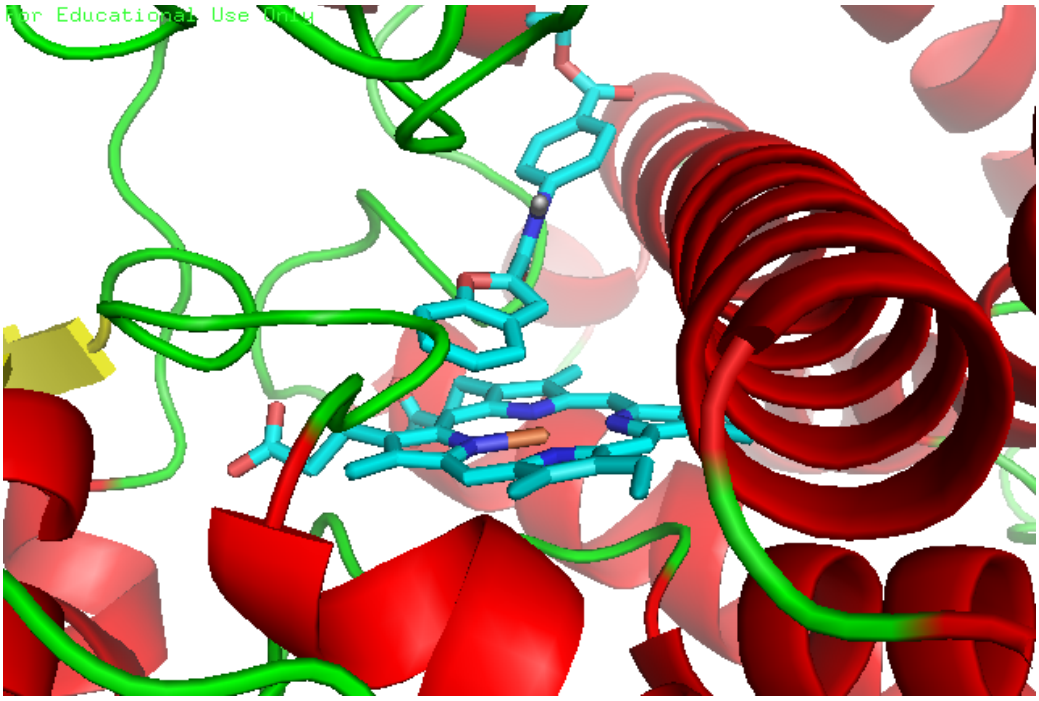


Figure A.22. Docking configuration of Ethyl 4-(benzofuran-2-carboxamido)benzoate.

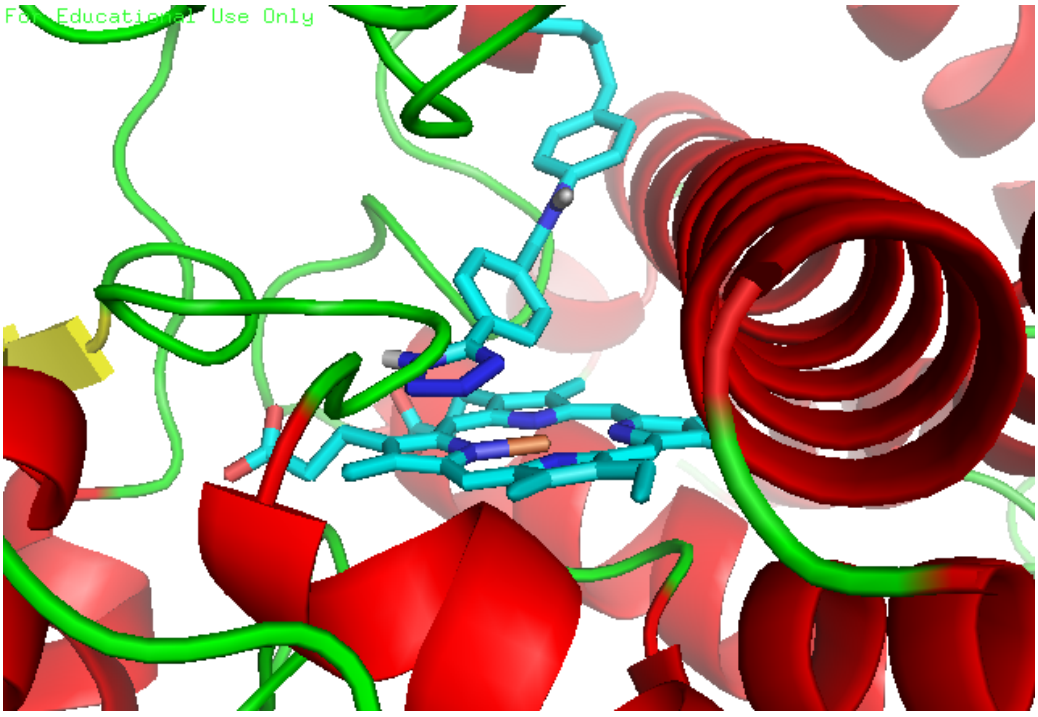


Figure A.23. Docking configuration of N-(4-butylphenyl)-4-(1H-tetrazol-5-yl)benzamide.

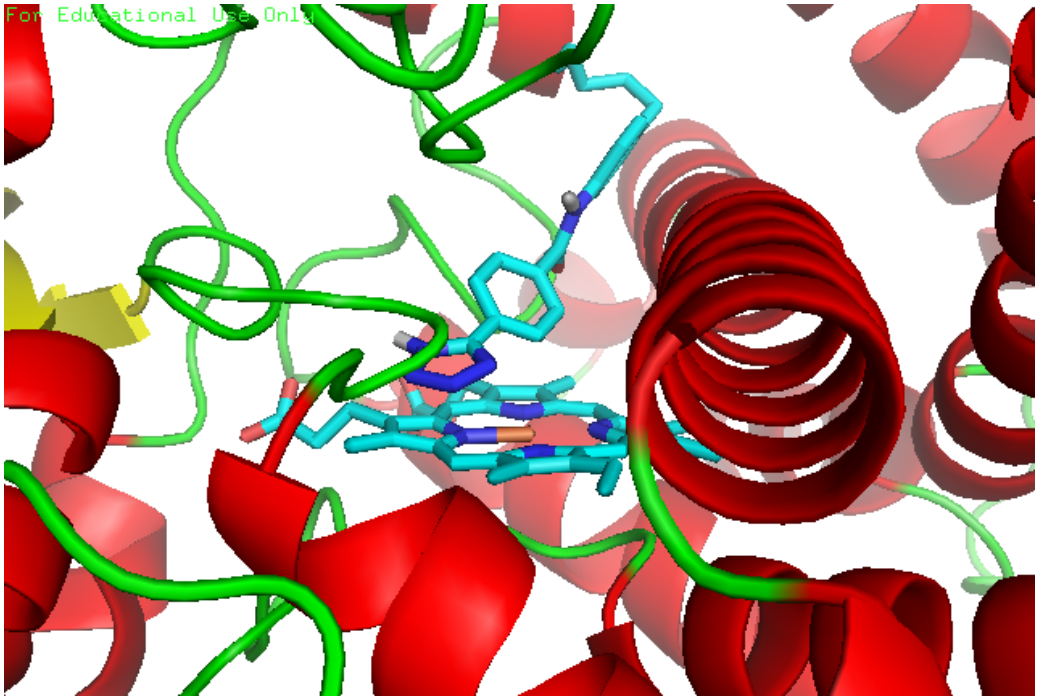


Figure A.24. Docking configuration of N-(4-pentylphenyl)-4-(1H-tetrazol-5-yl)benzamide.

# APPENDIX B: SPECTROSCOPY DATA

This section includes 1D NMR ($^{1}H$, $^{13}C$ NMR) spectroscopy of the synthesized products. Expansions were made on the NMR data for easy interpretation.

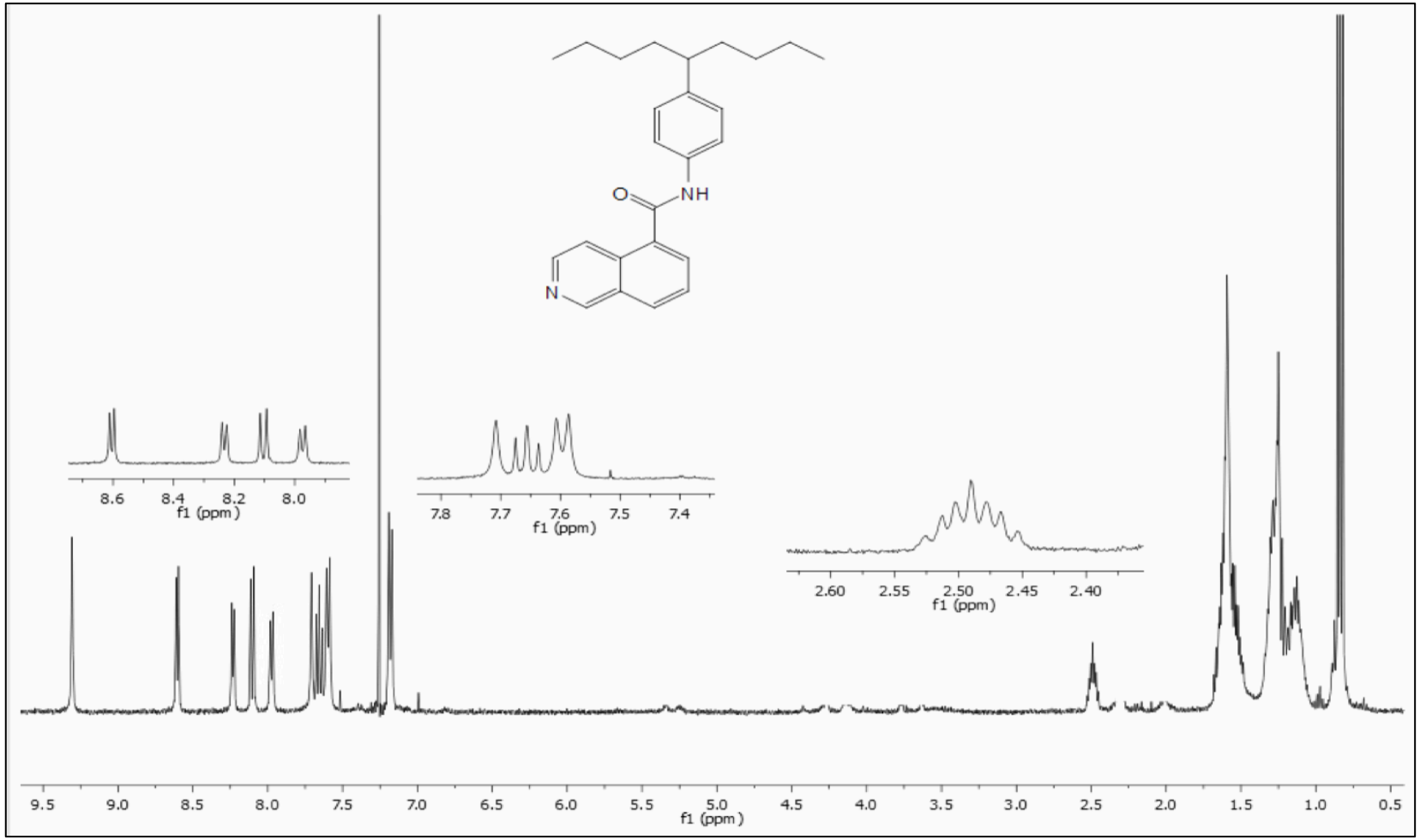


Figure B.1. $^{1}$H-NMR spectrum of *N*-(4-(nonan-5-yl)phenyl)isoquinoline-5-carboxamide.

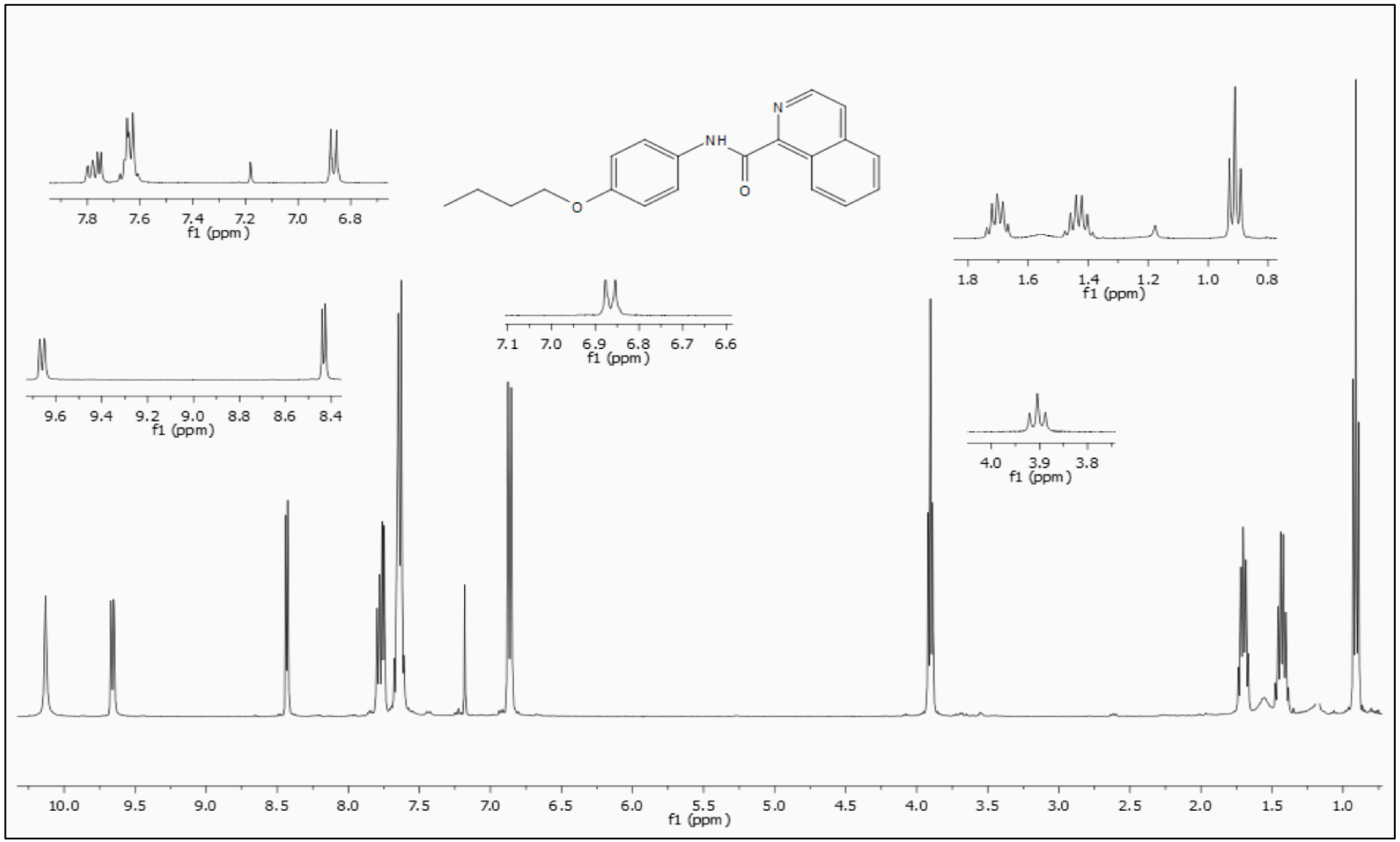


Figure B.2. $^{1}$H-NMR spectrum of N-(4-butoxyphenyl)isoquinoline-1-carboxamide.


Figure B.3. $^{13}$C-NMR spectrum of N-(4-butoxyphenyl)isoquinoline-1-carboxamide.

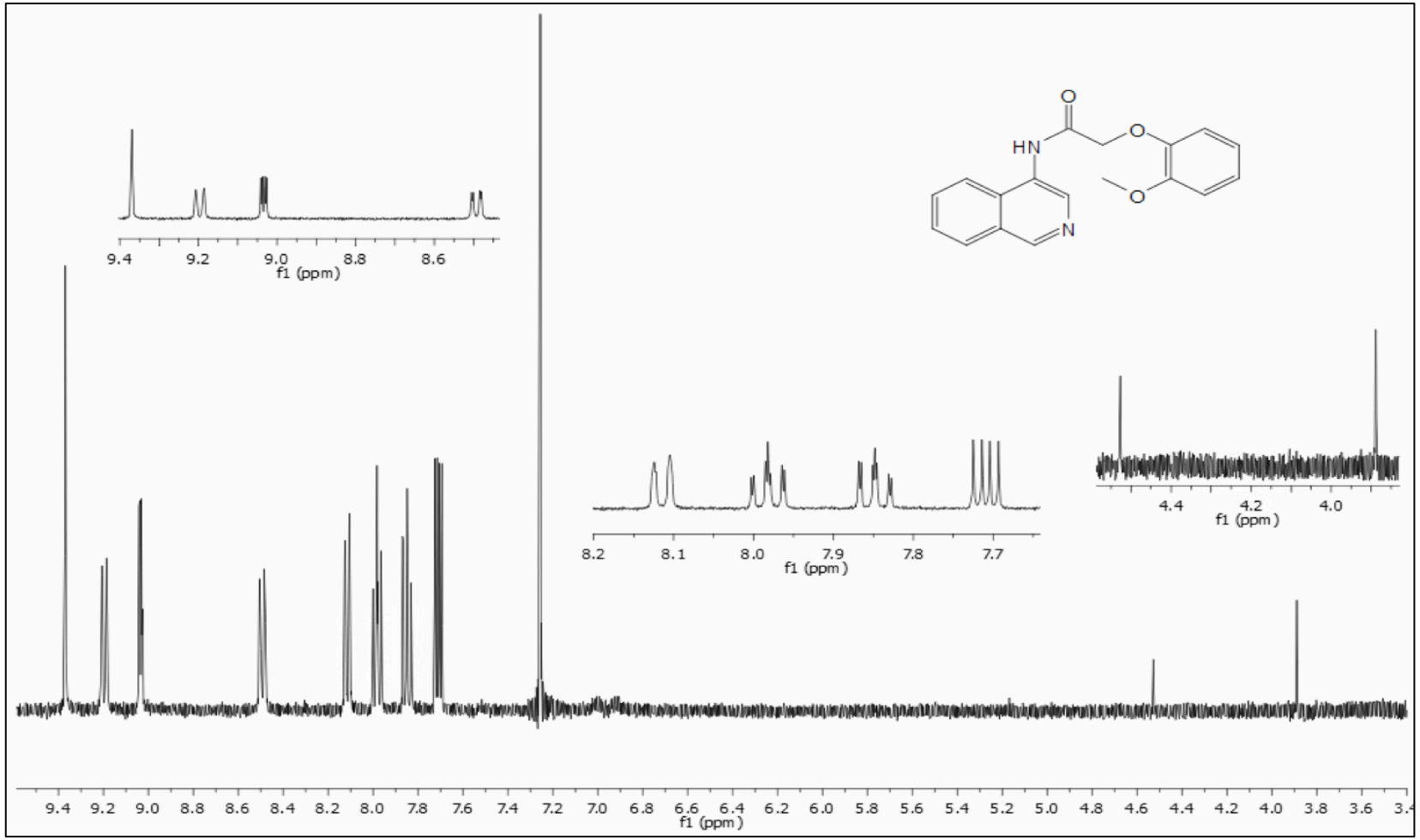


Figure B.4. $^{1}$H-NMR spectrum of *N*-(isoquinolin-4-yl)-2-(2-methoxyphenoxy)acetamide.

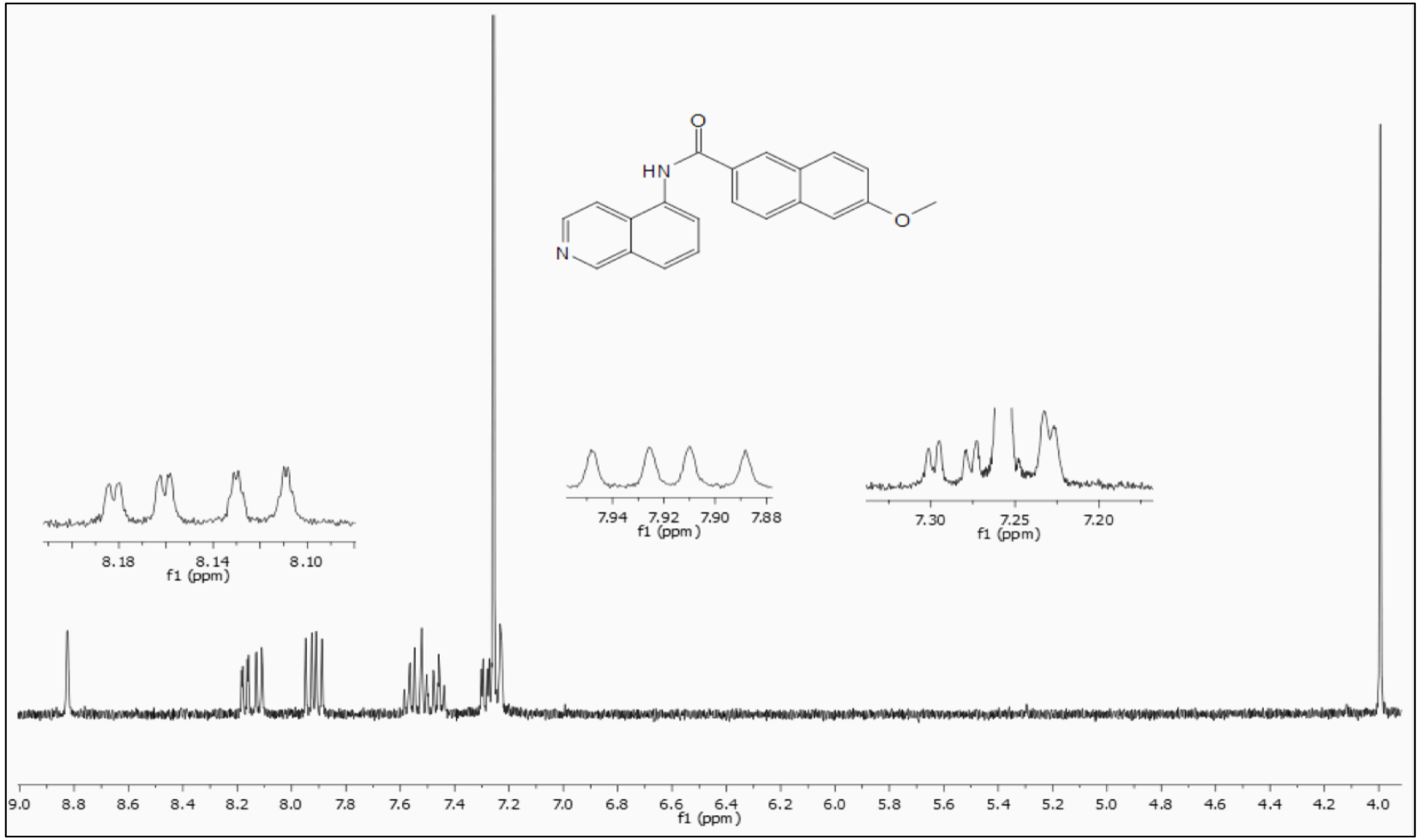


Figure B.5. $^{1}$H-NMR spectrum of *N*-(isoquinolin-5-yl)-6-methoxy-2-naphthamide.

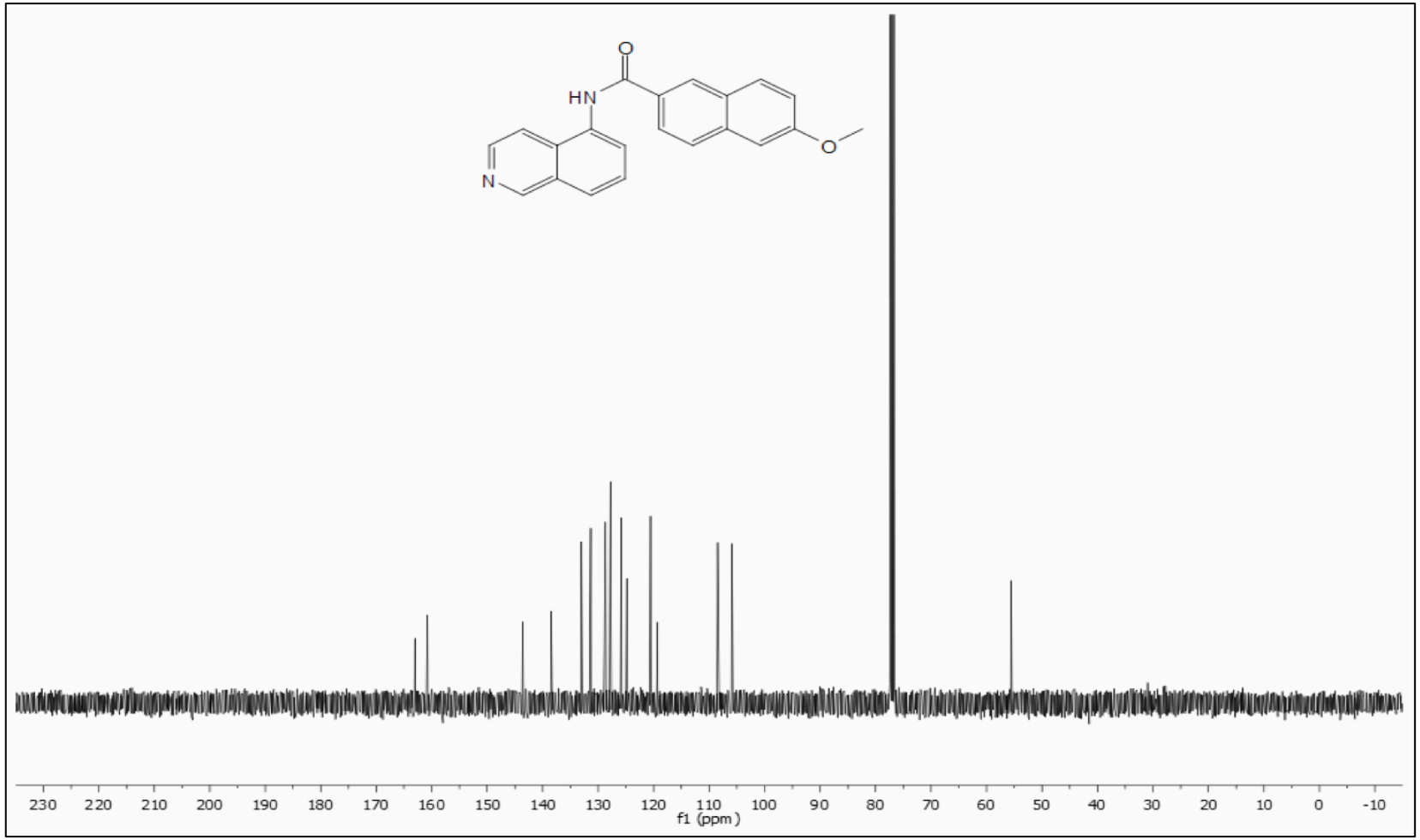


Figure B.6. $^{13}$C-NMR spectrum of *N*-(isoquinolin-5-yl)-6-methoxy-2-naphthamide.

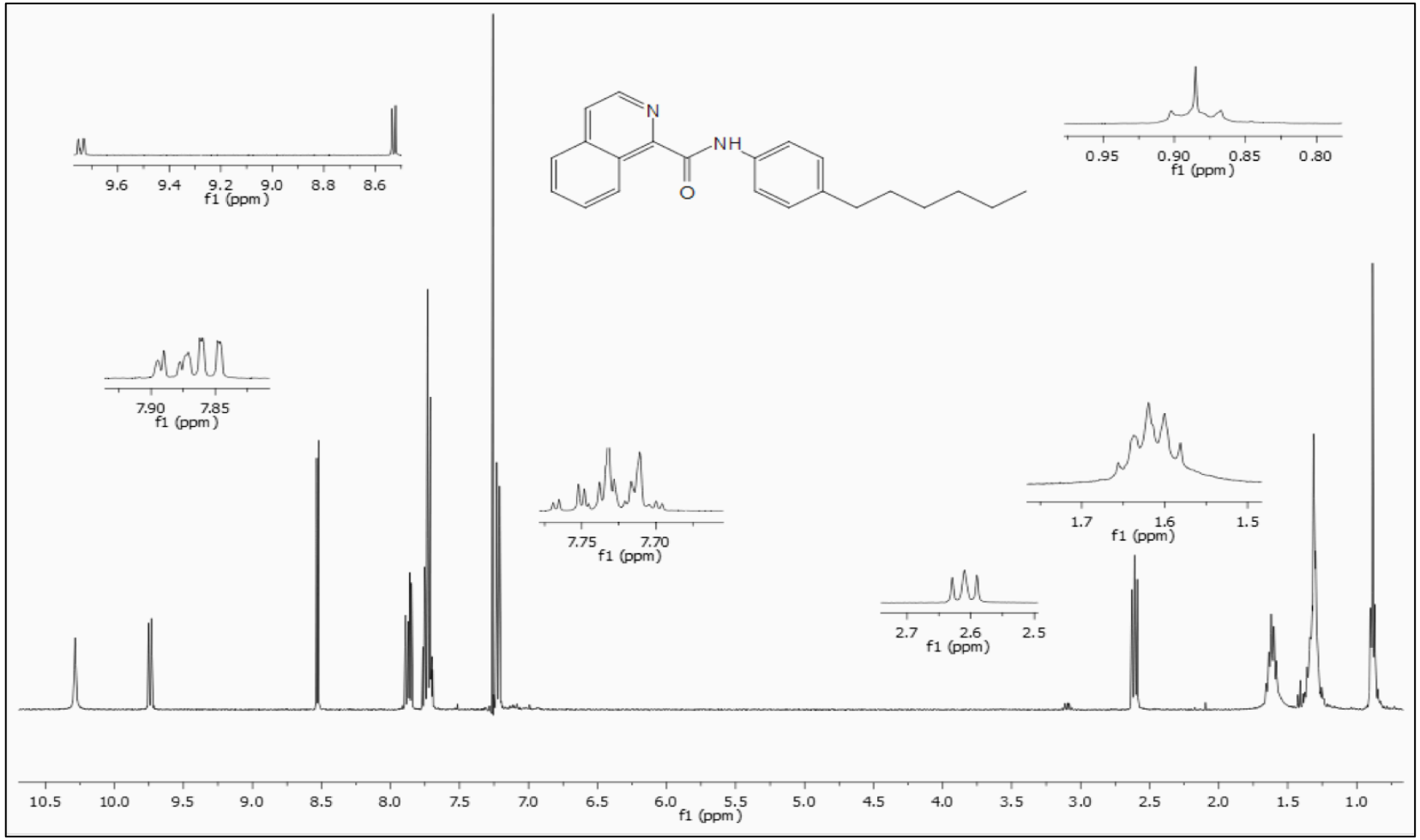


Figure B.7. $^{1}$H-NMR spectrum of *N*-(4-hexylphenyl)isoquinoline-1-carboxamide.

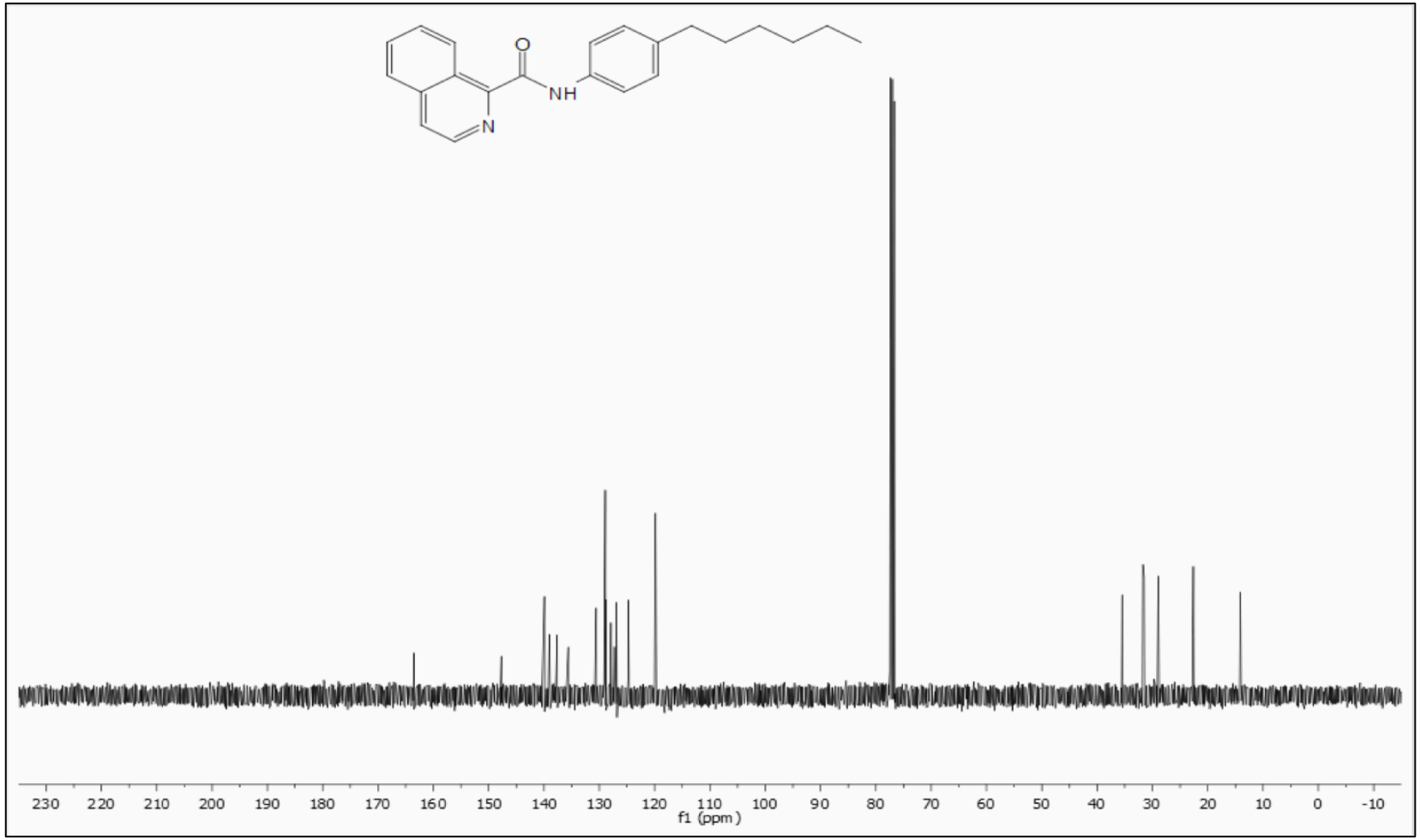


Figure B.8. $^{13}$C-NMR spectrum of *N*-(4-hexylphenyl)isoquinoline-1-carboxamide.

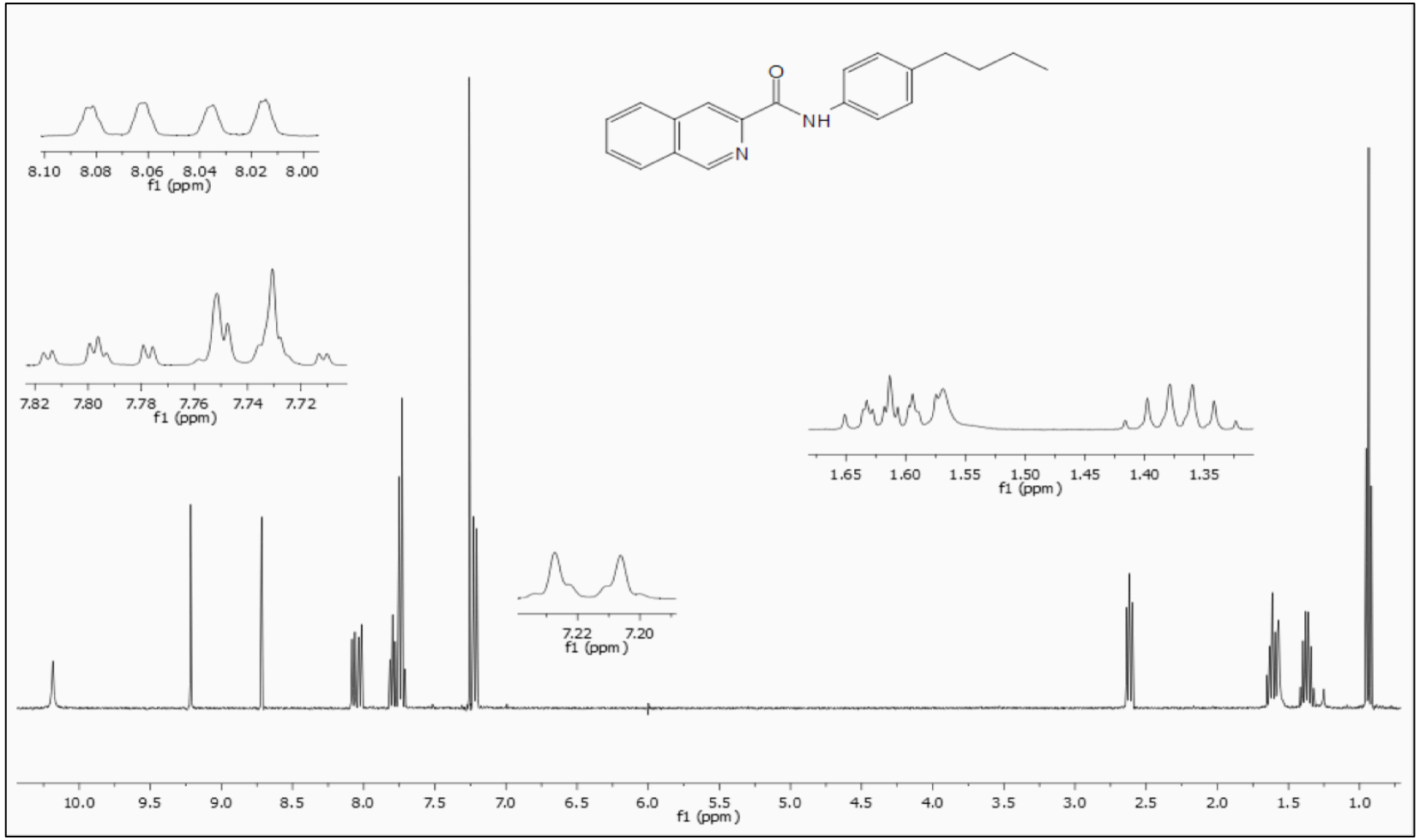


Figure B.9. $^{1}$H-NMR spectrum of N-(4-butylphenyl)isoquinoline-3-carboxamide.

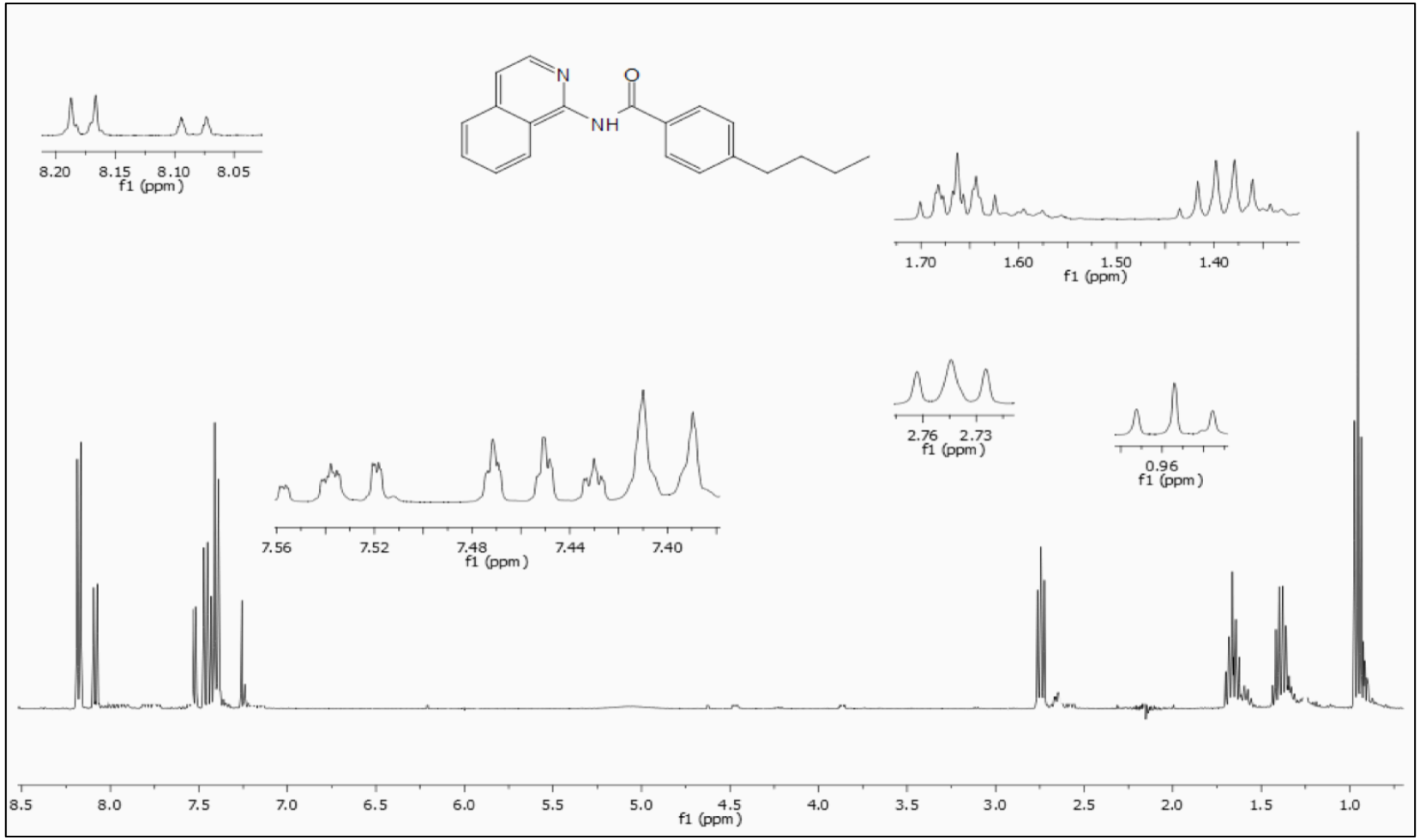


Figure B.10. $^{1}$H-NMR spectrum of 4-butyl-N-(isoquinolin-1-yl)benzamide.

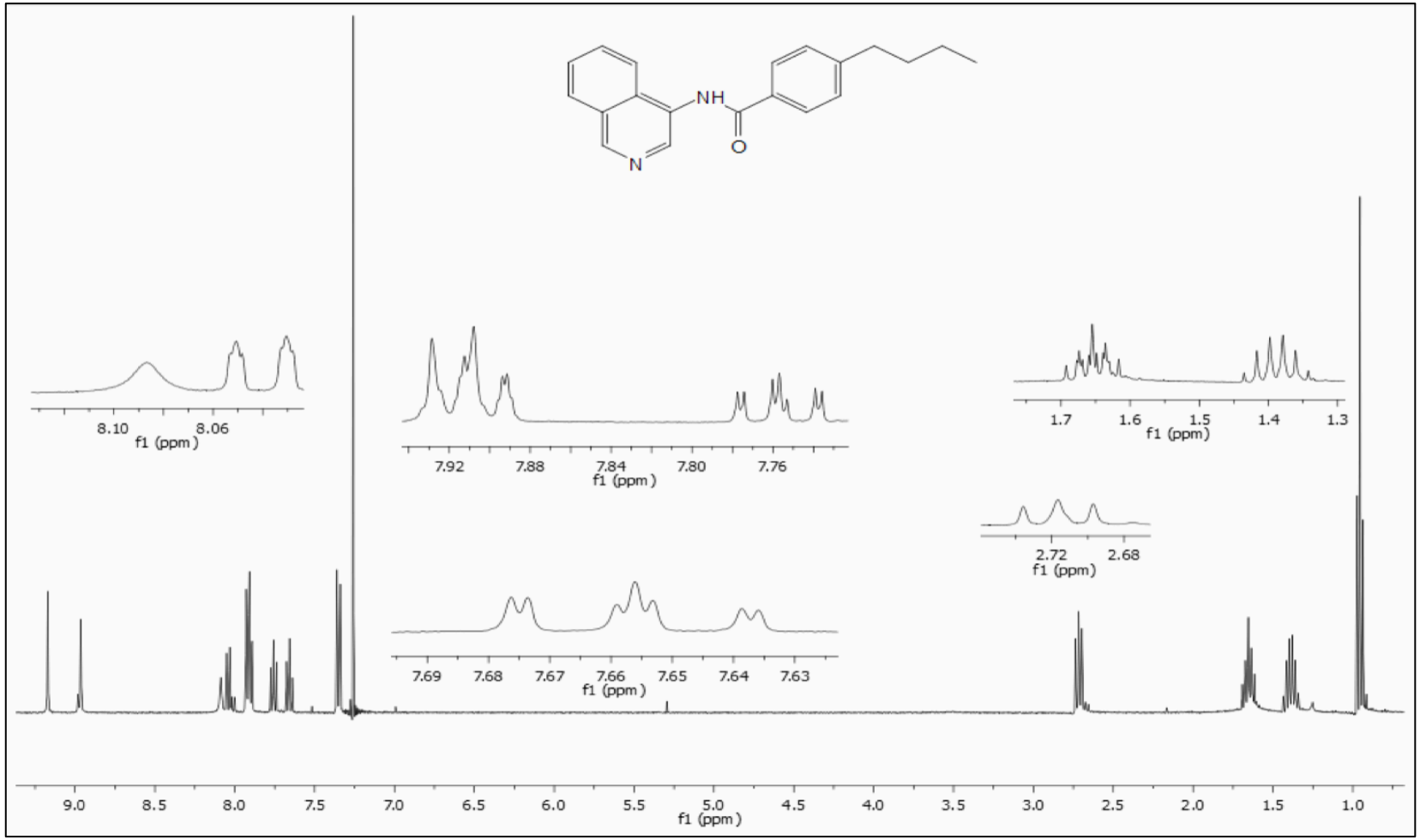


Figure B.11. $^{1}$H-NMR spectrum of 4-butyl-N-(isoquinolin-4-yl)benzamide.

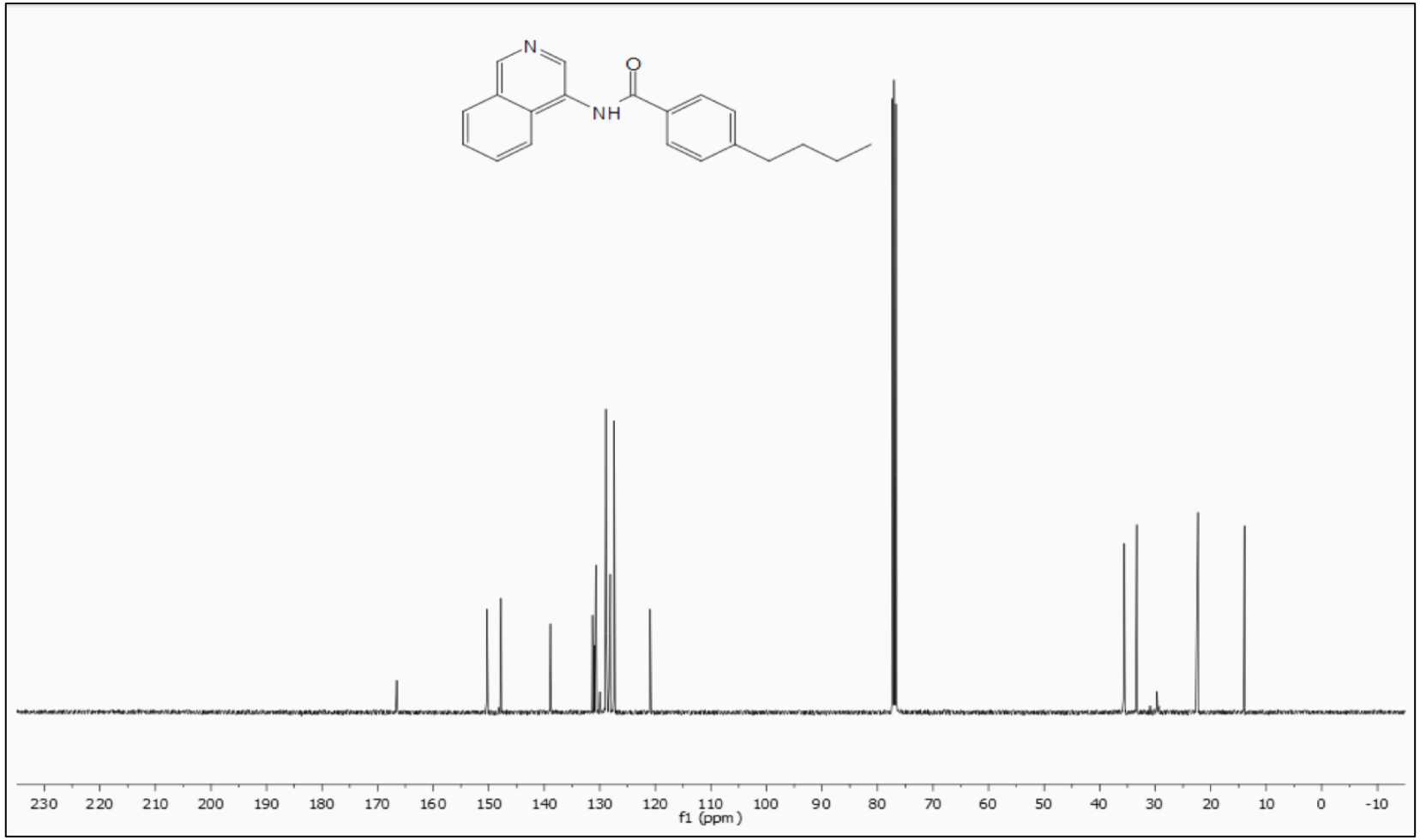


Figure B.12. $^{13}$C-NMR spectrum of 4-butyl-N-(isoquinolin-4-yl)benzamide.

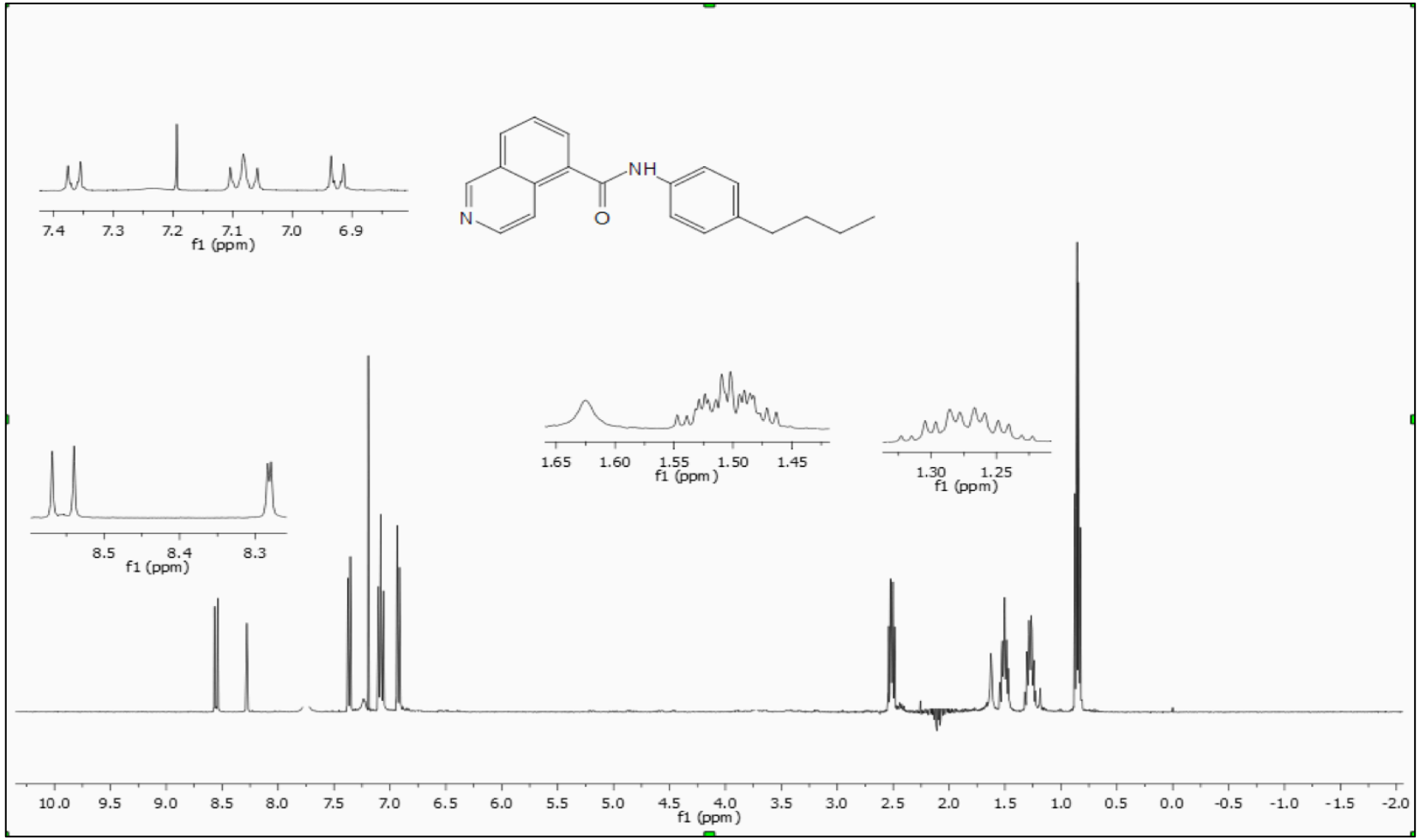


Figure B.13. $^{1}$H-NMR spectrum of 4-butyl-N-(isoquinolin-4-yl)benzamide.

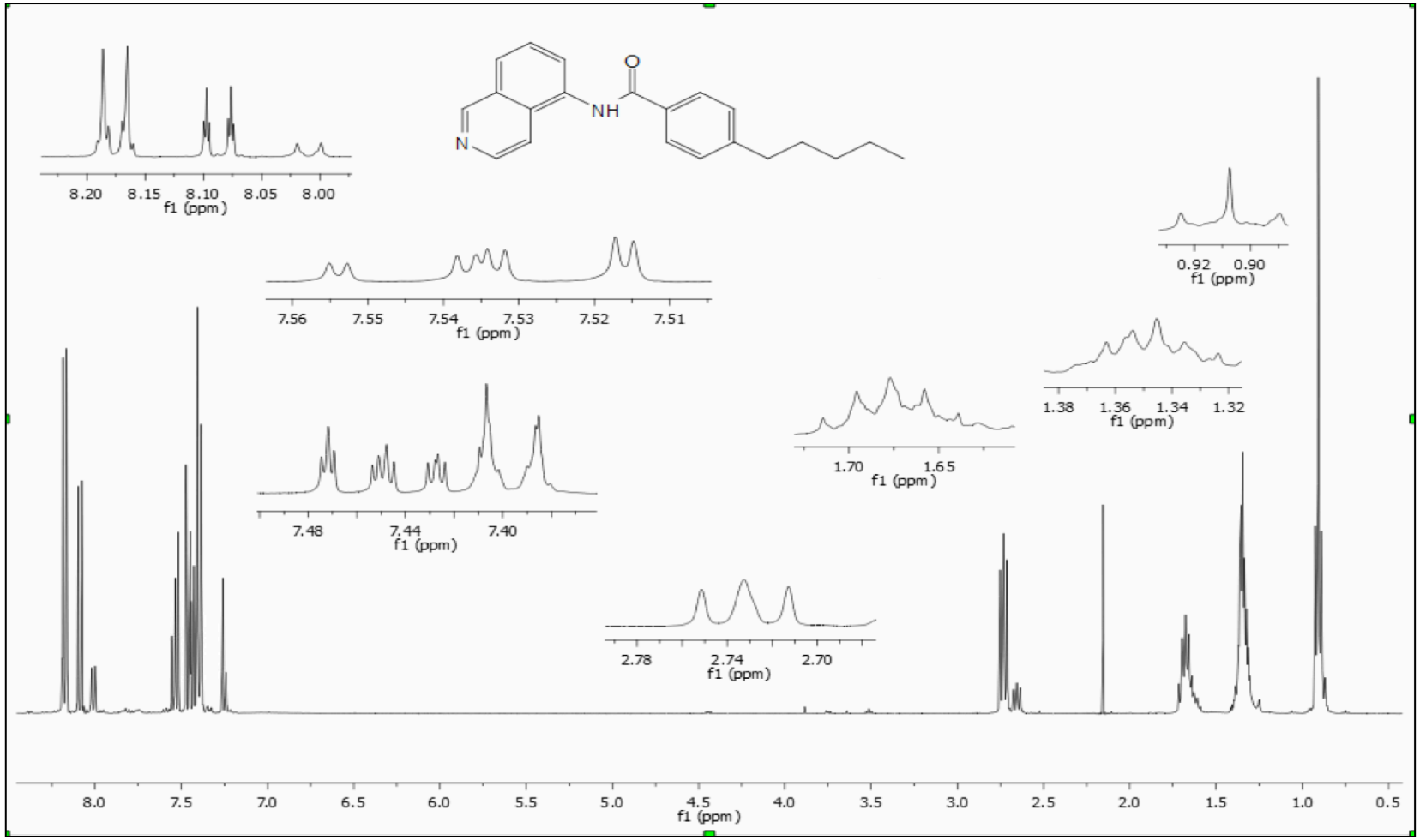


Figure B.14. $^{1}$H-NMR spectrum of N-(isoquinolin-5-yl)-4-pentylbenzamide.

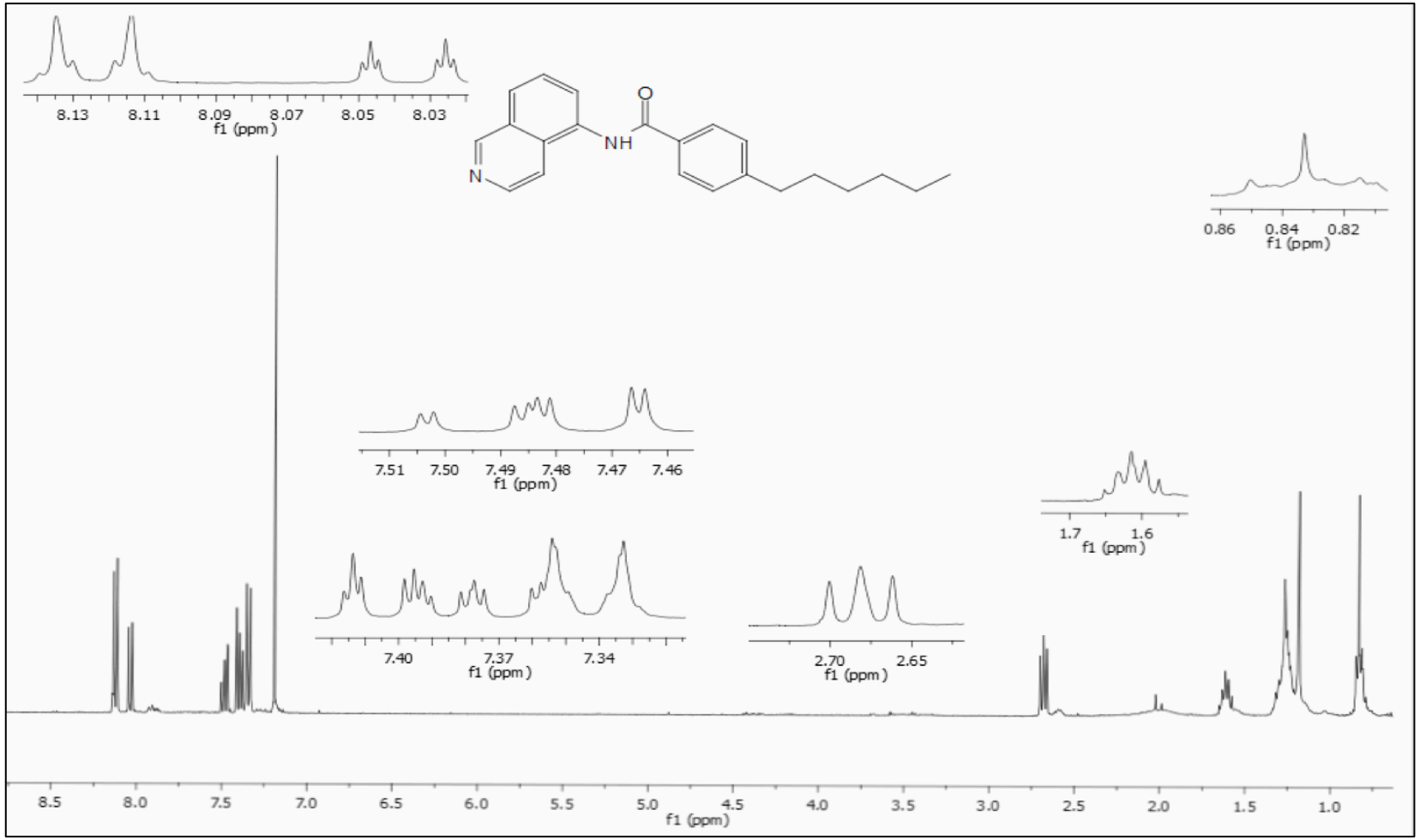


Figure B.15. $^{1}$H-NMR spectrum of N-(isoquinolin-5-yl)-4-hexylbenzamide.

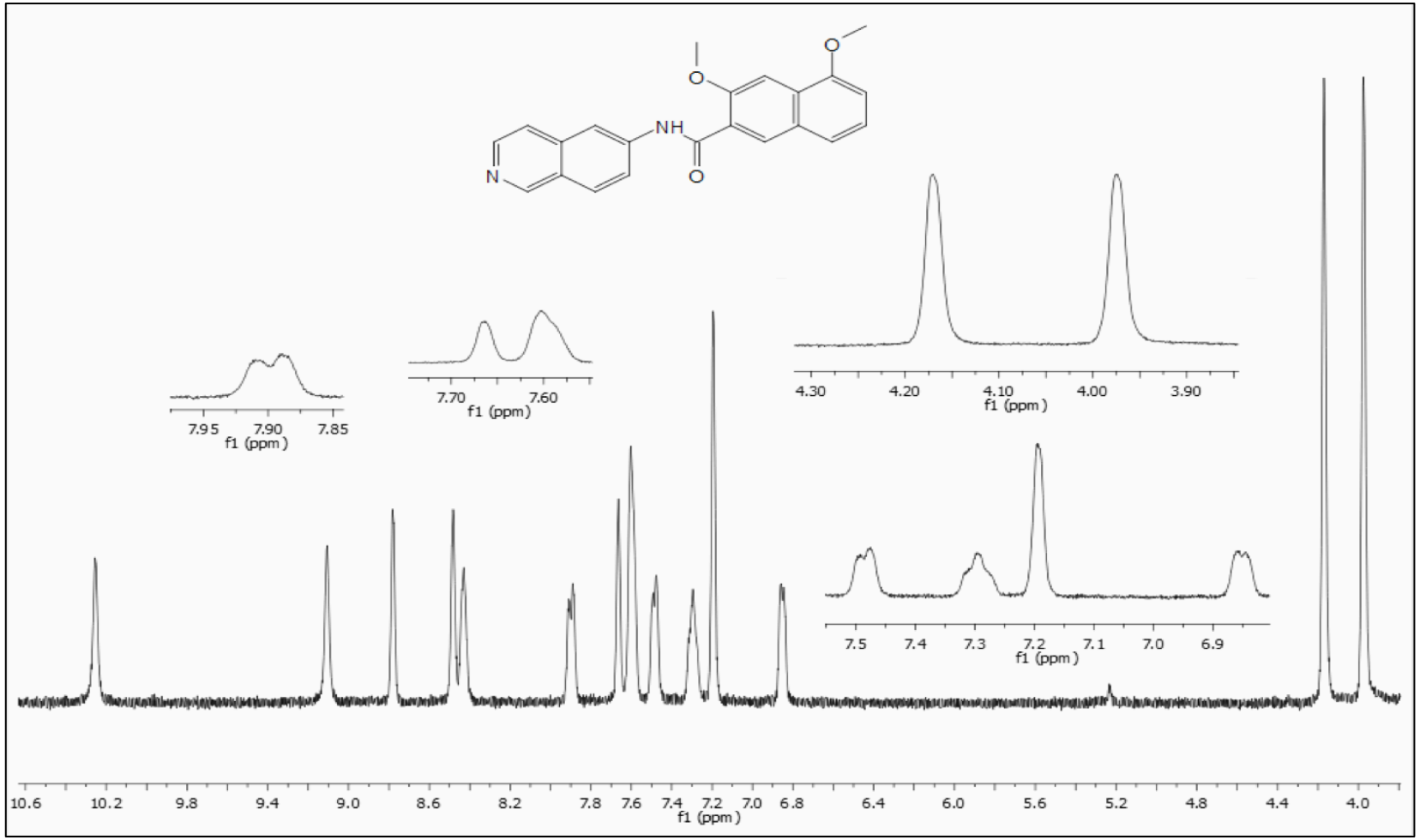


Figure B.16. $^{1}$H-NMR spectrum of N-(isoquinoline-6-yl)-3,5-dimethoxy-2-naphtamide.

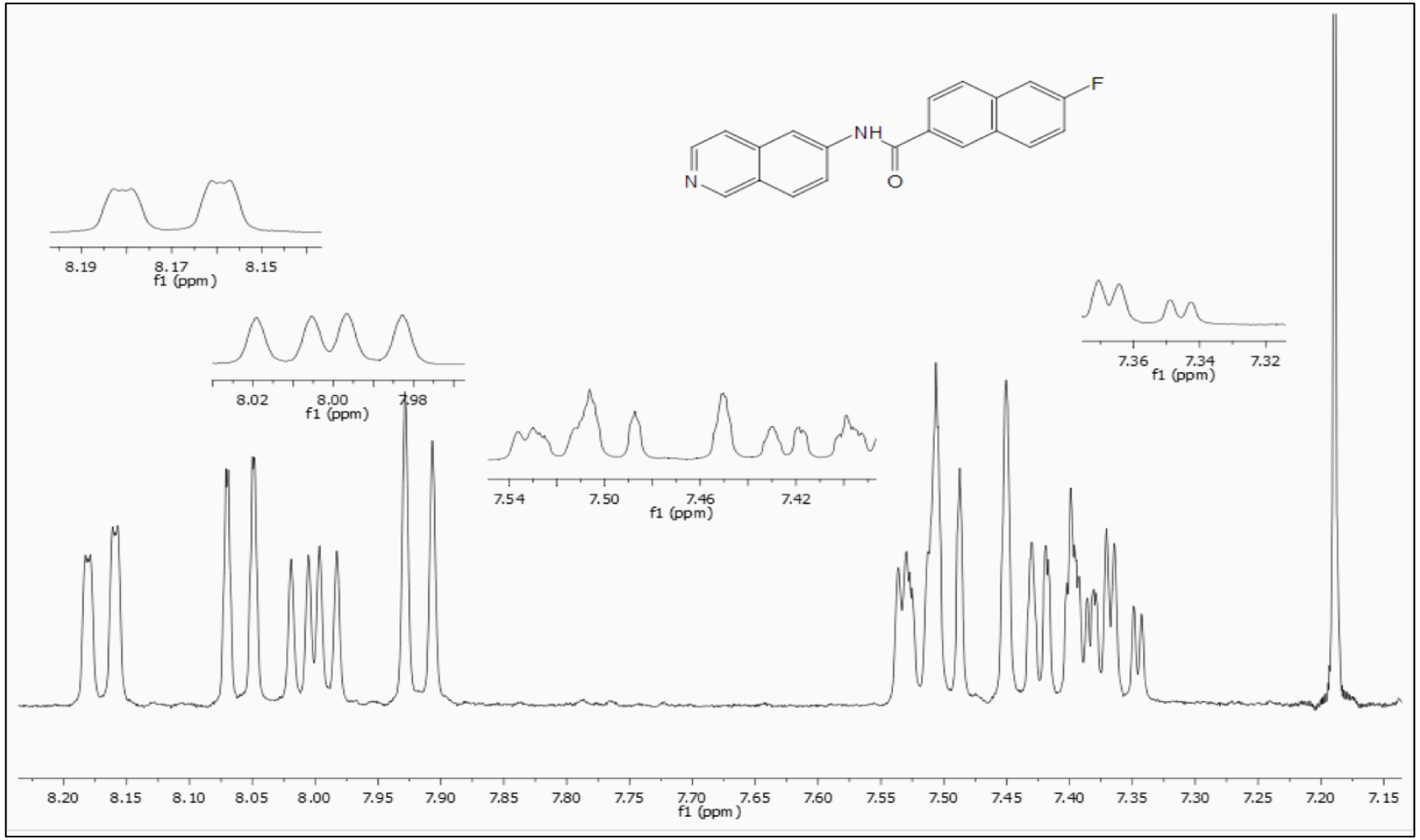


Figure B.17. $^{1}$H-NMR spectrum of 6-fluoro-N-(isoquinolin-6-yl)-2-naphthamide.

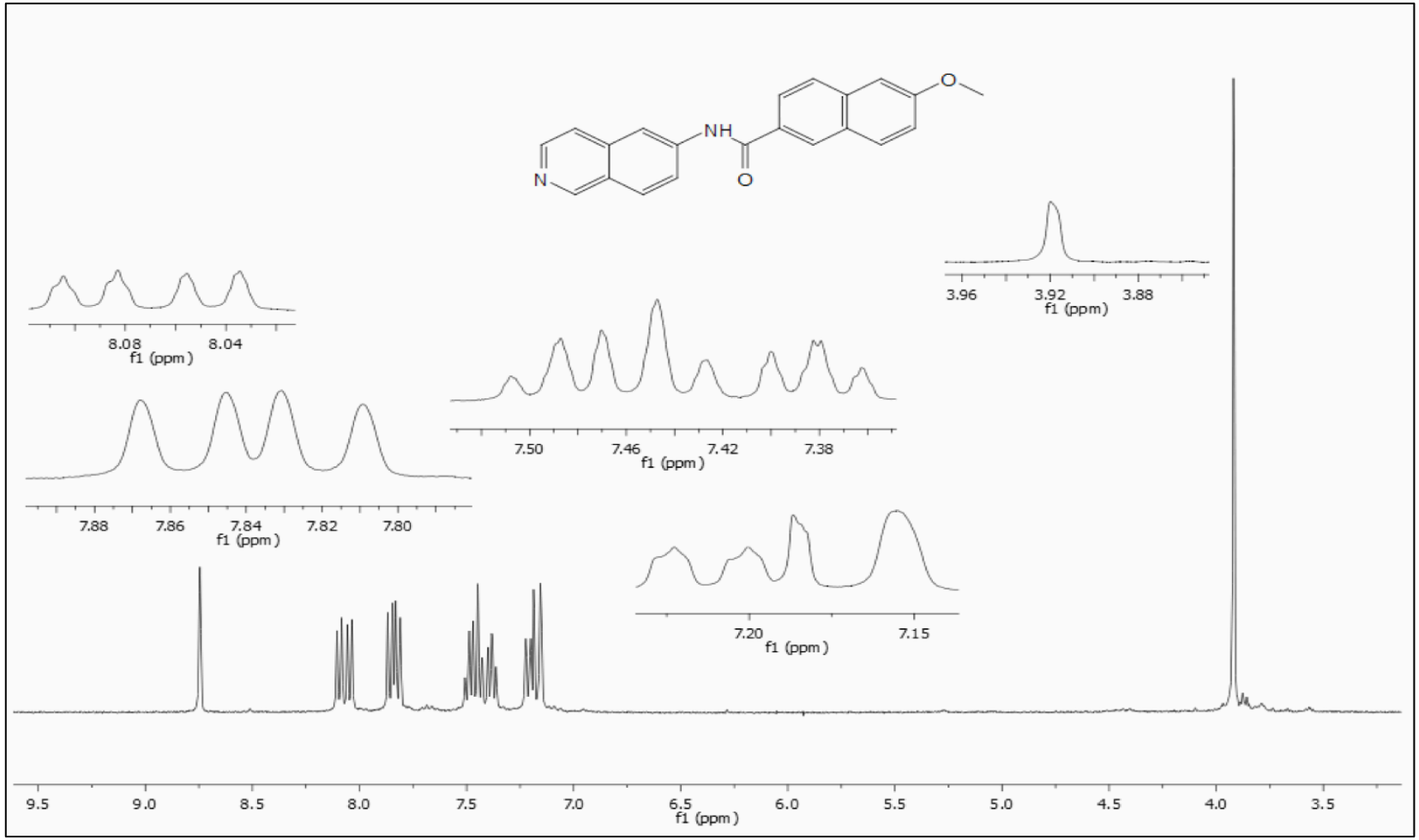


Figure B.18. $^{1}$H-NMR spectrum of N-(isoquinolin-6-yl)-6-methoxy-2-naphthamide.

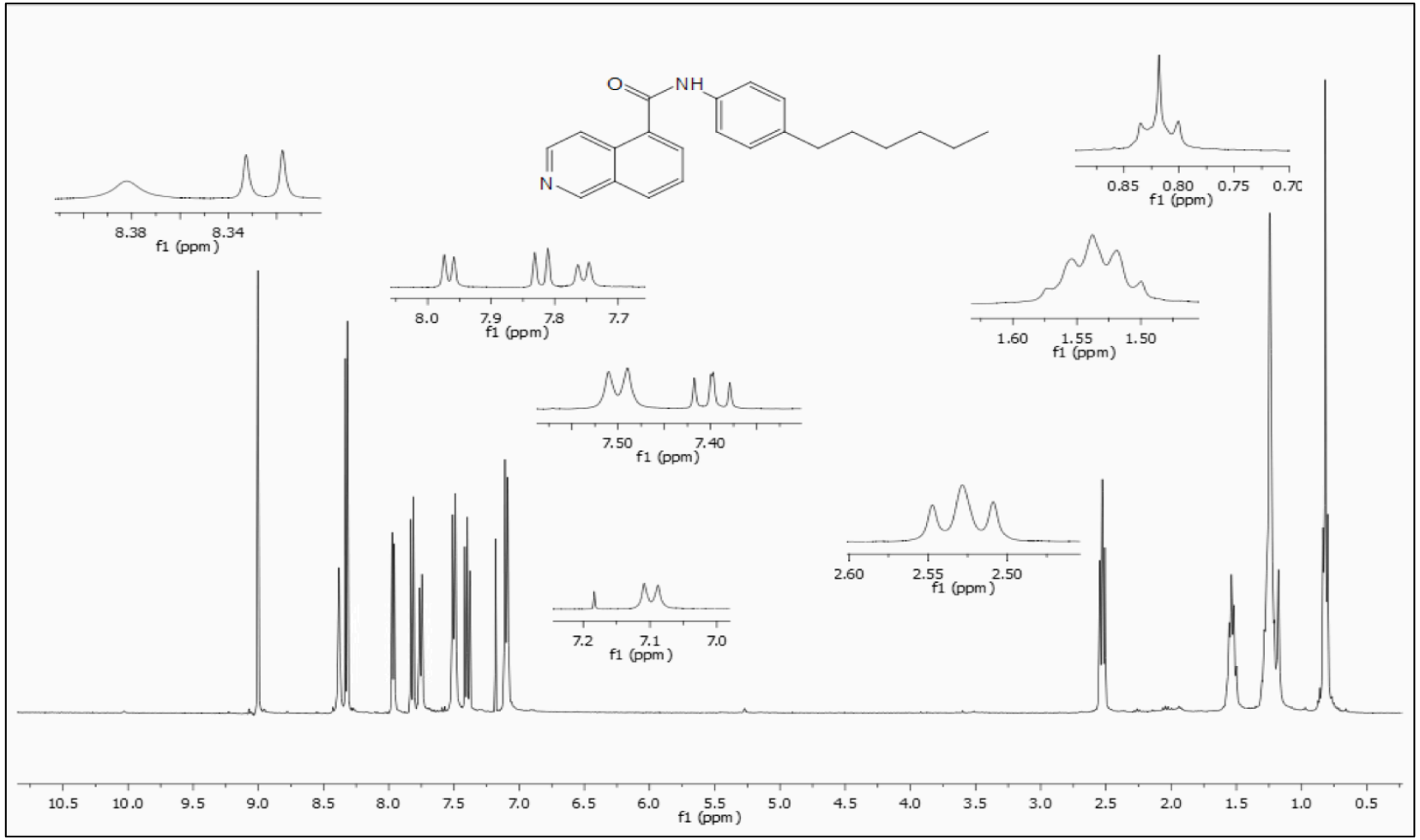


Figure B.19. $^{1}$H-NMR spectrum of N-(4-hexylphenyl)isoquinoline-5-carboxamide.

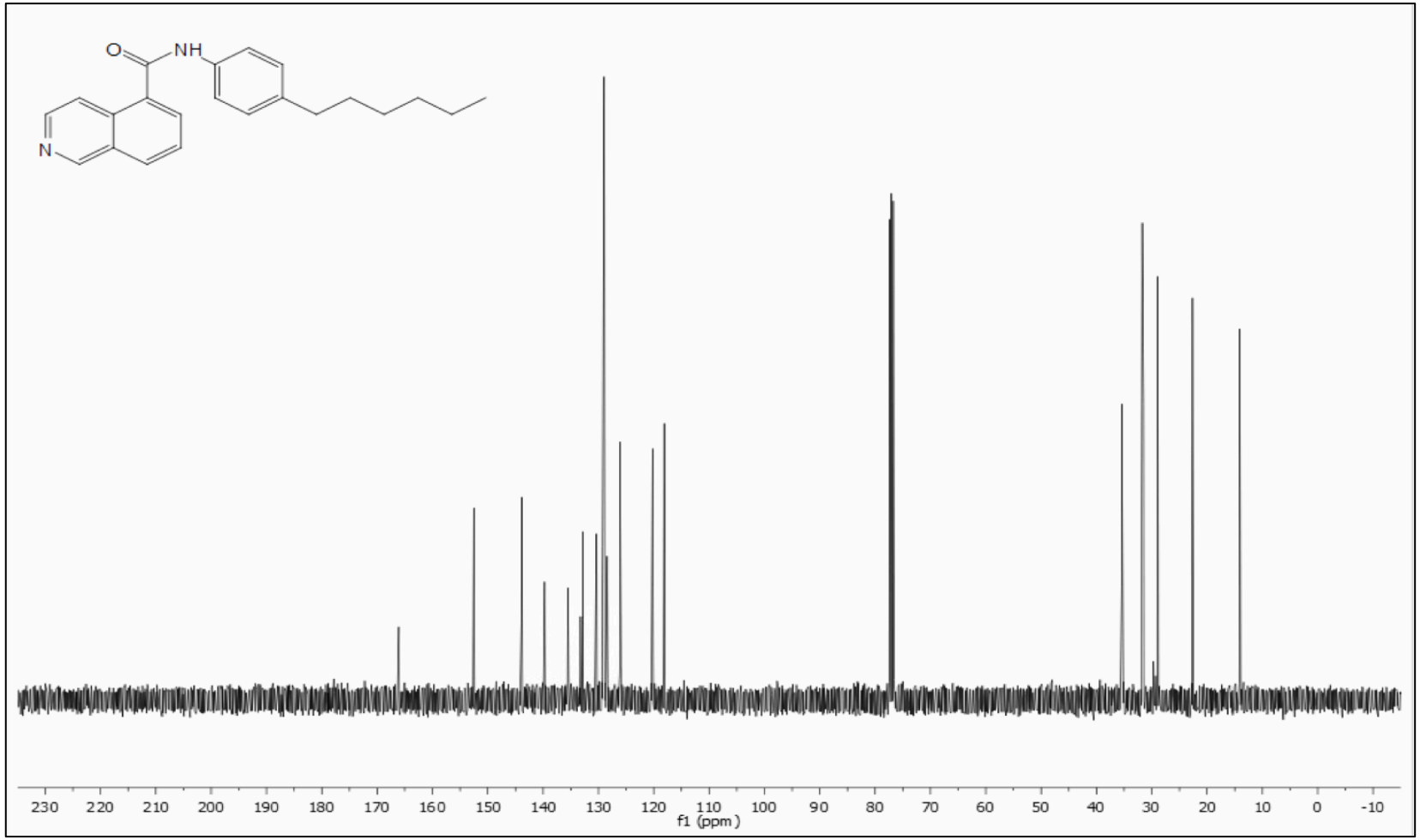


Figure B.20. $^{13}$C-NMR spectrum of N-(4-hexylphenyl)isoquinoline-5-carboxamide.

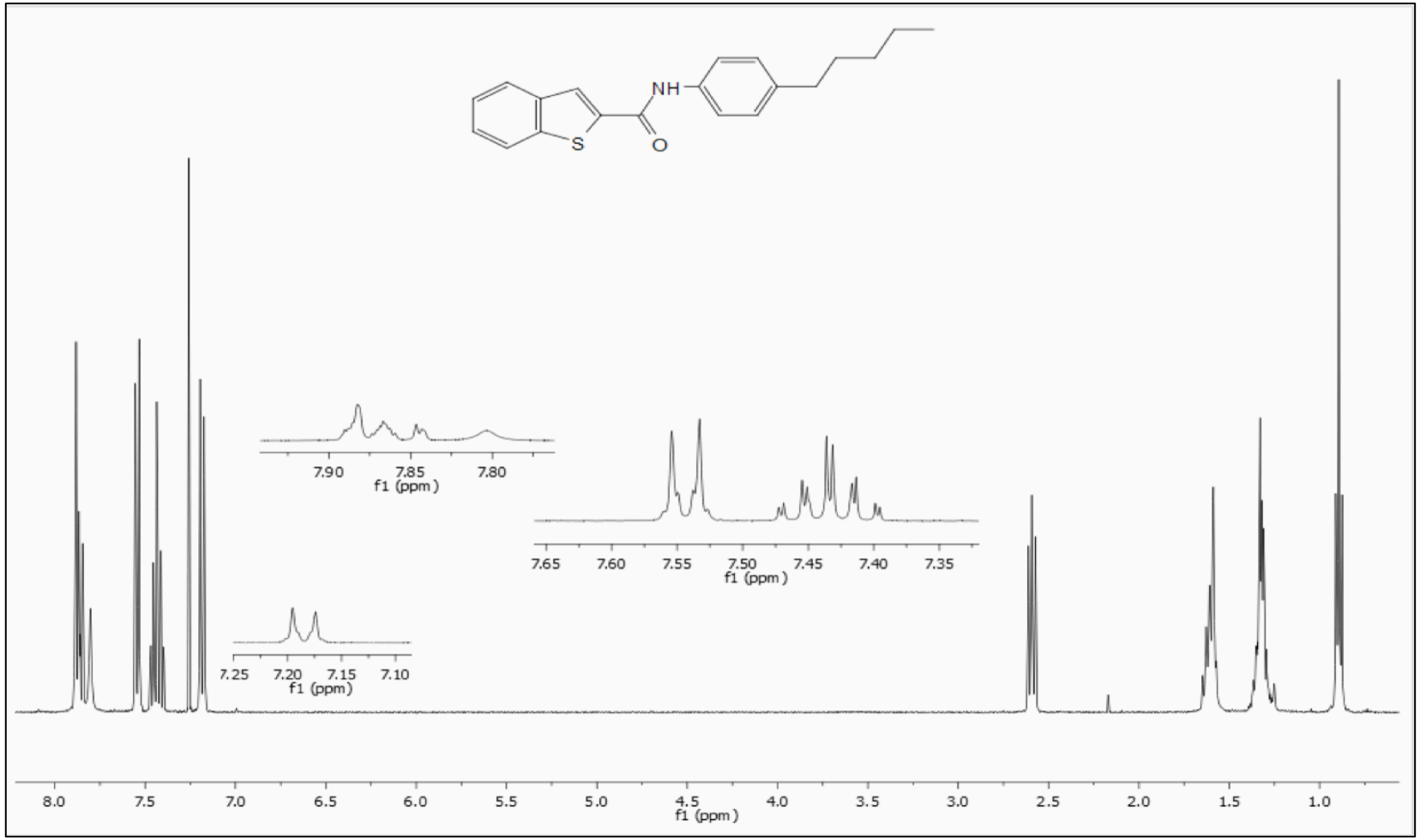


Figure B.21. $^{1}$H-NMR spectrum of 1-(Benzo[b]thiophen-2-yl)-2-(4-pentylphenyl)ethanone.

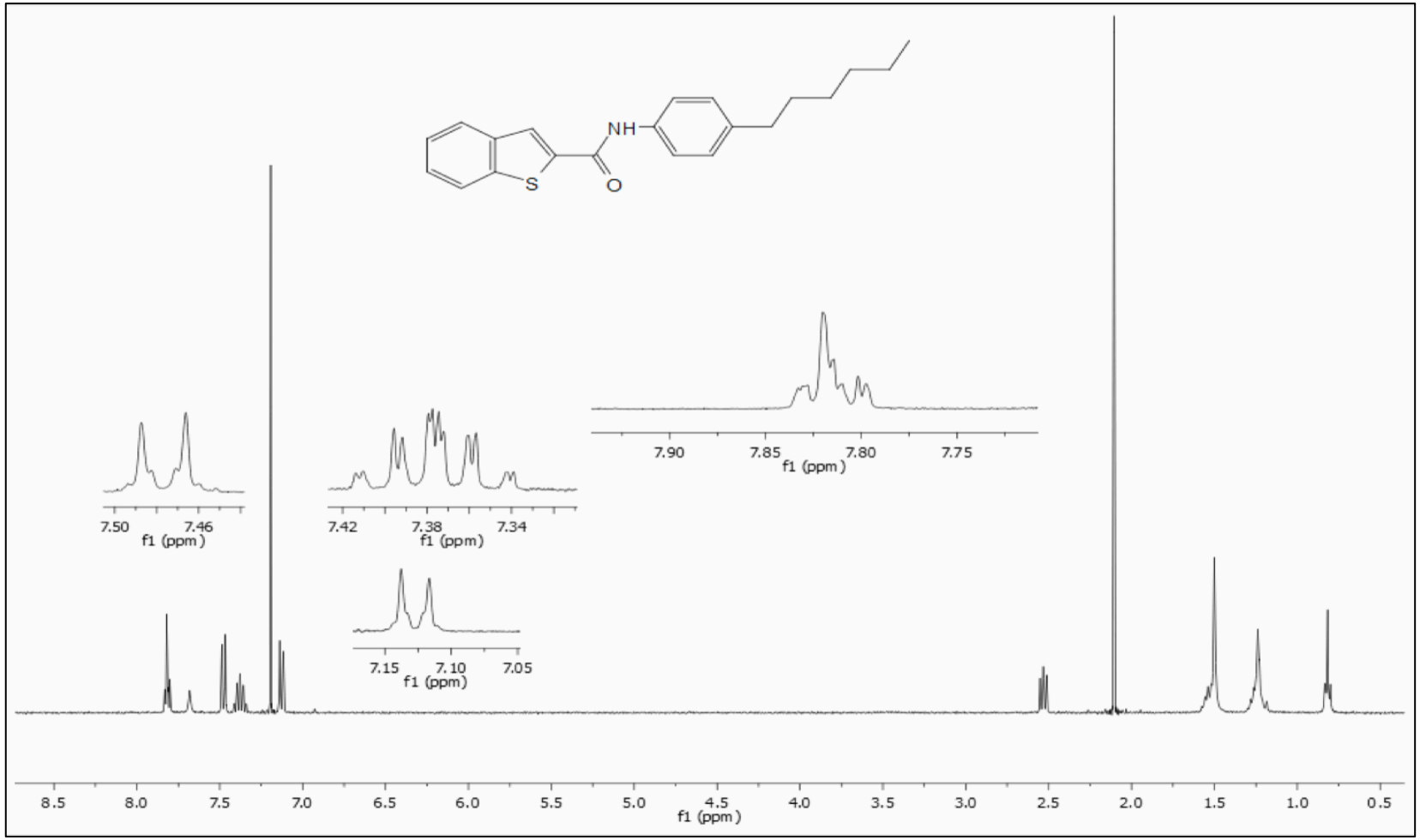


Figure B.22. $^{1}$H-NMR spectrum of 1-(Benzo[b]thiophen-2-yl)-2-(4-hexylphenyl)ethanone.

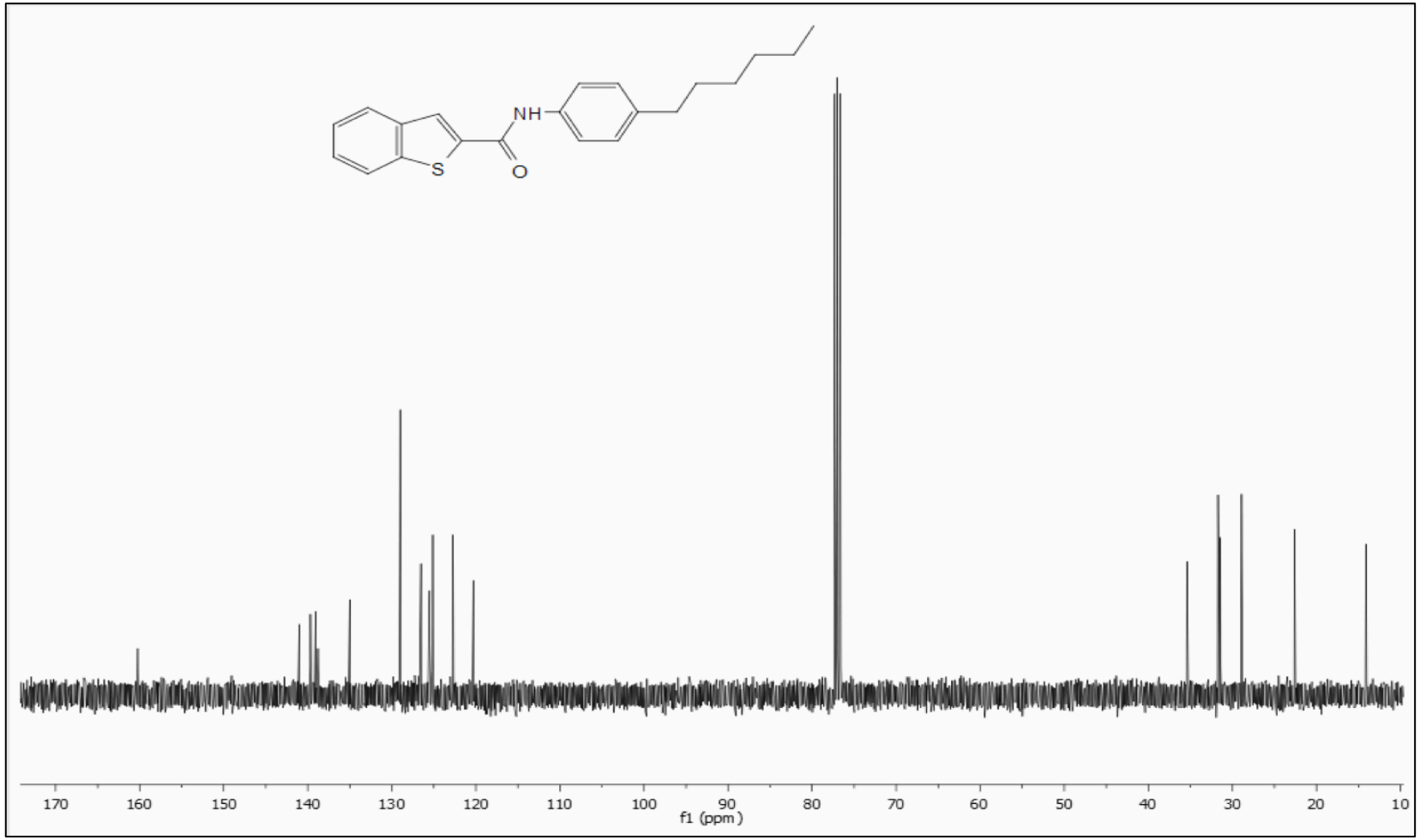


Figure B.23. $^{13}$C-NMR spectrum of 1-(Benzo[b]thiophen-2-yl)-2-(4-hexylphenyl)ethanone.

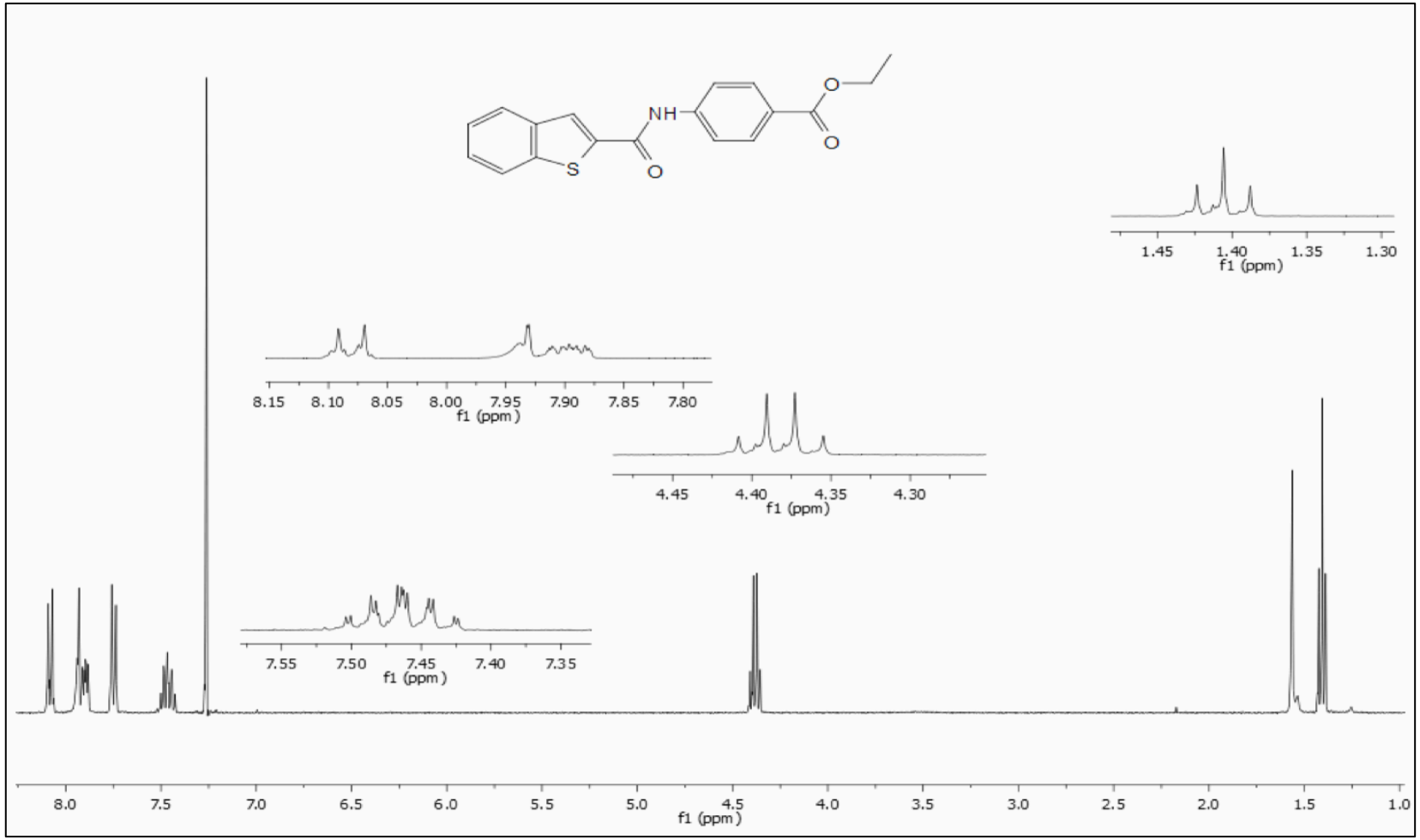


Figure B.24. $^{1}$H-NMR spectrum of Ethyl 4-(benzo[b]thiophene-2-carboxamido)benzoate.

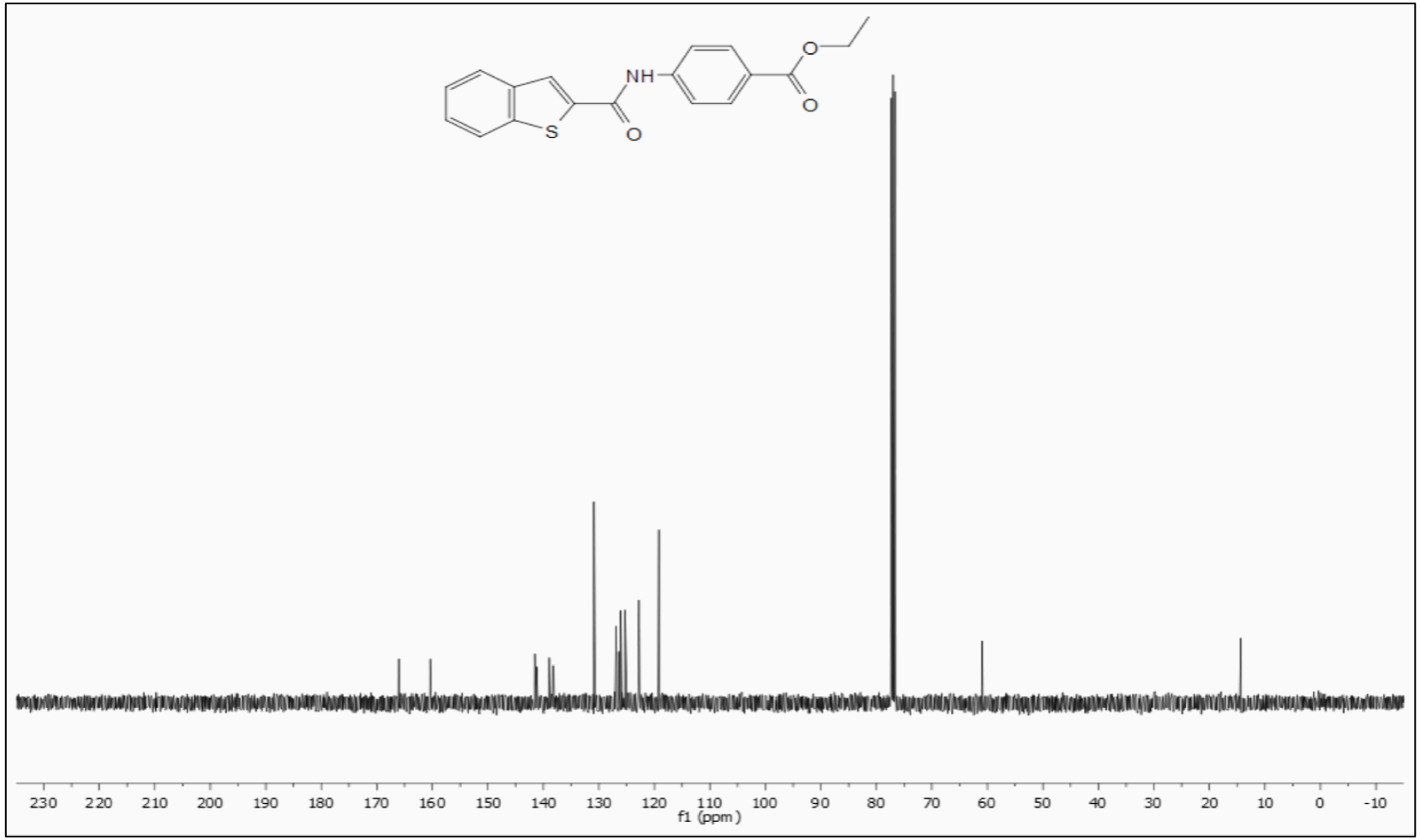


Figure B.25. $^{13}$C-NMR spectrum of Ethyl 4-(benzo[b]thiophene-2-carboxamido)benzoate.

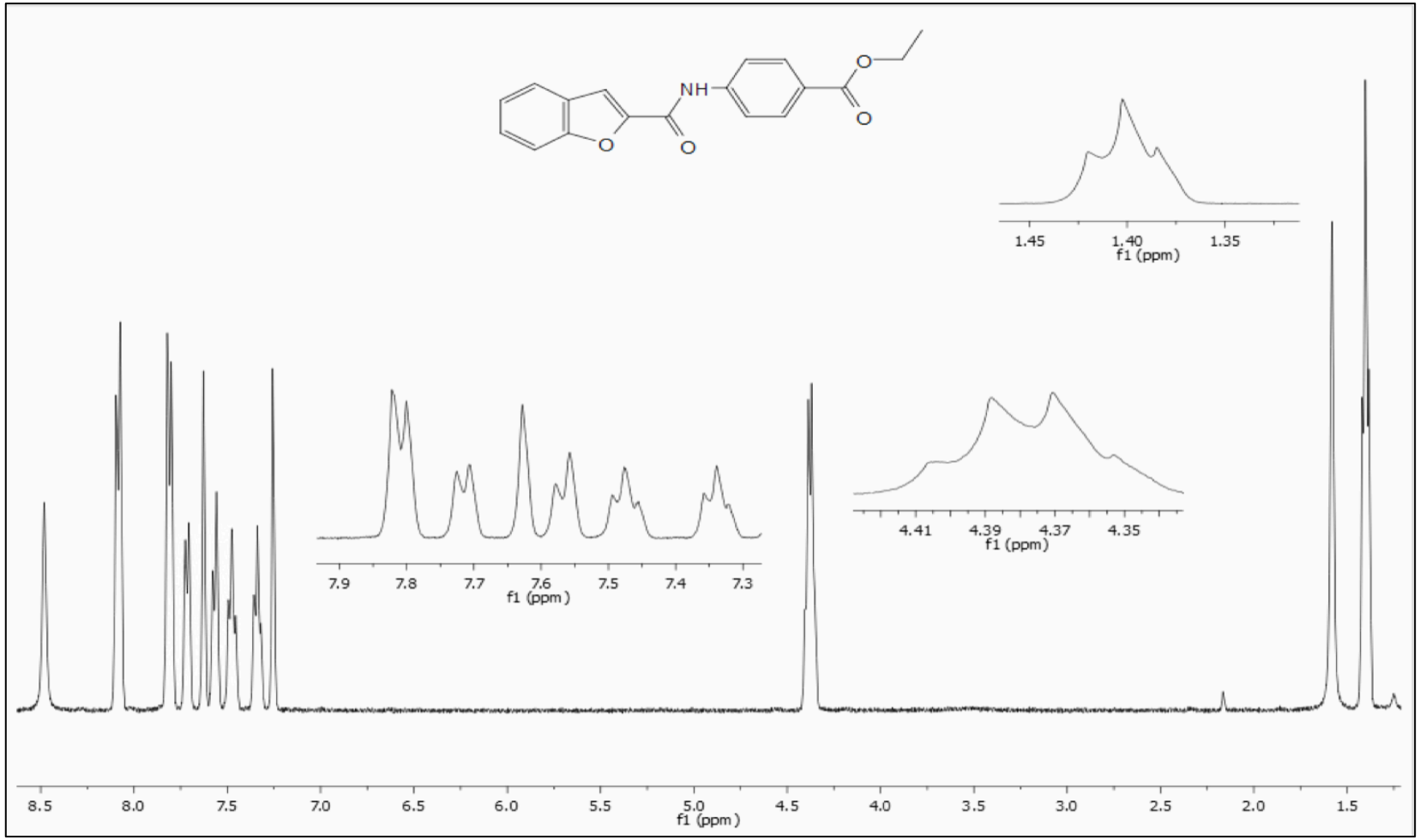


Figure B.26. $^{1}$H-NMR spectrum of Ethyl 4-(benzofuran-2-carboxamido)benzoate.

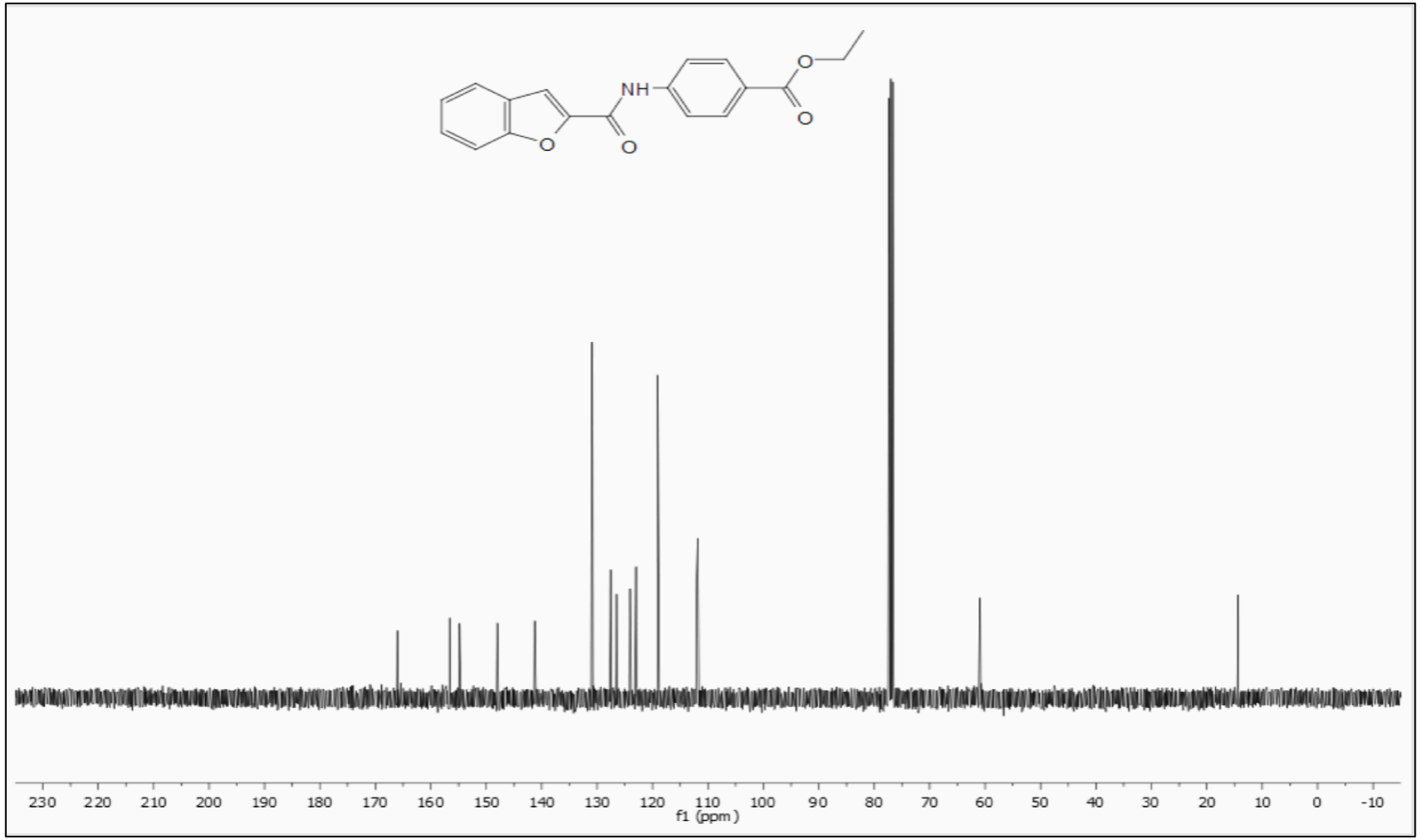


Figure B.27. $^{13}$C-NMR spectrum of Ethyl 4-(benzofuran-2-carboxamido)benzoate.

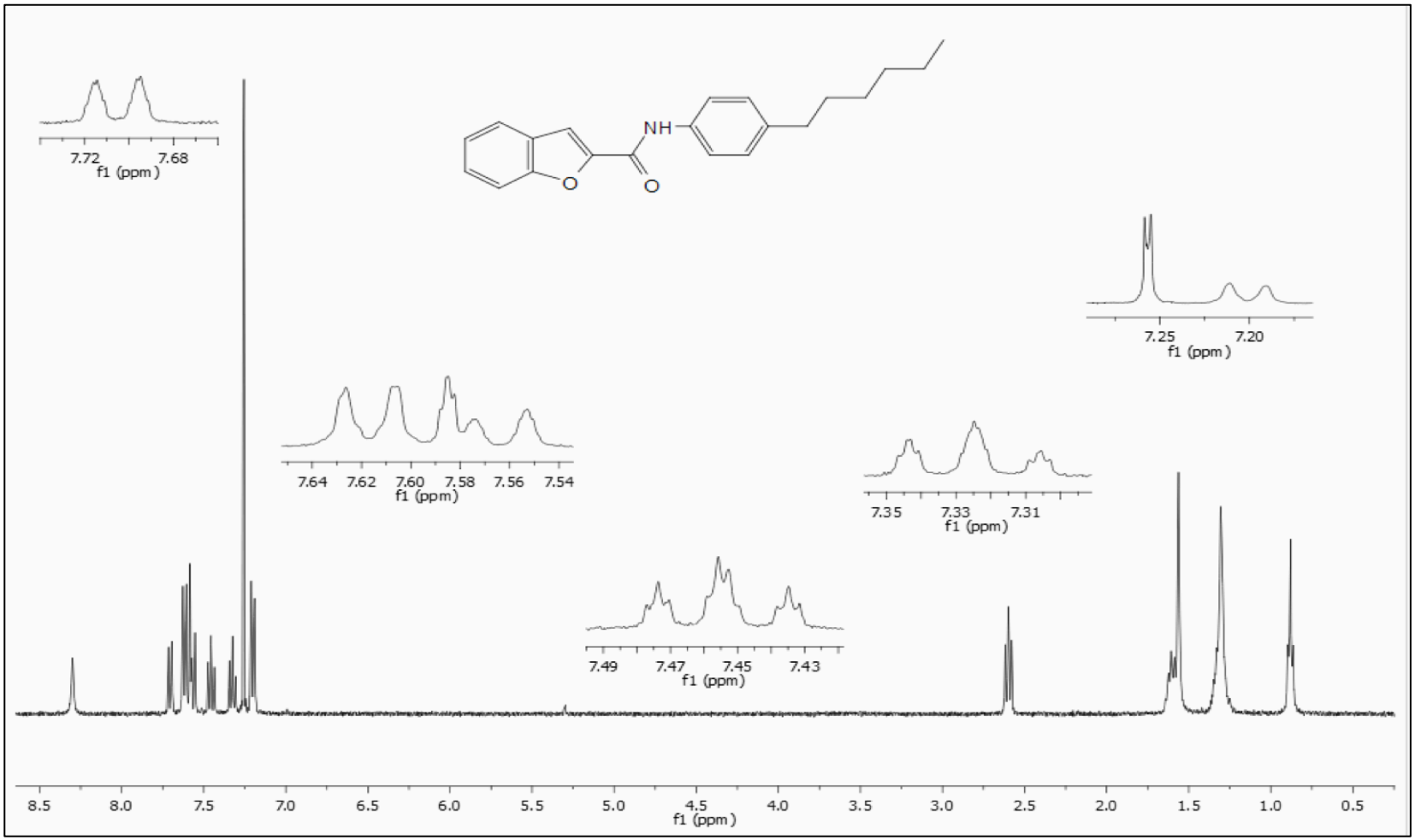


Figure B.28. $^{1}$H-NMR spectrum of N-(4-hexylphenyl)benzofuran-2-carboxamide.

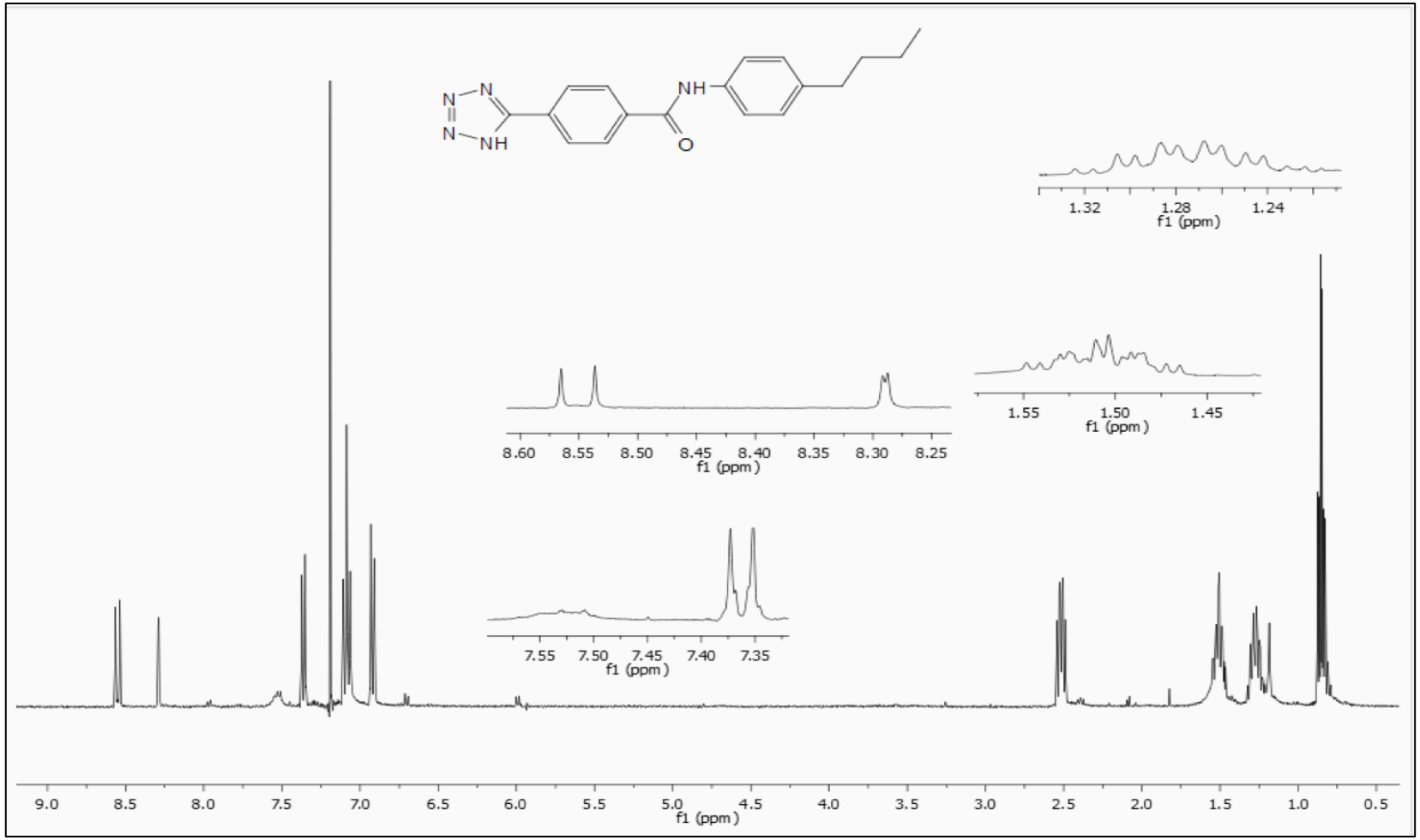


Figure B.29. $^{1}$H-NMR spectrum of N-(4-butylphenyl)-4-(1H-tetrazol-5-yl)benzamide.

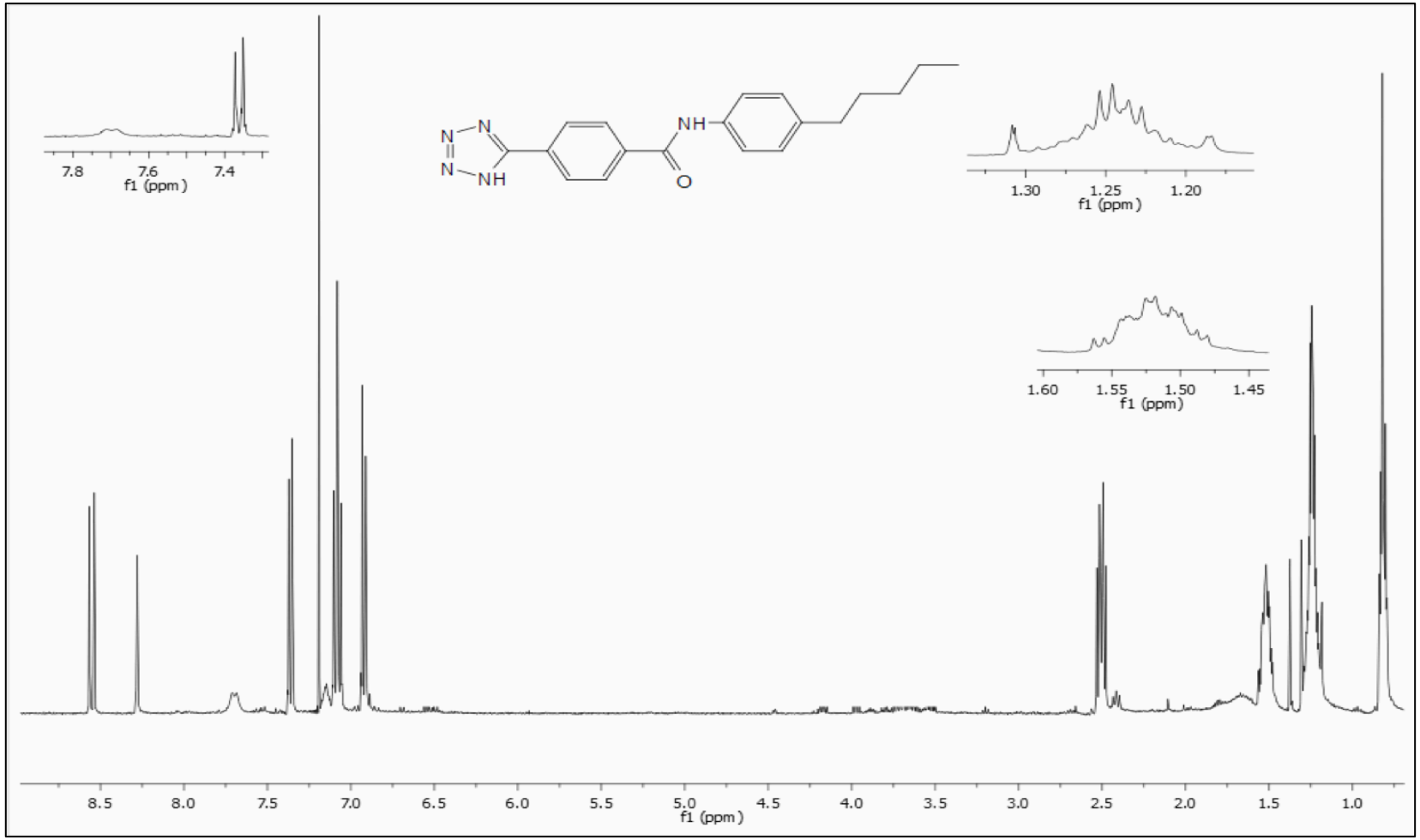


Figure B.30. $^{1}$H-NMR of N-(4-pentylphenyl)-4-(1H-tetrazol-5-yl)benzamide.

# REFERENCES


1. American Cancer Society, *"Cancer Facts & Figures",* 2015*,* http://www.cancer.org/acs/groups/content/@editorial/documents/document/acspc-044552.pdf, [Accessed June 2015].

2. Pories, S. E., M. A. Moses, and M. M. Lotz, *Cancer*, Greenwood Publishing Group, California, 2009.

3. American Cancer Society, *"The History of Cancer",* http://www.cancer.org/cancer/cancerbasics/thehistoryofcancer/the-history-of-cancer-modern-knowledge-and-cancer-causes, [Accessed June 2015].

4. American Cancer Society, *"Cancer Facts & Figures",* 2010*,* http://www.cancer.org/research/cancerfactsstatistics/cancerfactsfigures2010/index, [Accessed June 2015].

5. Wikipedia, *"Risk Factor",* https://en.wikipedia.org/wiki/Risk_factor, [Accessed July 2015].

6. Hartmann, R. W., Q. Hu, "The Renaissance of CYP17 Inhibitors for the Treatment of Prostate Cancer," in *Cancer Drug Design and Discovery*, Neidle S., P. B. Arimondo, N. Guilbaud, and C. Bailly, Editors, 2nd edition, Elseiver, pp. 319–56, 2014.

7. American Cancer Society, *"What are the risk factors for prostate cancer?"*, http://www.cancer.org/cancer/prostatecancer/detailedguide/prostate-cancer-risk-factors, [Accessed June 2015].

8. Wikipedia, *"Prostate"*, https://en.wikipedia.org/wiki/Prostate, [Accessed June 2015].

9. Visual Health Solutions, *"Prostate Cancer,"* http://visualhealthsolutions.com/index.php?page=asset_detail&asset_id=vpl_0137_001. [Accessed May 2015].

10. LeBeau, A.M., P. Singh, J.T. Isaacs, "Prostate-Specific Antigen is a 'Chymotrypsin-Like' Serine Protease With Unique P1 Substrate Specificity" *Biochemistry*, pp. 3490–3496, 2009.

11. Makarov, D., and H. Carter, "The Discovery of Prostate Specific Antigen as a Biomarker for the Early Detection of Adenocarcinoma of the Prostate" *Journal of Urology*, Vol. 176, No. II, pp. 2383–2385, 2006.

12. Miller, W., R. Auchus, and D. Geller, "The Regulation of 17,20 Lyase Activity" *Steroids*, Vol. 62, pp. 133–42, 1997.

13. van Leeuwen, P., D. Connolly, A. Gavin, M. Roobol, A. Black, C. Bangma *et al.,* "Prostate Cancer Mortality in Screen and Clinically Detected Prostate Cancer: Estimating the Screening Benefit" *European Journal of Cancer*, Vol. 46, pp. 377–83, 2010.

14. National Cancer Institute, *"Prostate"* http://www.cancer.gov/cancertopics/wyntk/prostate/page6, [Accessed August 2011].

15. National Cancer Institute, *"Treatment of Prostate Cancer"*, http://www.cancer.gov/cancertopics/pdq/treatment/prostate/Patient/page4#Keypoint19. [Accessed August 2011].

16. Neidle, S, P. B. Arimondo, N. Guilbaud, and C. Bailly, *Cancer Drug Design and Discovery*, 2nd Edition, Elseiver, London, 2014.

17. Cai, C., S. Chen, P. Ng, G. Bubley, P. Nelson, E. Mostaghel, *et al*., "Intratumoral *De Novo* Steroid Synthesis Activates Androgen Receptor in Castration-Resistant Prostate Cancer and is Upregulated by Treatment with CYP17A1 Inhibitors" *Cancer Research*, Vol. 71, pp. 6503–13, 2011.

18. Montgomery, R., E. Mostaghel, R. Vessella, D. Hess, T. Kalhorn, C. Higano, *et al.*, "Maintenance of Intratumoral Androgens in Metastatic Prostate Cancer: A Mechanism for Castration-Resistant Tumor Growth" *Cancer Research,* Vol. 68, pp. 4447–54, 2008.

19. Petrunak, E. M., N. M. DeVore, P. R. Porubsky, and E. E. Scott, "Structures of Human Steroidogenic Cytochrome P450 17A1 with Substrates," *Journal of Biological Chemistry*, Vol. 289, No. 47, pp. 32952–32964, 2014.

20. Attard, G., A. Reid, T. Yap, F. Raynaud, M. Dowsett, S. Settatree, *et al*., "Phase I Clinical Trial of a Selective Inhibitor of CYP17, Abiraterone Acetate, Confirms that Castration-Resistant Prostate Cancer Commonly Remains Hormone Driven" *Journal of Clinical Oncology*, Vol. 26, pp. 4563–71, 2008.

21. Picard, F., T. Schulz, and R. Hartmann, "5-Phenyl Substituted 1-Methyl-2-Pyridones And 4'-Substituted Biphenyl-4-Carboxylic Acids: Synthesis and Evaluation as Inhibitors of Steroid-5α-Reductase Type 1 and 2" *Bioorganic Medicinal Chemistry*, Vol. 10, pp. 437–48, 2002.

22. Yin, L. and Q. Hu, "CYP17 Inhibitors – Abiraterone, C17, 20-Lyase Inhibitors and Multi-Targeting Agents" *National Review of Urology*, Vol. 11, pp. 32–42, 2014.

23. Hartmann, R. W., Q. Hu, "The Renaissance of CYP17 Inhibitors for the Treatment of Prostate Cancer," *Cancer Drug Design Discovery*, pp. 319–356, 2014.

24. DeVore, N. M. and E. E. Scott, "Structures of Cytochrome P450 17A1 with Prostate Cancer Drugs Abiraterone and TOK-001" *Nature*, Vol. 482, No. 7383, pp. 116–119, 2012.

25. Ozdemir, M. E., *Structure-Based Drug Design for Prostate Cancer*, M.S. Thesis, Koc University, 2008.

26. Armutlu, T., M. E. Ozdemir, S. Ozdas, I. H. Kavakli, "Discovery of Novel CYP17 Inhibitors for the Treatment of Prostate Cancer with Structure-Based Drug Design," *Letters of Drug Design and Discovery*, Vol. 6, pp. 337–344, 2009.

27. Workman, P., and I. Collins, "Modern Cancer Drug Discovery: Integrating Targets, Technologies and Treatments for Personalized Medicine," *Cancer Drug Design and Discovery*, 2nd Edition, Neidle S., P. B. Arimondo, N. Guilbaud, and C. Bailly, Editors, Elseiver, pp. 3–43, 2014.

28. Grigoryev, D.N., B. J. Long, I. P. Nnane, V. C. Njar, Y. Liu, and M. Brodie, "Effects Of New 17alpha-Hydroxylase/C(17,20)-Lyase Inhibitors on Lncap Prostate Cancer Cell Growth *in Vitro* and *in Vivo*" *Brazilian Journal of Cancer*, Vol. 81, No. 4, pp. 622–630, 1999.

29. Montalbetti, N. and V. Falque, "Amide Bond Formation and Peptide Coupling," *Tetrahedron*, Vol. 61, No. 46, pp. 10827–10852, 2005.

30. Çavuşoğlu, N., *"Synthesis Of Branched Alkyl Substituted Potential Drug Molecules Active Against Prostate Cancer"*, M.S. Thesis, Boğaziçi University, 2011.

31. Yıldırım, T., "*Synthesis of Branched Alkyl Substituted Phenylene Derivatives as Potential Drug Molecules Active Against Prostate Cancer",* M.S Thesis, Boğaziçi University, 2012.

32. Köseoğlu, A., *"Aromatic Carboxamides as Non-Steroidal Inhibitors of CYP17 for the Treatment of Prostate Cancer"* , Ph.D. Thesis, Boğaziçi University, 2015.

33. Zengin, E., *"Synthesis of Isoquinoline and Pyrocatechol Derivatives as Potential Drug Molecules Active Against Prostate Cancer,"* M.S. Thesis, Boğaziçi University, 2013.